INFORMATION TO USERS

This manuscript has been reproduced from the microfilm master. UMI films the text directly from the original or copy submitted. Thus, some thesis and dissertation copies are in typewriter face, while others may be from any type of computer printer.

The quality of this reproduction is dependent upon the quality of the copy submitted. Broken or indistinct print, colored or poor quality illustrations and photographs, print bleedthrough, substandard margins, and improper alignment can adversely affect reproduction.

In the unlikely event that the author did not send UMI a complete manuscript and there are missing pages, these will be noted. Also, if unauthorized copyright material had to be removed, a note will indicate the deletion.

Oversize materials (e.g., maps, drawings, charts) are reproduced by sectioning the original, beginning at the upper left-hand corner and continuing from left to right in equal sections with small overlaps.

Photographs included in the original manuscript have been reproduced xerographically in this copy. Higher quality 6" x 9" black and white photographic prints are available for any photographs or illustrations appearing in this copy for an additional charge. Contact UMI directly to order.

ProQuest Information and Learning
300 North Zeeb Road, Ann Arbor, MI 48106-1346 USA
800-521-0600

Université d'Ottawa · University of Ottawa

BUTYL ACRYLATE/VINYL ACETATE EMULSION COPOLYMERIZATION:

Reaction Monitoring and Property Evaluation

by
Renata Jovanović

A thesis submitted to the Faculty of Graduate and Postdoctoral Studies
in fulfillment of the requirements for the degree of

Master of Applied Science
Chemical Engineering

Department of Chemical Engineering
UNIVERSTY OF OTTAWA

ABSTRACT

Several aspects of butyl acrylate/vinyl acetate (BA/VAc) polymerizations were investigated in this thesis. All of these originated from an attempt to establish links between different aspects of adhesive production (i.e. the polymerization process, inherent polymer properties and final product properties). Even though poly(vinyl acetate) based adhesives have been investigated in academia and industry for many years, there is a considerable lack of information about the relationship between the above mentioned aspects of BA/VAc emulsion based adhesives.

Polymerization process monitoring is a key factor in obtaining high quality products with prespecified properties. Therefore, a considerable part of this work was devoted to the real-time monitoring of BA/VAc emulsion polymerization reactions. An Attenuated Total Reflectance - Fourier Transform Infrared (ATR-FTIR) spectroscopy sensor was used for monitoring conversion and copolymer composition. Due to the novelty of this technique, in the first part of the study, the suitability of this technique for polymerization monitoring was investigated. Six BA and VAc homo- and co-polymerizations in toluene solution were monitored using standard techniques (gravimetry and ^{1}H-NMR) and ATR-FTIR spectroscopy. The ATR-FTIR monitoring technique involved the determination of characteristic absorbances of the functional groups of BA and VAc monomers. The consumption of monomer throughout the reaction was followed using these characteristic absorbances. The results obtained using ATR-FTIR compared favorably to standard techniques. In addition, the effect of solvent on BA and VAc solution polymerizations was investigated. The effect of solvent was found to contribute to the change of a lumped kinetic constant, $k_p/k_t^{0.5}$, with the concentration of solvent. Incorporated into a

JAVA™-based model for free radical polymerization modeling, these changes considerably improved the model predictions.

In the second part of this thesis, the knowledge obtained from the off-line monitoring of the solution polymerizations was employed for the real time monitoring of six high-solids BA/VAc emulsion polymerizations. Monomer consumption was monitored using the monomer characteristic absorbances via ATR-FTIR spectroscopy. The copolymers formed were not soluble in a range of organic solvents. This insolubility was assigned to the use of a polymeric surfactant poly(vinyl alcohol) and its possible grafting onto the particle surface. Thus, an indirect means of evaluating the accuracy of the ATR-FTIR measurements was employed. The results obtained using ATR-FTIR spectroscopy compared favorably to those obtained by gravimetry for most of the feed compositions. Temperature was discovered as a significant factor that affected the ATR-FTIR probe readings.

Finally, the latexes obtained in the second part of this thesis were characterized for a variety of polymer properties of interest to adhesive industry. Among the properties investigated were particle size, rheology, dynamic mechanical properties of the dry polymers and the shear and tensile strength of adhesive bonds when hard maple wood is used as a substrate. The existence of two glass transition temperatures (determined using dynamic mechanical analysis of dry polymers) in all cases was an indicator of the heterogeneity of the BA/VAc copolymers formed in a batch mode. Copolymer composition and its heterogeneity influenced the adhesive bond strength. The heterogeneity of the copolymers, measured as the difference between the glass transition temperatures of the homopolymer domains, increased with the increase in BA content. An increase in the average tensile strength of adhesive bonds with an increase in the BA

content in the copolymer was observed. On the other hand, increases in the BA content led to a decrease in the average shear strength of the adhesive bond.

The shear strength of the strongest BA/VAc adhesive produced was not significantly different from the shear strength of a commercial poly(vinyl acetate) based adhesive. The tensile strength of the adhesive bond for all of the produced BA/VAc adhesives was greater than the strength of the bond of a commercial adhesive. However, due to the low number of samples more work in this area should be performed in order to strengthen these conclusions.

RÉSUMÉ

Plusieurs aspects de la polymérisation du système acrylate de butyle/acétate de vinyle (BA/Vac) furent étudiés lors de cette étude. Chacun d'entre eux émergent de la tentative d'établir le lien entre les différents aspects de la production d'adhésifs (i.e. le procédé de polymérisation, les propriétés inhérentes des polymères et les propriétés du produit final). Malgré que les adhésifs à base de poly(acétate de vinyle) furent investigés en mileu académique et en industrie au cours des dernières années, il y a manque énorme quant aux études concentrées sur la relation entre les aspects mentionés ci-haut pour les adhésifs à base d'émulsion de BA/Vac.

La surveillance des procédés de polymérisation est un facteur clé pour l'obtention de produits de haute qualité comportant des propriétés pré-spécifiées. De ce fait, une partie considérable de cette étude a été dédiée à la surveillance en temps réel des réactions de polymérisation en émulsion du système BA/Vac. Une sonde qui utilise le facteur de réflexion total atténué - spectroscopie infrarouge de la transformation Fourier (ATR-FTIR) fût utilisée pour la surveillance de la conversion et de la composition des polymères. Puisque cette technique est encore très nouvelle, la première partie de cette étude fût d'étudier la convenance de cette technique pour la surveillance des réactions de polymérisation. Six BA et Vac homo et co-polymérisation furent surveiller en utilisant des techniques standards (gravimétries et H-NMR) et la spectroscopie ATR-FTIR. La technique ATR-FTIR de surveillance implique la détermination des absorbances charactéristiques des groupes fonctionels des monomères BA et Vac. La disparition des monomères au cours de la réaction a été suivie en utilisant ces absorbances charactéristiques. Les résultats obtenus en utilisant ATR-FTIR sont favorablement comparables aux techniques standards. De plus, l'effet du solvent sur la polymérisation en solution de BA et

Vac fût investigé. Il a été démontré que l'effet du solvent contribue au changement d'une constante cinétique, $k_p/k_t^{0.5}$, avec la concentration du solvent. Incorporés dans un programme JAVA pour la modélisation de polymérisations à radicaux libres, ces changements ont grandement améliorés les prédictions des modèles.

En seconde partie de cette thèse, les connaissances obtenues par la surveillance différée des polymérisations en solution furent utilisées pour la surveillance continue en temps réel de six polymérisations à émulsion de BA/Vac avec un contenu en solides élevé. La disparition des monomères a été suivie en utilisant les absorbances charactéristiques via la spectroscopie ATR-FTIR. Le copolymères formés n'étaient pas solubles dans une gamme de solvents organiques. Cette insolubilité est attribuée à l'utilisation d'un surfractant polymérique (poly(alcohol de vinyle)) et son possible attachement sur la surface des particules. Donc, une manière indirecte d'évaluer la précision des mesures de ATR-FTIR a été utilisée. Les résultats obtenus avec la spectroscopie ATR-FTIR comparent favorablement avec ceux obtenus par gravimétrie pour la plupart des compositions initiales de monomèes. Il a été découvert que la température affecte énormément les lectures effectuées par la sonde ATR-FTIR.

Finalement, les latex obtenus en seconde partie de cette étude furent charactériés pour une variété de propriétés d'intérèt à l'industrie des adhésifs. Parmi les propriétés étudiées figurent: la grosseur des particules, la rhéologie, les propriétés méchaniques dynamiques du polymère séché ainsi que la force de résistance et d'élasticité des liens adhésifs lorsque l'érable dur est utilisé comme substrat. L'existence de deux températures de transition vitreuse (déterminée par l'analyse des propriété méchaniques dynamiques des polymères séchés) dans chacun des cas était un indicateur de l'hétérogénéité des copolymères BA/Vac produits en système discontinu. La composition des copolymères ainsi que l' hétérogénéité influencent la

force du lien adhésif. L'hétérogénéité des copolymères, mesurée comme étant la différence entre les températures de transition vitreuse des homopolymères, augmente avec une augmentation du contenu en BA. Une augmentation dans la force d'élasticité des liens adhésifs avec une augmentation dans le contenu en BA dans le copolymère fût observée. De l'autre côté, une augmentation en contenu de BA a provoqué une diminution dans la force de résistance du lien adhésif.

La force de résistance de l'adhésif BA/Vac le plus fort produit n'est pas très différent de celui d'un adhésif commercial fait de poly(acétate de vinyle). La force d'élasticité des liens adhésifs pour tous les adhésifs BA/Vac produits était plus élevée que celle de l'adhésif commercial. Par contre, en vue du petit nombre d'échantillons, d'autres recherches devront êtres faites dans ce domaine afin de renforcer ces conclusions.

ACKNOWLEDGEMENTS

First of all I would like to express my gratitude to my supervisor Dr. Marc A. Dubé. There are different teachers (W.A. Ward): "The mediocre teacher tells. The superior teacher demonstrates. The great teacher inspires." You, Dr. Dubé, are a great teacher. Thank you for never giving up until my good was better and my better was the best. Thank you for your endless support and full-heart friendship.

I am grateful to Dr. M. Munro, (Department of Mechanical Engineering, University of Ottawa) for his assistance in the determination of adhesive properties, to Ms. A. Delgado (Institute for Research in Construction, National Research Council – Ottawa) for assistance in obtaining the DMA data and to Mr. F. Cotton (École Polytechnique – Montreal) for assistance with the viscosity measurements.

I would like to thank the technicians at the Department of Chemical Engineering, University of Ottawa, Gérard Nina, Frank Ziroldo and Louis Tremblay for the help they provided during this work. I am in debt to Mr. Tremblay especially, for his endless efforts and hours he put into the design and construction of the jigs for adhesive testing, for numerous glass ampules and all those "cumulative" small assistances that were needed for the smooth running of this project.

Thanks are also due to the members of the Polymer Reaction Engineering group Chris, Kim, Tony, Xiaodong, Yi and especially, Hong who convinced me that there are no strangers in the world just friends that we haven't met yet. Thanks, our discussions and friendship are precious to me.

Special thanks goes to my family, to those who taught me that any dream can become reality if I have enough courage to pursue it.

Special thanks also goes to my husband, Zoran, who shared all the joyful and sad times with me during not only these two, but the last fourteen years. Thank you for everything.

TABLE OF CONTENTS

LIST OF FIGURES

Chapter 4

Chapter 5

LIST OF TABLES

NOMENCLATURE

Symbols

A_i= area under the spectral peaks of monomer *i* obtained using ^{1}H-NMR spectroscopy

C_{fcta} = chain transfer agent rate constant

C_{fm} = chain transfer to monomer rate constant

C_{fs} = chain transfer to solvent rate constant

E' = storage modulus

E'' = loss modulus

f = initiator efficiency

$\overline{F}_i$ = weight fraction of monomer *i* bound into polymer

I = initiator

K = Mark-Houwink parameter

k_d = initiator decomposition rate constant

k_p = propagation rate constant

$k_p/k_t^{0.5}$ = lumped rate constant

k_{pIj} = propagation rate for the addition of monomer *j* to an initiator fragment

k_{pij} = rate constant of addition of monomer *j* to the radical ending with monomer unit *i*

k_t = termination rate constant

k_{tc} = termination by combination rate constant

k_{td} = termination by disproportionation rate constant

$M^\bullet$ = total concentration of all chain radicals

Mj = monomer *j*

m_i = mass of monomer *i*

M_n = instantaneous number average molecular weight

$[M]_p$ = monomer concentration inside a particle

M_w = instantaneous weight average molecular weight

MW_m = molecular weight of the repeat unit

N = number of latex particles

$\bar{n}$ = average number of radicals per particle

N_a = Avogadro's number

n_i = mole of monomer i

N_c = refractive index of ATR crystal

N_{sc} = ratio between the sample and crystal refractive indices

P = polymer

$R^\bullet$ = primary radical

R_I = rate of initiation

$R_m^\bullet$ = growing polymer chains size of m

$R_n^\bullet$ = growing polymer chains size of n

$R_{r,j}^\bullet$ = radical of chain length r ending in monomer unit j

$R_{r+1,j}^\bullet$ = radical of chain length $r + 1$ ending with monomer unit j

R_p = rate of polymerization

r_i = reactivity ratio of monomer i

R_t = rate of termination

t = time

T_g = glass transition temperature

W = wavenumber

X = overall conversion

x_i = conversion of monomer I

Greek Leters

α = Mark-Houwink parameter

β = molecular weight contribution due to termination by combination

γ = shear rate

η = viscosity

τ = molecular weight contribution due to termination by disproportionation and transfer to small molecules

Θ = angle of incidence

LIST OF ABBREVIATIONS

AIBN = 2,2'-azobisiso-butyronitrile

APS = ammonium persulfate

ASTM = American Society for Testing and Materials

ATR-FTIR = Attenuated total reflectance Fourier transform infrared

BA = butyl acrylate

CTA = chain transfer agent

DP = depth of penetration

DMA = dynamic mechanical analysis

GPC = gel permeation chromatography

MIR = mid infrared

MWD = molecular weight distribution

NIR = near infrared

PBA = poly (butyl acrylate)

PSD = particle size distribution

PVAc = poly (vinyl acetate)

PVOH = poly (vinyl alcohol)

SDS = sodium dodecyl sulfate

THF = tetrahydrofuran

VAc = vinyl acetate

WSI = water soluble impurities

^{1}H-NMR = ^{1}H -nuclear magnetic resonance

Chapter 1

INTRODUCTION

There is great industrial and academic interest in emulsion-based polymers. While both industry and academia are interested in the fundamental understanding of the polymerization process itself, there has been a divergence of interests where the properties of the formed polymers are concerned. Academia has tended to investigate inherent polymer properties such as copolymer composition, molecular weight and molecular weight distribution, and particle size and distribution. It therefore, has focused on the modelling and control of the polymerization process to obtain these desired inherent polymer properties. On the other hand, industry has been more interested in final product performance properties such as adhesion, flow, mechanical properties, etc. They have tended to model, control and optimize the polymerization process in order to yield these final product properties. There is a considerable lack of work connecting process reaction conditions, inherent polymer properties and final product performance. In other words, almost no structure–property relations are reported for many polymer systems.

One emulsion polymer of great interest to both industry and academia is the butyl acrylate/vinyl acetate (BA/VAc) emulsion copolymer. VAc is a major component of adhesives (i.e. pressure sensitive, wood and hot melt adhesives) as well as other products (architectural coatings, sealants etc.) and BA is used to enhance and/or change inherent copolymer and final product properties. The complexity of the reaction kinetics of BA/VAc emulsion copolymerization makes it an interesting research subject. In addition, despite the industrial interest in this system, there is almost four times more work reported in the open literature for butyl acrylate/styrene and butyl acrylate/methyl methacrylate than for butyl acrylate/vinyl acetate copolymerizations. Clearly, there is a need to study this copolymerization system.

1.1 Objectives of the study

In this study, the polymerization reaction conditions, inherent polymer properties and final product performance properties were investigated for a series of butyl acrylate/vinyl acetate emulsion-based adhesives.

This study comprised two objectives. One was to establish structure-property relationships for BA/VAc emulsion-based adhesives. The other objective involved the investigation of an in-line emulsion polymerization monitoring method using ATR-FTIR spectroscopy to track conversion and polymer composition. The results of ATR-FTIR monitoring were to be compared to standard polymer characterization techniques (i.e. gravimetry and ^{1}H-NMR spectroscopy).

Emulsion polymerization processes are heterogeneous, involve different reaction stages, and may be influenced by differences in reactivity ratios and the solubility of the different monomers involved. This, coupled with the novelty of the ATR-FTIR monitoring technique, made the use of the monitoring technique in an off-line mode a logical first step. A series of butyl acrylate and vinyl acetate homo- and copolymerizations was performed in toluene. The objective of this part of the study was to obtain important information about the ATR-FTIR monitoring of these particular monomers. The more straightforward nature of solution polymerizations and less demanding off-line monitoring using ATR-FTIR spectroscopy were considered beneficial for this purpose. The characteristic wavenumbers and calculation methods used in this part of the study were to be employed for future in-line emulsion polymerization monitoring. Furthermore, being aware of the considerable lack of information on solvent effects in butyl acrylate and vinyl acetate homo- and copolymerizations, a secondary objective was to

investigate these effects. After completing the investigation of the ATR-FTIR monitoring technique, final product properties of the produced emulsion copolymers (i.e. viscosity, dynamic mechanical properties and adhesive bond performance under shear and tensile stresses) were to be tested and the relationship between these properties and the inherent polymer properties and the polymerization process characteristics were to be established.

1.2 Thesis structure

The thesis is based on the following three scientific publications (submission status indicated). Further details of the thesis content can be seen in Figure 1.1.

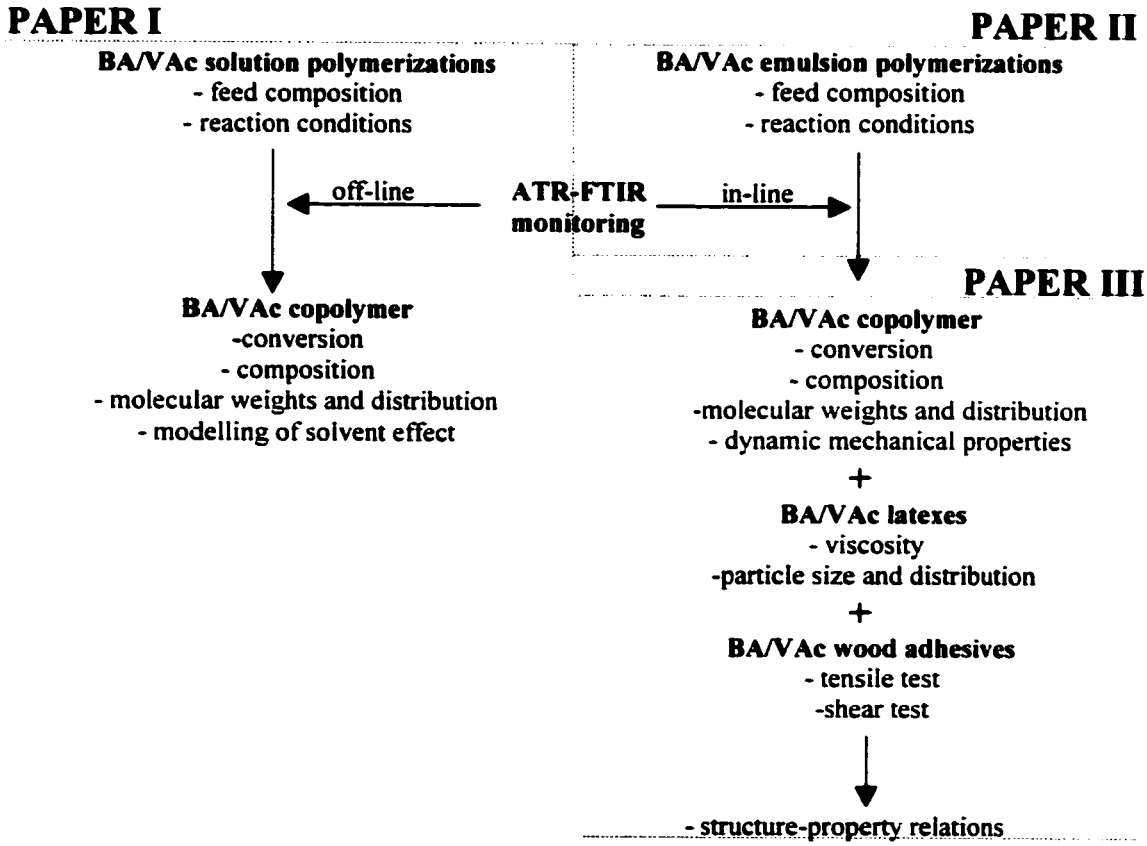

Figure 1.1 Thesis structure

PAPER I **Jovanović, R.**, and Dubé, M.A. Monitoring of butyl acrylate and vinyl acetate homo- and copolymerizations in toluene. Journal of Applied Polymer Science, accepted January 2001.

PAPER II **Jovanović, R.**, and Dubé, M.A. (2000) Butyl Acrylate/Vinyl Acetate Emulsion Polymerization: In-line Monitoring Using ATR-FTIR Spectroscopy, Macromolecules (to be submitted)

PAPER III **Jovanović, R.**, and M.A. Dubé (2000) Butyl Acrylate/Vinyl Acetate Latexes and Latex-Based Adhesives Properties, (to be submitted)

In **PAPER I,** the results obtained for a series of solution homo- and copolymerizations of butyl acrylate and vinyl acetate in toluene are presented. The results include: 1. The characterization of BA and VAc homo- and copolymerizations in toluene for kinetics, solvent effects, copolymer composition, average molecular weights and molecular weight distribution. 2. Establishment of ATR-FTIR spectroscopy as an off-line reaction monitoring technique including absorbance peak selection and assignment procedures, and the use of characteristic peaks for off-line polymerization monitoring. 3. The evaluation of ATR-FTIR spectroscopy as an off-line monitoring method in comparison to standard ^{1}H-NMR spectrometry and gravimetric techniques. 4. Modelling of the effect of solvent on the copolymerization kinetics.

In **PAPER II,** the results obtained for a series of BA/VAc emulsion polymerizations are presented. The results include: 1. The characterization of BA/VAc emulsion polymerizations. 2. The establishment of ATR-FTIR as an in-line polymerization monitoring technique, including absorbance peak selection and assignments, and the use of real-time peak profiles for in-line polymerization monitoring. 3. The advantages and disadvantages of using ATR-FTIR spectroscopy as an in-line monitoring technique for these systems.

PAPER III is an extension to PAPER II. The polymers obtained in the emulsion polymerization experiments are further characterized for final performance properties. The following results are presented: 1. The rheological properties of latexes including viscosity, and particle size and distribution. 2. The dynamic mechanical properties of the copolymer films. 3. The adhesive properties of the latexes including the tensile and shear strengths of the adhesive bond. 4. An attempt to establish structure-property relationships for synthesized polymers.

The results of this project were also presented as the following refereed conference presentations:

1. **Jovanović, R.**, and Dubé, M.A. (2000) In-line monitoring of butyl acrylate/vinyl acetate copolymerizations. 50th Canadian Chemical Engineering Conference, Montreal, QC, Oct 15-18.
2. **Jovanović, R.**, Hua, H., and Dubé, M.A. (2000) Multicomponent polymerization monitoring using an MIR probe. 13th Canadian High Polymer Forum, Aylmer, QC, Aug 13-16 (oral presentation).
3. **Jovanović, R.**, Hua, H., and Dubé, M.A. (2000) Multicomponent polymerization monitoring using an MIR probe. 13th Canadian High Polymer Forum, Aylmer, QC, Aug 13-16 (poster presentation).
4. Dubé, M.A. Hua, H., and **Jovanović, R.**, (2000) In-line monitoring of emulsion polymerization. Polymer Reaction Engineering IV, Palm Coast, FL, March 19-24.

Chapter 2

THEORY

In this section, the fundamentals of polymerization processes are described. It is a guide to the homogenous and heterogeneous polymerizations of butyl acrylate and vinyl acetate monomers. Next, various reaction monitoring techniques are described with emphasis on Attenuated Total Reflection-Fourier Transform Infrared spectroscopy for monitoring conversion and copolymer composition. Finally, the basics of adhesive bonding and adhesive bond testing are presented. This information is necessary to the understanding of the scope of this project and the conclusions that were reached.

Basic definitions. *Polymers* are built up by linking together a large number of small molecular compounds called *monomers* through a chemical reaction termed *polymerization*. There are several classifications of polymers and polymerization reactions. Homo-, co- and terpolymer denote polymer consisting of one, two and three types of repeating units, respectively. According to the polymerization mechanism, there are two classes of polymerization reactions: step growth polymerizations (usually involving the existence of functional groups on the monomer and the elimination of small molecules) and chain growth polymerizations (involving the existence of unsaturated carbon bonds on the monomer(s)). A subclass of chain growth polymerization, free radical polymerization, is of interest in this study. Free radical polymerizations are conventionally divided into two groups: *homogenous* and *heterogeneous* polymerizations, according to the number of phases that exist. These reactions can be performed in batch, semi-batch or continuous reactors.

2.1 Homogeneous Free Radical Polymerization

Homogenous free radical polymerizations include bulk and solution polymerizations. The following are typical free radical copolymerization reactions.[1]

Initiation: This is the first step in a polymerization reaction and it involves the creation of highly reactive free radicals. The initiator, I, undergoes a homolytic decomposition. Two identical free radicals ($R^\bullet$) called primary radicals, are formed according to the following reaction scheme

$$I \xrightarrow{k_d} 2\,R^\bullet \tag{1}$$

where k_d is a temperature dependent rate constant for initiator decomposition. The decomposition can be thermally, chemically or radiation induced and it has an efficiency, f.

A free radical can add to monomer 1 or 2, M_j.

$$\begin{aligned} R^\bullet + M_1 &\xrightarrow{k_{p1}} R^\bullet_{1,1} \\ R^\bullet + M_2 &\xrightarrow{k_{p2}} R^\bullet_{1,2} \end{aligned} \tag{2}$$

$R^\bullet_{r,j}$ denotes a radical of chain length r ending in monomer unit j, and k_{pj} denotes the propagation rate for the addition of monomer j to an initiator fragment.

The rate of initiation, R_I, is given as:

$$R_I = 2fk_d[I] \tag{3}$$

Propagation: In this step, polymer chains continue to grow by addition of monomer. The possible propagation reactions for a copolymerization case are given as:

$$\begin{aligned} R^\bullet_{r,1} + M_1 &\xrightarrow{k_{p11}} R^\bullet_{r+1,1} \\ R^\bullet_{r,1} + M_2 &\xrightarrow{k_{p12}} R^\bullet_{r+1,2} \\ R^\bullet_{r,2} + M_1 &\xrightarrow{k_{p21}} R^\bullet_{r+1,1} \\ R^\bullet_{r,2} + M_2 &\xrightarrow{k_{p22}} R^\bullet_{r+1,2} \end{aligned} \tag{4}$$

where k_{pij} denotes the rate constant of addition of monomer j to the radical ending with monomer unit i. $R^{\bullet}_{r+1,j}$ denotes a radical of chain length $r + 1$ ending with monomer unit j. When modeling the propagation step, the reactivity of a radical center is of importance. The terminal model considers that the reactivity of the radical center is dependent only upon the last monomer unit bound in the polymer chain whereas the penultimate model assumes that the two last monomer units bound into the polymer chain affect the reactivity of a radical center.

The rate of polymerization, R_p, is given as

$$R_p = k_p[M^{\bullet}][M] \tag{5}$$

where k_p is the propagation rate constant, $[M^{\bullet}]$ is the total concentration of all chain radicals and $[M]$ is the monomer concentration. One characteristic of the propagation step for multicomponent polymerizations is the difference in the tendency of monomers to enter the polymer chain. The reactivity ratios are used to represent the reactivity of radicals ending in monomer unit 1 toward monomer 1 or monomer 2 in the reaction mixture. If $r_1>1$ then homopolymeric growth is preferred. On the other hand, heteropolymeric growth is preferred when $r_1<1$.

$$r_1 = \frac{k_{p11}}{k_{p12}} \qquad r_2 = \frac{k_{p22}}{k_{p21}} \tag{6}$$

The greater the difference in the reactivity ratios, the greater the possibility of composition drift. Composition drift is the change in chemical composition of the polymer formed throughout the reaction. This is the case in BA/VAc batch copolymerizations because r_{BA}=5.93 and r_{VAc}=0.026.[2] Thus, the copolymer formed will be richer in BA at the beginning of the reaction while near the end, more VAc will be incorporated into the copolymer.

Termination: Termination may occur via two different chemical processes. The first, termed termination by *combination*, involves two unpaired free radicals forming a paired electron bond; the result is one dead polymer chain:

$$R_m^\bullet + R_n^\bullet \xrightarrow{k_{tc}} P_{m+n} \tag{7}$$

where $R_m^\bullet$ and $R_n^\bullet$ denote growing polymer chains size of m and n respectively, P denotes a dead polymer chain of length $m+n$ and k_{tc} is the termination by combination rate constant. The second termination reaction involves atom (usually hydrogen) abstraction and is known as termination by *disproportionation*. The result is the formation of two dead polymer chains, P_m and P_n, one of which is terminally unsaturated. This terminal unsaturation is a potential reactive site.

$$R_m^\bullet + R_n^\bullet \xrightarrow{k_{td}} P_m + P_n \tag{8}$$

k_{td} denotes the termination by disproportionation rate constant. Even though the energy barrier to this reaction makes it less likely than the disproportionation reaction in the case of VAc monomer, there are considerable numbers of these reactions occurring. The result is a large number of branched polymer chains.

The rate of termination, R_t, is given as

$$R_t = k_t[R^\bullet]^2 \tag{9}$$

"Termination rate constant" is a misnomer because the "constant" changes with the viscosity of the reaction medium, i.e. it is diffusion-controlled. There are three diffusion-controlled intervals during the course of a polymerization depending on the viscosity of the reaction medium. The first interval is called segmental-diffusion control. The low viscosity environment at conversions up to 15% enables two macroradical chains to move and terminate easily. The next interval, translational diffusion control, occurs in the medium viscosity range at conversions ranging from

15 to ~85%. The translational movements of chains are restricted and termination is possible due to the movement of chain segments that bear a radical at the end. At the final stages of the reaction, the viscosity is so high that the chains can hardly move. Thus, the approach of two reactive centers can only be accomplished by the addition of monomer. This is known as reaction-diffusion control. The termination rate constant under high conversion is one of the subjects of active research in polymer reaction kinetics and modeling. Successful modeling of free radical polymerizations requires successful modeling of these three diffusion-controlled intervals. When modeling an emulsion polymerization, it should be noted that, due to the high viscosity in the main locus of polymerization (i.e. the particles), the rates of termination and propagation might be diffusion-controlled even at low conversion levels.

Chain transfer reactions: Atom transfer or atom abstraction reactions with subsequent propagation of the new radical species are called chain-transfer reactions. These involve transfer to initiator, monomer, chain transfer agent (a deliberately added substance to induce the transfer in order to control molecular weight), solvent or polymer. These are represented with the general reaction scheme:

$$RM_n^{\bullet} + X \xrightarrow{k_{tr,x}} P_n + X^{\bullet} \tag{10}$$

where X can be the initiator, monomer, polymer, solvent or chain transfer agent and $k_{tr,x}$ is the chain transfer rate constant. The transferred radical may or may not to continue to react.

$$X^{\bullet} + M_i \xrightarrow{k_p^i} R_{i,t}^{\bullet} \tag{11}$$

The most prevalent form of chain transfer, in the absence of chain transfer agent, is transfer to monomer. VAc is one of the monomers where considerable chain transfer to monomer and polymer occurs. Acrylates are also among the monomers prone to chain transfer to polymer. When chain transfer to polymer occurs, the fraction of branched chains increases. The chain

transfer reactions may not greatly affect the overall rate of polymerization, but they are dominant in controlling the molecular weight.

The equation for the rate of polymerization (Equation (5)) can be rearranged into a more useful expression by using a steady-state assumption (i.e. the concentration of radicals reaches a steady-state almost instantaneously) and by incorporating the rate of initiation:

$$R_p = \frac{k_p}{k_t^{1/2}}[M](fk_d[I])^{1/2} \tag{12}$$

The term $\frac{k_p}{k_t^{1/2}}$ is a lumped constant and it can be obtained directly from experimental measurements using Equation 12. The absolute values of the rate constants can only be obtained using sophisticated techniques such as pulsed laser polymerization. However, systems where both rate constants are considerably high, such as VAc and BA, are difficult to study using pulsed laser polymerization.[3]

The free radical polymerization mechanism does not change in the presence of solvent but the viscosity of the reaction mixture will decrease, leading to better heat transfer and mixing, and affecting the diffusion control of the reaction. The presence of solvent can also affect the kinetic parameters in the polymerization. VAc is a monomer that is affected by the presence of solvent to a great extent, whereas BA is less affected.[4] These effects include not only a propensity towards chain transfer reactions but an apparent effect on the lumped constant, $k_p/(k_t)^{1/2}$. It is, at present, unclear whether the propagation rate constant or the termination rate constant or both are affected because it is experimentally difficult to establish their absolute values. In a review on solvent effects in free radical polymerizations of different monomers, Coote and Davis[5] considered that the presence of solvent affects the propagation rate constant due to the formation of radical-solvent complexes which reduce the apparent k_p. On the other

hand, there is also an effect of solvent on k_t. Recent studies that involved VAc and BA homopolymerizations in toluene and ethyl acetate showed that the rate of reaction depends on the initial solvent concentration.[6,7,8] The effect of solvent on the lumped constant can be attributed to the chain length dependence of the termination rate constant.[9] Shorter chains will terminate more quickly than longer ones. For BA and VAc, chain transfer to solvent is high, therefore, many short chains are generated. The more solvent in the system, the higher the proportion of short chains and the higher the termination rate constant and the lower the lumped constant.[6,7,10]

2.2 Heterogeneous Free Radical Polymerization

Polymers can be obtained in heterogeneous reactions such as emulsion, suspension, dispersion or precipitation polymerizations. Conventional emulsion polymerization is of interest in this project.

The importance of emulsion polymerizations was recognized during the First World War during attempts to obtain synthetic rubber. In 1995, it was estimated that 30% of commercial polymers were produced by free radical polymerization and 40-50% of these were emulsion polymerizations.[11] The popularity of emulsion polymerizations is due to the following advantages. Emulsion polymerizations tend to have higher reaction rates compared to homogeneous polymerizations. In addition, their lower viscosity enables better heat transfer and mixing. Finally, the latex may be directly used (e.g. in architectural coatings, adhesives and sealants). On the other hand, if the latex is not used directly, cleanup and purification might be a tedious procedure due to the presence of many components.

A typical emulsion polymerization recipe includes the following components: water, monomer(s), initiator(s), and emulsifier(s). Buffer and chain transfer agent are usually added. *Water* is a main ingredient: It acts to maintaining low viscosity and good heat transfer. In addition, it isolates the polymerization loci. Termed as compartmentalization, it is one of the greatest advantages of emulsion versus bulk or solution polymerization in terms of the ability to adjust the polymerization rate. It is also a medium for the transfer of various reactive species between the phases. *Monomers* are vinyl type (e.g. styrene, acrylonitrile, vinyl acetate) or disubstituted vinyls (e.g. acrylates, methacrylates). *Initiators* in conventional emulsion polymerization are water-soluble (e.g. potassium or ammonium peroxodisulfate are usually employed). The formation of $SO_4^{-\bullet}$ radicals has a high activation energy so these initiators are usually employed at temperatures above 50°C.

$$S_2O_8^{2-} \xrightarrow{\Delta} 2SO_4^{-\bullet} \tag{13}$$

Sulfate radicals can react with water to produce HSO_4^- which alters the pH.

$$SO_4^{-\bullet} + H_2O \longrightarrow HSO_4^- + HO^\bullet \tag{14}$$

This can considerably reduce the initiator efficiency if the pH <3. The increased acidity catalyses the hydrolysis of VAc and BA. The hydrolysis of poly(vinyl acetate) produces acetic acid while the hydrolysis of poly(butyl acrylate) forms poly(acrylic acid) and butanol. The small molecules can act as plasticizers in dry polymer film. For adhesives applications this can be highly undesirable.[12] Therefore, a *buffer* (e.g. $CaCO_3$, $NaHCO_3$ or Na_2CO_3) is usually employed to obtain latex with a neutral pH. This ensures that latex with minimum hydrolysis can be obtained. *Emulsifiers* (a.k.a. surfactants) are used to impart colloidal stability to the latex particles. There are three types of emulsifiers: electrostatic – to prevent coagulation by electrostatic repulsion, polymeric (steric) – to prevent coagulation by entropic repulsion, and electrosteric – a

combination of the previous two. Because of use of poly(vinyl alcohol), PVOH, in this project, it is described in more detail.

PVOH is produced by the hydrolysis of poly(vinyl acetate). Its properties depend on its degree of hydrolysis and molecular weight. It is usually employed as emulsifier in VAc emulsions polymerizations. The current understanding of steric stabilization lags behind that of electrostatic stabilization. As opposed to its role in particle stabilization, the role of PVOH in particle nucleation has been mentioned only sporadically in the literature. According to O'Donnell at al.[13], there are no micelles formed in VAc emulsions stabilized with partially hydrolysed PVOH, but the PVOH does act as the main locus of nucleation. This suggestion was also accepted by Lepizzera and Hamielec[14], who studied seeded emulsion polymerization of VAc in the presence of PVOH. In both cases, a detailed mechanism for particle nucleation was not given. On the other hand, Gavat et al.[15] suggested that nucleation takes place within monomer microdroplets that are stabilized by PVOH.

Poly(vinyl acetate) emulsion protected with PVOH often have a combination of large particles and a rather wide particle size distribution (PSD).[16] The combination of particle sizes and PSD yields an emulsion that does not change its viscosity considerably when it experiences high shear conditions. A comparison between PVOH and an ionic emulsifier is shown below:[17]

PVOH	**Ionic surfactant**
EMULSION PROPERTIES	
Large particle size	Fine particle size
Wide PSD	Narrow PSD
Strong wet tack	Poor wet tack
Good flow stability	Poor flow stability
Good machining	Relatively poor machining
Rapid setting	Relatively slow setting
Near-Newtonian rheology (does not shear thin)	Thixotropic behavior (thins with shear)

PVOH		Ionic surfactant
	FILM PROPERTIES	
Hazy film		Clear film
Flat film		Glossy film
Water sensitive		Water resistant

Other advantages of PVOH protection are the following: PVOH gives unique properties to emulsion stabilized with it. It enhances the adhesive properties of PVAc. PVOH-protected emulsions are easily modified to reinforce specific adhesive properties. Solvent and oil resistance are increased and creep is decreased.

The disadvantages of the use of PVOH are in the possibility of grafting to the formed polymer or promotion of the agglomeration of small particles.[18]

Other ingredients added to emulsions include components such as chain transfer agents for molecular weight control, and electrolytes to induce particle size monodispersity.

It is convenient to divide a conventional batch emulsion polymerization reaction into the three intervals summarized in Table 2.1.[11]

Table 2.1 Different stages of an emulsion polymerization reaction

Interval	Typical % conversion range	Micelles	Monomer droplets	Particle number	Particle size
I	0-10	Present	present	increases	increases
II	10-40	Absent	present	constant	increases
III	40-100	Absent	absent	constant	~ constant

Interval I - The emulsifier is dissolved in water at a concentration above the critical micellar concentration. An excess of emulsifier molecules aggregates together to form colloidal clusters – micelles. Monomer is dispersed in droplets (diameter = 0.1-1 mm) that serve as monomer reservoirs. Monomer diffuses from the droplets through the water phase into the micelles to

achieve a thermodynamic equilibrium. A small fraction of monomer is dissolved in the water phase. A schematic representation of interval I is given in Figure 2.1.

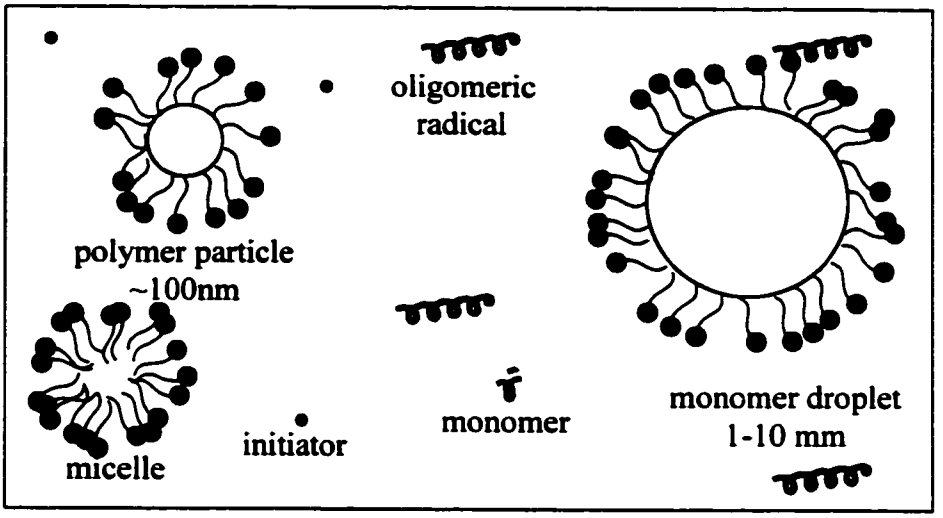

Figure 2.1 Schematic representation of interval I of emulsion polymerization stabilized by electrostatic emulsifier (e.g. sodium dodecyl sulphate)
(note: dimensions are not proportional)

Free radicals are generated in the water phase and can undergo several distinctive reactions in the water phase:

1. Radicals can add monomer molecules present in water phase according to reactions (2) and (4). It is considered that when the number of monomer units added is about 7 (note: this depends on monomer system), the oligomer becomes hydrophobic and enters the organic phase (i.e. polymer particle or micelle). By entering a micelle, it nucleates a new particle. This is known as heterogeneous or micellar nucleation. There is another type of nucleation termed homogeneous nucleation that occurs in the water phase. Its importance increases with the increase in the water solubility of monomers. Polymerization takes place almost exclusively in the interior of the

micelles because of their high monomer concentration and their high surface to volume ratio compared to the monomer droplets.[1]

2. Radicals can react with water-soluble impurities:

$$R^{\bullet}_{r,i} + WSI \xrightarrow{k_{zj}} P(WSI) \tag{15}$$

where *P(WSI)* is a dead molecule and k_{zj} is the rate constant for reaction of water-soluble impurity, *j*, with monomer *i*-ended radical. Water-soluble impurities (e.g. oxygen) may cause an induction period by consuming large amounts of radicals.

3. The radicals may terminate upon encountering another radical according to reactions 7 and 8.

4. The initiator fragments may recombine. The efficiency factor accounts for this phenomenon.

5. Radicals may be captured by monomer droplets. Droplet nucleation may occur under high shear (high rate of mixing).

6. Radicals can be desorbed from the polymer particles. This phenomenon is restricted to small molecules, usually as a result of chain transfer to monomer, monomer-soluble impurity or chain transfer agent.

7. Desorbed radicals may be resorbed into the polymer particle.

8. Radicals may be captured by micelles.

9. Radicals may be captured by particles.

The "fate" of radicals in the organic phase (e.g. when the radical is captured by polymer particles, micelles or monomer droplets) is the same as in the bulk and solution polymerizations. The radicals can undergo propagation (see equation 4), termination (see equations 7 and 8), or chain transfer reactions (see equations 10 and 11). The concept of diffusion-controlled rate constants applies here as well. During this interval, the particle size and the polymerization rate increase with time.

Interval II - After approximately 15% conversion of the initially charged monomer, micelles are exhausted. No new particles are generated. Monomer diffuses from the monomer droplets, through the aqueous phase and into the latex particles, to maintain saturation swelling and support the propagation reaction.[19]

Interval III - After approximately 40%-60% conversion, the monomer droplets disappear, at which point the polymerization rate tends to decrease as a result of the decrease in concentration of monomer inside the particles. During this stage, only the latex particles and the aqueous phase are present. The remaining monomer located in the latex particles is being consumed.

The number of polymer particles is the prime determinant of the rate of polymerization. The rate of polymerization, R_p, and the number-average degree of polymerization for emulsion polymerization, $\overline{X}_n$, are given by the following equations:

$$R_p = k_p[M]_p \bar{n} N / N_a \tag{16}$$

$$\overline{X}_n = k_p[M]_p \bar{n} N / R_I \tag{17}$$

where k_p is the propagation rate constant, $[M]_p$ is the monomer concentration inside the particle. $\bar{n}$ represents the average number of radicals per particle, N is the number of latex particles, N_a is Avogadro's number and R_I is the initiation rate. The greatest advantage of emulsion polymerization kinetics is the ability to simultaneously increase both the polymerization rate and the molecular weight of polymer which is not possible in bulk or solution polymerizations.

2.3 Free Radical Polymerization Modeling

Used either for process design, control and optimization or inference of unmeasured properties, models are valuable engineering tools. They serve as a pool of knowledge about a process and enhance process understanding. The objective in polymerization modeling is to create flexible models to simulate different homo-, co- and multicomponent polymerizations in bulk, solution or emulsion. In addition, these models should preferably simulate different reactor configurations (i.e. batch, semi-batch or continuous) and different temperature regimes such as isothermal or non-isothermal conditions. The basic reaction scheme given for homogeneous and heterogeneous polymerizations, mass and energy balance equations, and equations for molecular weight development are the basis for free radical polymerization modeling. Other practical aspects of free radical polymerization modeling summarized by Dubé et al.[20] and Gao and Penlidis[21,22] include the segmental diffusion control model,[23] the reaction diffusion control model,[24] parallel[25] or serial[26] approaches for the overall termination rate parameter, diffusion-controlled k_t and its chain length dependency[9,27] and diffusion-controlled initiator efficiency.[28] All these were incorporated into a comprehensive model developed by Gao and Penlidis[21] for bulk/solution free radical polymerization. This model was a basis for the first JAVA-based model for free radical polymerizations in bulk and solution developed by Badeen and Dubé.[29]

Apart from the work of Buback et al.[26,30] and Dubé et al.[31] there are no recent modeling data on butyl acrylate polymerization in bulk. Dubé and Penlidis[2] also modeled the BA co- and terpolymerizations with VAc and methyl methacrylate in emulsion.

In order to model the solvent effect, models with a variable lumped constant, $\frac{k_p}{k_t^{1/2}}$, for BA and VAc solution polymerizations were employed by Othman et al.,[10] McKenna et al.,[6] and McKenna and Villanueva[7]. Modeling of VAc polymerization in different reactor configurations can be found in Hamer and Ray,[32] Hamer et al.,[33] and Teymour and Ray.[34]

Due to their complex reaction mechanism and heterogeneous nature, modeling of emulsion polymerizations is challenging. In some advanced models, not only conversion, copolymer composition and molecular weight can be predicted but also sequence length distribution and particle size and distribution.[35,36] Very useful reviews on mathematical modeling of emulsion polymerizations are given by Penlidis et al.[35] and Dubé et al..[20] Use of a model for emulsion polymerization of BA and VAc emulsion copolymerizations were reported by Penlidis et al.,[35] Dubé and Penlidis,[2] and Othman et al.[10]

2.4 Free Radical Polymerization Monitoring

Ever increasing demands on product quality, process control and safety drive the development of new and improved polymerization monitoring techniques. The complex and viscous nature of polymerization reactions is the main obstacle to efficient monitoring. In addition, there are only limited numbers of variables that can be monitored. The polymerization monitoring techniques can be divided into three groups: off-line, on-line and in-line techniques.

Even though accurate, off-line techniques have long measurement delays which can impede effective process control. Sometimes, off-line monitoring requires sophisticated and expensive instrumentation such as ^{1}H-NMR spectrometers. On the other hand, on-line monitoring techniques are fast enough to enable continuous monitoring but they require the

removal of defined amounts of sample through a sampling loop. Due to the shear sensitivity of emulsion polymerization reaction mixtures this might present a serious challenge. Phase separation or polymer build up inside the sampling loop can seriously hamper continuous monitoring. In-line monitoring is preferable: *in situ* monitoring of the reactor contents using a hardware sensor.

There are several variables of interest for continuous monitoring. These are conversion and copolymer composition, molecular weight, and in the case of emulsion polymerization, particle size. In one of the first reviews on polymerization monitoring techniques, Chien and Penlidis[37] predicted that many of the techniques they reported as off-line techniques could be soon used on-line. In reviews on the monitoring techniques given by Hergeth,[38] Shork[39] and Kammona et al.[40] some of the up-to-date monitoring techniques are evaluated. For conversion and copolymer composition on-line and in-line monitoring, the following techniques can be used: densitometry, gas chromatography, calorimetry/energy balance, ultrasound and different spectroscopic techniques (fluorescence, near and mid infrared, and Raman spectroscopy). On-line molecular weight monitoring can be accomplished using viscometry and gel permeation chromatrography. For on-line particle size monitoring, dynamic light scattering, turbidimetry or size exclusion chromatography can be employed. Below, some conversion and copolymer composition monitoring techniques are discussed.

Densitometry is based on density differences between monomer and polymer. As the polymerization proceeds, the density difference leads to an increase in density of the reaction mixture and to an overall shrinkage of its volume. Both changes can be measured continuously on-line and conversion can be calculated at any time knowing the amount of ingredients initially

charged.[41] The disadvantages of this method are the existence of a sampling loop and its associated problems described earlier and possible temperature control difficulties.

Gas chromatography can be employed on-line for the determination of residual monomer[42] or as an in-line monitoring technique when used for analysis of the gas in the head space of a polymerization reactor.[43] The disadvantage in the first case is related to the use of a sample loop and in the second case, the need to account for monomer partitioning between the various phases in the reaction mixture.

Changes in temperature or heat flux during the course of a polymerization are the basis for *calorimetry/energy balances* as a monitoring technique.[44] It is a relatively simple method but suffers from problems related to noise in the calorimetric measurements.

Ultrasound propagation velocity as a monitoring technique is receiving increasing attention.[45] It is based on measuring the velocity of a high-frequency sound wave passing through the sample. It is employed as an in-line technique.

The basis for *fluorescence spectroscopy* is the emission of electromagnetic radiation when an electronically excited state species returns to its ground state. It has been used to monitor photocuring of acrylic monomers.[46]

2.4.1 Infrared (IR) Spectroscopy for Polymerization Monitoring

Among the techniques that are increasingly used for conversion and copolymer composition monitoring are *infrared spectroscopic techniques.* The basis of infrared spectroscopy is the absorption of infrared radiation by a molecule. The absorption of infrared radiation corresponds to energy changes on the order of 8-40 kJ/mole. Radiation in this energy

range corresponds to the range encompassing the stretching and bending vibrational frequencies of the bonds in most covalent molecules.[47] Since every type of bond has a different natural frequency of vibration, and since two of the same type of bond in two different compounds are in two slightly different environments, no two molecules of different structure have exactly the same infrared absorption spectrum.[48] The basis for employment of IR spectroscopy in quantitative analysis thus, in reaction monitoring, is the Beer-Lambert law, where absorbance of the component is proportional to its concentration. Absorbance can be measured as peak height, peak height ratio, peak area or peak area ratio.

There are different IR spectroscopic instruments currently in use.[48] Multiplex IR instrumentation is commonly employed. A multiplex optical device, such as the Michelson interferometer, measures spectral information about the intensities at individual frequencies while measuring the intensities of all frequencies simultaneously. Fourier transform infrared spectroscopy uses the Michelson interferometer. The most important properties of multiplexing are higher signal-to-noise ratios, rapid scanning, accurate wavelength measurements due to calibration with an internal laser and high energy throughput because no slits are required.

The quality of IR spectra does not depend only on the instrumentation used but also on sampling methods. The selection of the sampling method (e.g. transmission, internal reflection etc.) depends on the sample properties of interest. The transmission FTIR method is usually applied to the characterization of solid polymer samples, thin films obtained by solvent casting or polymer powders. Internal reflection spectroscopy (a.k.a. attenuated total reflection, ATR) is used for the analysis of polymer samples with low transmission (i.e. liquids and semisolids).[49] Therefore, the ATR-FTIR sampling method has been found to be potentially suitable for monitoring polymerization reactions. ATR-FTIR is a contact sampling method that involves a

crystal with a high refractive index and low IR absorption in the IR region of interest. The infrared beam enters the crystal at an angle, which exceeds the critical angle for total internal reflection. The infrared beam can reflect several times (multireflection ATR) before it leaves the crystal. Once inside the crystal, a standing wave of radiation is set up, called an evanescent wave. A unique property of the evanescent wave is that it is slightly bigger than the crystal, allowing it to penetrate a small distance into the sample. This distance is called the depth of penetration, DP, and it is analogous to the path length in transmission sampling techniques. DP is defined as the depth at which the evanescent wave is attenuated to 36.8% of its initial value and is given by the following equation:[50]

$$DP = \frac{1}{2\pi W N_c (\sin^2 \Theta - N_{sc}^2)^{1/2}} \tag{25}$$

where W is the wavenumber, N_c and N_{sc} are the crystal refractive index and ratio between the sample and crystal refractive indices, respectively, and Θ is the angle of incidence. It can be seen that the absorption intensity at a certain frequency is proportional to the wavenumber for constant N_c, N_{sc} and Θ. As a consequence, the peaks are more intense at low wavenumber than at high wavenumber since the low wavenumber radiation penetrates further into the sample. Software is available to perform the calculation on the ATR spectra that will remove this dependence. The selection of the ATR crystal (e.g. germanium, zinc selenide, diamond) depends on the IR region of interest.

Spectroscopic techniques based on near (14000-4000 cm^{-1}) and mid (4000-600 cm^{-1}) infrared ranges are used increasingly in reaction monitoring. Both techniques are employed in-line and offer structural and kinetic information. In NIR spectroscopy, most absorbances are overtones or combinations of bands of fundamental vibrations. Thus, they are typically weaker than MIR absorbances. NIR spectroscopy was used to monitor solution homo-and

copolymerization of styrene and isoprene at low conversion levels.[51] NIR spectroscopy was also employed to monitor bulk polymerization of methyl methacrylate[52] and styrene/methyl methacrylate semi-batch copolymerization.[53] Wu et al.[54] employed NIR spectroscopy for styrene emulsion polymerization.

The MIR range is richer in information than the NIR range and absorbances are the result of fundamental vibrations; thus, well-defined (i.e. strong, sharp) absorbance peaks are the result. In-house built instruments using MIR spectroscopy were employed by Mijovic et al.[55] and Chatzi et al.[56] for conversion and copolymer composition monitoring. A commercially available instrument, the ReactIR™ 1000 (ASI Applied Systems Inc.) based on ATR-FTIR (Attenuated Total Reflectance – Fourier Transform Infrared) spectroscopy was used by Full et al. (1995)[57] for monitoring tetrahydrofurfuryl methacrylate microemulsions. The same instrument was employed for monitoring living carbocationic polymerization of isobutylene,[58-61] the free radical polymerization of styrene[62] and an ester-exchange polymerization mechanism.[63]

2.5 Latex-Based Adhesives

Adhesive is one application where latex is used "as is" (i.e. no further purification or polymer isolation). Poly(vinyl acetate), PVAc, latexes are mainly used as non-structural adhesives, for bonding substrates such as wood and paper or for temporary bonding (pressure sensitive films).[12] PVAc emulsions have an exceptionally good adhesion to porous surfaces (wood, paper, leather).[13] There are four theories describing the process of adhesion: mechanical interlocking theory, diffusion theory, electronic theory and adsorption/specific adhesion theory.[64] A mechanical interlock is formed between polymer and porous wood fibers when an adhesive

spreads, penetrates and wets a wood surface. However, in many cases, good adhesion can be obtained between perfectly smooth surfaces, indicating that this theory might not be widely applicable. This contribution is not easily isolated and measured.[65] Diffusion theory states that the intrinsic adhesion of an adhesive to a substrate is due to mutual diffusion of polymer molecules across their interface. This suggests that the macromolecules of both the adhesive and substrate (wood), or chain segments of them, possess sufficient mobility and are mutually soluble. This theory was criticized by Anand et al.,[66] who suggested that the dependence of the bonded joint's strength on time of contact and polymer molecular weight can be explained by the effect of wetting of the substrate surface. The authors suggested that the increase in bonded joint strengths is due to an increasing degree of interfacial contact and that the mechanism of adhesion depends instead on the formation of secondary Van der Waals and hydrogen forces across the interface of the adhesive and wood. Electronic theory, which proposes the occurrence of electron transfer upon contact of the two surfaces, is the most criticized adhesion theory. Pizzi[64] stated that there was no experimental evidence for the existence of this contributory factor in wood adhesion. Thus, this theory is not applicable in wood adhesion. Adsorption theory states that an adhesive will adhere to a substrate because of the inter- and intramolecular forces between the atoms and molecules of the two materials. This is the most widely accepted and applicable theory of adhesion. In wood adhesion, primary bonds (e.g. covalent, ionic, coordinate) as well as secondary bonds (i.e. van der Waals, hydrogen bonds, electrostatic interactions) are present. Some authors distinguish between these two and introduce the covalent bonding theory as an additional theory in wood adhesives. High solid contents (~50 wt%) and relatively low viscosity of PVAc-based adhesives enables easy application (i.e. by roller, spray or brush) and rapid-setting. In addition, high bond strength, a colorless bond line and less environmental hazards

than solvent-based adhesives are among their characteristics.[12] As a saturated molecule, PVAc is resistant to oxygen, microorganisms and UV radiation.[16] On the other hand, these adhesives are not suitable for applications requiring sustained resistance to high temperatures or elevated moisture level due to their thermoplastic nature. They are also unsuitable for joints that are under a continuous load. Major changes can be made to the adhesive properties of PVAc by copolymerization (e.g with BA, ethylene or others), changing the polymerization method (e.g. to batch or semi-batch), changing the emulsifier (e.g. to ionic or polymeric emulsifiers), modifying the degree of branching, or by adding a variety of functional groups. The high temperature sensitivity, for example, can be improved by copolymerization, high molecular weight development and the employment of PVOH as emulsifier.[12]

The investigation of adhesive properties includes inherent polymer properties such as copolymer composition, molecular weight and distribution, particle size and distribution, viscosity, dynamic mechanical properties, and thermal stability. In addition, the characterization includes testing of performance properties such as the durability of the adhesive bond under different stress conditions (e.g. tension, shear, impact, fatigue, torsion, compression etc.) or under different chemical (i.e. organic solvents, acids and basis) or environmental factors (e.g. exposure to light, moisture, oxidation). Thermal and biological stability can also be assessed.[67]

2.5.1 Characterization of Inherent Adhesive Polymer Properties

A standard technique for the determination of *copolymer composition* is ^{1}H-NMR spectroscopy. Determination of BA/VAc copolymers using this technique is described by Dubé and Penlidis.[68] Other techniques can also be employed. A detailed description of these can be

found in part 2.4: monitoring of free radical polymerizations. Related to adhesive performance properties, the introduction of BA units to a PVAc chain increases the flexibility of the chain because the bulky butyl side groups allow greater intermolecular movement and also separates the polymer chains so that they can slip past one another easily.[16] This chain flexibility is necessary for good adhesion.

Molecular weight and molecular weight distribution (MW and MWD) can be assessed using gel permeation chromatography, a separation technique based on the hydrodynamic volume of the molecules in solution. MW and MWD contribute to tensile strength, toughness, and flexibility of PVAc-based adhesives. The branching that usually occurs during VAc polymerization increases the tensile strength, toughness and heat resistance of the adhesive.[16] The MWD of BA/VAc copolymers, obtained in a batch emulsion polymerization has been found to depend slightly on the BA content.[69]

Particle size and distribution can be determined using different techniques (e.g. light scattering, small angle X-ray scattering, centrifuge methods). PVAc-based emulsions intended for use as wood adhesives have a relatively large particle size (0.3-5 μm[12]). The average particle size of batch BA/VAc copolymer latexes is independent of copolymer composition, which is not the case for semi-batch produced copolymers. In a batch process, due to the reactivity ratio difference, the latex particles are comprised of a PBA-rich core and a PVAc-rich shell.[69] The same authors found that surface morphology and film formation of BA/VAc latexes depends on BA content in the particle.

Dynamic mechanical measurements are the most powerful methods for studying the mechanical behavior of polymer films under small strains in the so-called linear viscoelastic regime. Dynamic mechanical analysis is increasingly applied to latex films.[70] In a dynamic

experiment, a sinusoidally varying strain is applied to a sample, and the resulting stress, which also oscillates sinusoidally, is determined. From the stress and strain, the dynamic modulus of the sample is evaluated. It consists of two parts, the storage modulus, E', which is proportional to the maximum deformation energy per unit volume stored during one oscillation, and the loss modulus, E'', which is proportional to the dissipated energy (i.e. energy loss). Two basic geometries can be used for these measurements: longitudinal extension or parallel plate geometry. The dependence of modulus on temperature at constant frequency or dependence of modulus on frequency at various temperatures can be determined. In the latter case, a master curve at the reference temperature can be evaluated. The polymerization mode (batch or semi-batch) can influence the dynamic mechanical behavior of BA/VAc latex films. The heterogeneity of BA/VAc copolymers in the batch mode has been confirmed by the existence of two glass transition temperatures (determined form the peaks of E'' vs. temperature curve).[69,71] The modulus of BA/VAc copolymers change with composition and molecular weight.[12]

2.5.2 Performance Properties of Latex-Based Adhesives

Performance tests are conducted for a variety of reasons. For example:

1. To choose among materials or processes;
2. To monitor the quality of a product;
3. To confirm the effectiveness of a bonding process ;
4. To investigate parameters or process variables that may lead to measured differences in the performance of a bond.

End-use tests (i.e. tensile or shear tests) are those which try to simulate the type of loading and service conditions to which a joint will be subjected. These tests are relatively straightforward but their correlation to inherent polymer properties is not.[67] There are a number of standard tests for adhesives specified by the American Society for Testing and Materials (ASTM) as well as other organizations. These standardized tests can be used to compare the strength of various adhesives and to isolate and quantitatively define the variables that ultimately determine the performance of a joint. On the other hand, the results of a standard test can be different from test results of an actual joint in service due to, for example, differences in stress loading (usually more complex in practice then in standard testing) or environmental aging which is always more severe under service conditions (laboratory tests usually "accelerate aging" in order to complete the testing in a reasonable time). Thus, the most reliable test is to measure the strength of an actual assembly under actual operating conditions. Unfortunately, these tests are often expensive and impractical.[67]

In the tension test (ASTM D 897), an adhesive joint is subjected to forces acting perpendicular to the plane of the joint. The results are reported as the tensile strength of the adhesive. Pizzi[64] has found that on beech strips, in tension, PVAc can easily reach strength of 7500 N due to the thermoplastic nature of the PVAc polymer. In a shear test (i.e. see ASTM- D 905), the forces are acting in the plane of the adhesive joint. The results are reported as shear stress at failure. Pure shear is seldom encountered in adhesive assemblies and substantial tension components are usually found.[67] These two tests are among the ASTM recommended tests for the standard specification of PVAc based emulsion adhesives (ASTM D 4317).

2.6 Literature

1. G. Odian, *Principles of Polymerization*, 2nd ed., John Wiley & Sons, New York, 1981
2. M.A. Dubé and A. Penlidis, *Polymer International*, **37**, 23 (1995)
3. R.A. Hutchinson, J.R. Richardson, and M.T. Aronson, *Macromolecules*, **27**, 4530 (1994)
4. G.E. Ham, *Vinyl Polymerization*, Vol. 1 and 2, Marcel Dekker Inc., New York 1967
5. M.L. Coote, T.P. Davis, B. Klumperman, and M.J. Monteiro, *Journal of Macromol. Sci. - Rev. Macromol. Chem. Phys.*, **C38**(4), 567 (1998)
6. T.F. McKenna, A. Villanueva, and A.M. Santos, *J. Polym. Sci.: Part A: Polym. Chem.*, **37**, 571 (1999)
7. T.F. McKenna and A. Villanueva, *J. Polym. Sci.: Part A: Polym. Chem.*, **37**, 589 (1999)
8. M. Fernandez-Garcia, M. Fernandez-Sanz, and E. Lopez Madruga, *Macromol. Chem. Phys.*, **201**(14), 1840 (2000)
9. G.T. Russell, R.G. Gilbert, and D.H. Napper, *Macromolecules*, **25**, 2459 (1992)
10. S. Othman, I. Barudio, G. Fevotte, and T.F. McKenna, *Polym. Reac. Eng.*, 7(1), 1 (1999)
11. R.G. Gilbert, *Emulsion Polymerization: A Mechanistic Approach*, Academic Press, London, 1995
12. T.M. Goulding, in *Wood Adhesives: Chemistry and Technology*, A. Pizzi, Marcel Dekker, Inc., New York, 1983
13. J.T. O'Donnell, R.B. Mesrobian, and A.E. Woodward, *J. Polym. Sci.*, **XXVIII**, 171 (1958)
14. S.M. Lepizzera and A.E. Hamielec, Macromol.Chem. Phys., **195**, 3103 (1994)
15. I. Gavat, V.Dimone, D. Donescu, C. Hagiopol, M. Munteanu, K. Gosa and T. Deleanu, J. Polym. Sci.: Polym. Symp., 64, 125 (1978)
16. H.J. Jaffe, F.M. Rosenblum and W. Daniels, in *Handbook of Adhesives*, 3rd ed., I. Skeist, Van Nostrand Reinhold, New York, 1990
17. H.J. Jaffe and F.M. Rosenblum, in *Handbook of Adhesives*, 3rd ed., I. Skeist, Van Nostrand Reinhold, New York, 1990
18. D.C. Blackley, *Polymer Latices: Science and Technology*, Vol.2, Chapman & Hall, London. 1997
19. P. Rempp and E.W. Merrill, *Polymer Synthesis*, Huethig & Wepf Verlag, Basel, 1986
20. M.A. Dubé, J.B.P. Soares, A. Penlidis, and A.E. Hamielec, *Ind. Eng. Chem. Res.*, **36**, 966. (1997)
21. J. Gao and A. Penlidis, *J. Macromol. Sci. - Rew. Macromol. Chem. Phys.*, **C36**(2), 199 (1996)
22. J. Gao and A. Penlidis, *J. Macromol. Sci. - Rew. Macromol. Chem. Phys.*, **C38**(4), 653 (1998)
23. K. Mahabdi and K.F. O'Driscoll, *J. Polym. Sci., Polym. Chem. Ed.*, **15**, 283 (1977)
24. M. Stickler, D. Panke, and A.E. Hamielec, *J. Polym. Sci., Polym. Chem. Ed.*, **22**, 2243 (1984)
25. W.Y. Chiu, G.M. Carratt, and D.S. Soong, *Macromoleucles*, **16**, 348 (1983)
26. M. Buback, B. Degener, and B. Huckestein, *Makromol. Chem. Rapid. Commun.*, **10**, 311 (1989)
27. M. Kammachi, *Makromol. Chem. Suppl.*, **14**, 17 (1985)
28. S. Zhu, Y. Tian, A.E. Hamielec, and D.R. Eaton, *Macromolecules*, **23**, 1144 (1990)
29. C. Badeen, MASc thesis, Department of Chemical Engineering, University of Ottawa, 2000

30. M. Buback, *Makromol. Chem.*, **191**, 1575 (1990)
31. M.A. Dubé, K. Rilling, and A. Penlidis, *J. Appl. Polym. Sci.*, **43**, 2137 (1991)
32. J.W. Hamer and W.H. Ray, *Chem. Eng. Sci.*, **41**(12), 3095 (1986)
33. J.W. Hamer, T.A. Akramov, and W.H. Ray, *Chem. Eng. Sci.*, **36**(12), 1897 (1981)
34. F. Teymour and W.H. Ray, *Chem. Eng. Sci.*, **44**, 1967 (1989)
35. A. Penlidis, J.F. MacGregor, and A.E. Hamielec, *AIChE J.*, **31**(6), 881 (1985)
36. A. Urretabizkaia, G. Arzamendi, and J.M. Asua, *Chem. Eng. Sci.*, **47**(9-11), 2579 (1992)
37. D.C.H. Chien and A. Penlidis, *J. Macromol. Sci. – Rev. Macromol. Chem. Phys.*, **C30**, 1 (1990)
38. W.D. Hergerth, in *Polymeric Dispersions: Principles and Applications*, J.M. Asua, NATO ASI Series, Kluwer Academic Publishers, Dordrecht, 1996
39. F.J. Schork, in *Emulsion Polymerization and Emulsion Polymers*, P.A. Lowel and M.S. El-Aasser, John Wiley & Sons, Chichester, 1997
40. O. Kammona, E.G. Chatzi, and C. Kiparissides, *J. Macromol. Sci. -Rev. Macromol. Chem. Phys.*, **C39**(1), 57 (1999)
41. F.J. Schork and W.H. Ray, *J. Appl. Polym. Sci.*, **34**, 1259 (1987)
42. A. Urretabizkaia, J.R. Leiza, and J.M. Asua, *AIChE J.*, **40**, 1850 (1994)
43. M. Alonso, M. Alivers, L. Puigjaner, and M. Recasens, *Ind. Eng. Chem. Res.*, **26**, 65 (1987)
44. P. Guinot, N. Othman, G. Fevotte, and T.F. McKenna, *Polym. Reac. Eng.*, **8**(2), 115 (2000)
45. G. Storti, A.K. Hipp, and M. Morbidelli, *Polym. Reac. Eng.*, **8**(1), 77 (2000)
46. O. Valdes-Aguilera, C.P. Pathak, and D.C. Neckers, *Macromolecules*, **23**, 689 (1990)
47. D.L. Pavia and G.M. Lampman, *Introduction to spectroscopy: a guide for students of organic chemistry*, 2nd ed., Harcourt Brace College Publishers, Forth Wort, 1996
48. J.L. Koenig, *Spectroscopy of polymers*, 2nd ed., Elsevier, Amsterdam, 1999
49. B.C. Smith, *Fundamentals of Fourier Transform Infrared Spectroscopy*, CRC Press, Boca Raton, 1996
50. N.B. Colthup. L.H. Daly, and S.E. Wiberley, *Introduction to Infrared and Raman Spectroscopy*, Academic Press, Inc., Boston, 1990
51. T.E. Long, H.Y. Liu, B.A. Schell, D.M. Teegarden, and D.S. Urez, *ACS Symp. Ser.*, **71**, 146 (1994)
52. P.K. Aldridge, D.H. Burns, J.J. Kelly, and J.B. Callis, *Process Control Qual.*, **4**(2), 155 (1993)
53. P.D. Gossen, J.F. MacGregor, and R.H. Pelton, *Appl. Sprctros.*, **47**,1852 (1993)
54. C. Wu, J.D.S. Danielson, J.B. Callis, M. Eaton, and N.L. Ricker, *Process Control Qual.*, **8**(1), 1 (1996)
55. J. Mijovic and S. Andjelic, *Polymer*, **38**(8), 1295 (1996)
56. E.G. Chatzi, O. Kammona, and C. Kiparissides, *J. Appl. Polym. Sci.*, **63**, 799 (1997)
57. A.P. Full, J.E. Puig, L.U. Gron, E.W. Kaler, J.R. Minter, T.H. Mourey, and J. Texter, *Macromolecules*, **25**, 5157 (1992)
58. R.F. Storey, A.B. Donnalley, and T.L. Maggio, *Macromolecules*, **31**, 1523 (1998)
59. T.L. Maggio and R.F. Storey, *Polymer Prep.*, **40**(2), 958, (1999)
60. R. F. Storey and A.B. Donnalley, *Macromolecules*, **32**, 7003 (1999)
61. R.F. Storey and T.L. Maggio, *Macromolecules*, **33**, 681 (2000)
62. A.J. Pasquale and T.E. Long, *Macromolecules*, **32**, 7954 (1999)
63. J.R. Bradley and T.E. Long, *Polymer Prep.*, **40**(1), 546 (1999)
64. A. Pizzi, *Advanced Wood Adhesives Technology*, Marcel Dekker, Inc., New York, 1994

65. L. Gollob and J.D. Wellons, in *Handbook of Adhesives*, ed. I. Skeist, Van Nostrand Reinhold, New York, 1990
66. J.N. Annad, *J. Adhes.*, **5**, 256 (1973)
67. E.M. Petrie, *Handbook of Adhesives and Sealants*, McGraw-Hill, New York, 2000
68. M.A. Dubé and A. Penlidis, *Macromol. Chem. Phys.*, **196**, 1101 (1995)
69. M.S. El-Aasser, T. Makgawinata, J.W. Vanderhoff, and C. Pichot, *J Polymer Sci.:Poymer Chem. Ed.*, **21**, 2363 (1983)
70. A. Zosel, *Polymers for Advanced Technologies*, **6**, 263 (1995)
71. C. Jourdan, J.Y. Cavaille, and J. Perez, *J. Polym. Eng. Sci.*, **28**(20), 1318, (1988)

Chapter 3

PAPER I

Off-Line Monitoring of Butyl Acrylate and Vinyl Acetate Homo- and Copolymerization in Toluene

Renata Jovanović and Marc A. Dubé*
Department of Chemical Engineering, University of Ottawa,
161 Louis Pasteur, P.O. Box 450 Stn. A, Ottawa, ON, K1N 6N5 Canada
* dube@genie.uottawa.ca

SUMMARY:

A study of butyl acrylate (BA) and vinyl acetate (VAc) solution homo- and copolymerization in toluene was carried out. Conversion and copolymer composition were monitored using traditional techniques (gravimetry and ^{1}H-NMR spectroscopy) and ATR-FTIR spectroscopy with a diamond-composite probe and light conduit technology. The peak height of characteristic absorbances of monomer(s) during the course of the reaction was used to calculate conversion and copolymer composition for the ATR-FTIR monitoring case. The data obtained using the ReactIR™ 1000 reaction analysis system in the off-line mode showed very good agreement with data obtained using traditional techniques. Solvent effects on BA and VAc solution homo- and copolymerizations in toluene were also investigated. Improvement to model predictions was obtained by allowing the lumped constant ($k_p/k_t^{0.5}$) to vary with solvent concentration. Experimental data and model predictions of number- and weight-average molecular weights for the investigated systems are also presented.

Key words: butyl acrylate, vinyl acetate, solution polymerization, ATR-FTIR spectroscopy, copolymerization kinetics, modeling

INTRODUCTION

Vinyl acetate (VAc) is a widely used monomer for the production of architectural coatings, adhesives, sealants and a variety of other products. Some applications require the modification of some of the final product properties. In these applications, VAc monomer is copolymerized with another monomer such as butyl acrylate (BA). Polymer product properties are affected by copolymer composition, molecular weight and molecular weight distribution which are in turn affected by the reactivities of the individual monomers. The monomer reactivities are described by the monomer reactivity ratios, parameters in the Mayo-Lewis equation (a.k.a. terminal model). Because the reactivity ratios for BA and VAc are quite different, r_{BA}=5.93 and r_{VAc}=0.026, copolymer composition drift is inevitable during batch polymerizations.[1] One way to deal with composition drift is to predict it with a model and/or to monitor the polymerization reaction in real-time and take appropriate steps when composition drift is observed (e.g. using semi-batch control policies[2]).

There are several models proposed for the simulation of free-radical polymerizations. Extensive overviews of the models developed in the last two decades were given by Gao and Penlidis[3,4] and Dubé et al.[5] These overviews present models developed for the simulation of free-radical homopolymerizations and copolymerizations in bulk and solution under a variety of conditions, reactor configurations and operating modes. These models were the basis for a model developed by Badeen.[6] This JAVA™-based model for the simulation of free-radical

polymerizations in bulk and solution is used in this work. The model employs terminal model kinetics and the pseudo-kinetic rate constant method.[2] The free-volume approach was used for the modeling of diffusion-controlled rate constants.[7]

Techniques for monitoring polymer composition drift have been rather limited to date. Despite their accuracy, traditional techniques (e.g. gravimetry and ^{1}H-NMR spectroscopy) are not very useful when the real-time monitoring of polymerization reactions is required because they result in significant time lags. In recent years, several attempts have been made to utilize various dielectric, acoustic and spectroscopic techniques to monitor polymerization reactions.[8,9] Kammona et al.[10] summarized the recent developments in hardware sensors for on-line conversion and copolymer composition monitoring. Techniques such as near infra-red (NIR) and mid infra-red (MIR) spectroscopy are most attractive to utilize for real-time reaction monitoring since they offer much information about the reaction system at the molecular level. Most of the early work reported the utilization of NIR spectroscopy[11,12,13] or MIR spectroscopy[14,15] through instruments developed in-house.

A commercial instrument, the ReactIR™ 1000 (ASI Applied Systems Inc.), has recently been developed for monitoring chemical reactions. Attenuated total reflectance – Fourier transform infrared spectroscopy (ATR-FTIR) was combined with new technological achievements (i.e. light conduit technology and a diamond composite insertion probe) to form a powerful tool for real-time, *in situ,* as well as off-line chemical process monitoring. Reaction pathway and kinetic information can be obtained without complicated reactor modifications and sample handling. Some results on the use of this state-of-the-art instrument in polymer reaction engineering have already been reported: Storey et al.[16,17] used the ReactIR™ 1000 to monitor carbocationic polymerizations of isobutylene while Pasquale and Long[18] used it to monitor stable

free radical polymerizations of styrene. The excellent performance of the instrument was outlined therein.

BA and VAc solution homo- and copolymerizations in toluene have been investigated only sparingly. Aside from the work by McKenna et al.,[19] McKenna and Villanueva,[20] and Othman et al.,[21] recent literature on solution homo- and copolymerizations of BA and VAc are scarce. Copolymerization of these two monomers in aromatic solvents such as toluene can be challenging for process modeling since very significant radical-solvent effects take place. Even though there are several mechanisms by which solvent can affect the propagation kinetics of free radical polymerization reactions, it is commonly believed that, in the case of vinyl monomers, the formation of complexes of the propagating radicals and an aromatic solvent is taking place.[22,23] Coote et al.[23] stated that radical-solvent complexes are favored in systems containing unstable radical intermediates (such as VAc) in which complexation may lead to the stabilization of these radicals and therefore, to the reduction of the propagation rate constant. On the other hand, the termination rate constant might be chain-length dependent.[19,20,21,24] In case of extremely high rates of transfer to solvent this would lead to an increase in the termination rate constant with solvent concentration.[19,20,21] Gaining insight about the influence of solvent on the propagation and termination rate constants is further complicated by the fact that even with the pulsed laser polymerization technique it is difficult to determine absolute values of these constants for BA and VAc.[25] In light of these challenges, the most suitable approach at this time is to estimate the value of the "lumped" kinetic constant (the ratio of the propagation rate constant over the square root of the termination rate constant, $k_p/k_t^{0.5}$). This approach was recently used by McKenna et al.[19] and McKenna and Villanueva[20] for the solution

homopolymerizations of BA and VAc in toluene and ethyl acetate and the copolymerization of BA/VAc in ethyl acetate.

The primary focus of the work reported herein was to monitor the homo- and copolymerizations of BA and VAc in toluene solution using an ATR-FTIR probe. The first steps involved the use of the probe in an off-line mode to determine conversion and copolymer composition and to compare these results to those using conventional off-line measurement techniques. This procedure involved the identification of characteristic IR absorbance peaks for each monomer and the use of these peaks to follow the reaction profile. A secondary goal was to continue ongoing polymerization model development. The data collected in this study were used to evaluate our JAVA™-based model and to direct further experimentation. Investigation of suspected solvent effects was also undertaken.

EXPERIMENTAL CONDITIONS AND TECHNIQUES

Reagent purification

Butyl acrylate (BA) and vinyl acetate (VAc) (Sigma-Aldrich) were received inhibited by 0.05 ppm hydroquinone. To remove the inhibitor, VAc was distilled under vacuum and BA was washed three times with a 10% (vol/vol) sodium hydroxide solution, three times with distilled de-ionized water, dried over calcium chloride and vacuum distilled. Distillations were completed a maximum 24h prior to polymerization and the monomers were stored at –10°C. The initiator, 2,2'-azobisiso-butyronitrile (AIBN) (Sigma-Aldrich) was recrystallized three times in absolute methanol. Toluene solvent (ACP Chemicals) and n-dodecyl mercaptan chain transfer agent

(CTA) (Sigma-Aldrich) were used without further purification as were all other solvents used for sample characterization.

Experimental procedure

The monomer feed was prepared by weighing the monomer(s), solvent, CTA and initiator into a flask. The feed was pipetted into a series of 5mL glass ampoules (length = 17cm; outer diameter 0.8cm). The ampoules were degassed by several freeze-thaw cycles under high vacuum. After sealing, the ampoules were weighed and subsequently submerged in a constant temperature water bath. At the appropriate time interval, two ampoules were removed from the bath simultaneously and placed in an ice bath to quench the reaction.

One ampoule was used for the determination of conversion by the traditional gravimetric technique. The ampoule was broken, the contents poured into a pre-weighed crystallizing dish, and a 10-fold excess of ethanol was added. After evaporation of the solvents, the precipitated polymers were dried in a vacuum oven at 30°C until a constant weight was reached. Once dried, the polymers were weighed and analyzed for conversion. In the case of copolymerization, the dry polymers were analyzed for cumulative copolymer composition using ^{1}H-NMR spectrometry.

The second ampoule was used for the ATR-FTIR measurements. When the ampoule was broken, part of its contents was weighed and toluene was added to the vial to ensure that enough sample was present to fully immerse the probe. After the collection of spectra of air as a background, the ATR-FTIR probe was immersed in the vial and spectra were recorded at a resolution of 8 cm^{-1}. The number of scans was 64 and less than one minute was required to collect a spectra.

The cumulative number- and weight-average molecular weights were determined using gel permeation chromatography.

The solution polymerization experimental conditions are summarized in Table 3.1 All reactions were carried out at 60 °C.

Table 3.1: Experimental conditions

Experiment	BA (wt %)	VAc (wt %)	Toluene (wt %)	AIBN (mol L^{-1})	CTA (mol L^{-1})
BT55	50	-	50	0.002	0.02
BT28	20	-	80	0.002	0.02
VT55	-	50	50	0.105	0.02
VT28	-	20	80	0.105	0.02
BVT55	25	25	50	0.002	0.02
BVT28	20	40	50	0.002	0.02

Product characterization

ATR-FTIR. Polymerization reactions were monitored off-line using an attenuated total reflectance (ATR) Fourier Transform infrared (FTIR) spectrometer – ReactIR™ 1000 (ASI Applied Systems Inc). The instrument is primarily designed for in-line monitoring of chemical reactions in the mid infrared spectral region (4000-650 cm^{-1}) but our intention was to employ it off-line in order to test its capabilities and limitations before its in-line utilization in our pilot

scale reactor. In this reaction monitoring system, the traditionally used fiber optic probe technology has been replaced by light conduit technology, which consists of six mirrors and three tubes that provide a purged path through which the infrared beam travels to a remote sampling device and back to a detector. The sampling device is a DiComp (diamond composite) insertion probe with stainless steel body (length 7.25", diameter 0.625") and a six reflection bi-layer ATR element with a diamond surface element (6mm diameter, 0.25mm thickness) at the top. Interfacing with the diamond and acting as a focusing element is an IR transmitting optic (a focusing crystal made of composite material). The design enables IR radiation to enter the focusing crystal and then, in a controlled manner, the side of the diamond disk. Once inside the disk, it forms a standing wave of radiation called an evanescent wave that penetrates a finite distance into a sample. The distance is called the depth of penetration, DP, and it is analogous to the path length in transmission sampling techniques. DP is given by the following equation:[26]

$$DP = \frac{1}{2\pi W N_c (\sin^2 \Theta - N_{sc}^2)^{1/2}} \tag{3.1}$$

where W is the wavenumber, N_c and N_{sc} are the crystal refractive index and ratio between the sample and crystal refractive indices, respectively, and Θ is the angle of incidence. It can be seen that the absorption intensity at a certain frequency is proportional to the wavenumber for constant N_c, N_{sc} and Θ. As a consequence, the peaks are more intense at low wavenumber than at high wavenumber since the low wavenumber radiation penetrates further into the sample.

The basis for monitoring polymerization reactions is the determination of the characteristic peaks that represent functional groups inside a monomer or polymer and monitoring their absorbances throughout the course of the reaction. The determination of characteristic peaks is straightforward since the mid-IR spectra consist of well-defined fundamental vibrational frequencies that correspond to specific functional groups and

interactions between them. According to Beer's law, the concentration of a component is proportional to the absorbance, which can be measured as peak height, peak height ratio, peak area or peak area ratio. In our case, the peak height has been found to give the best results. The peak heights were determined after a baseline correction. Following the general rule that the less manipulation of the original spectra, the less error induced in the quantitative analysis,[26] the subtraction of the solvent spectra was omitted because the solvent was not absorbing at the same wavelength as the chosen characteristic peaks. The following equations were used for determination of the conversion, x, of individual monomers:

$$x(mol\%) = 1 - \frac{peak\ height\ at\ time\ t}{peak\ height\ at\ time\ t = 0} \tag{3.2}$$

and the overall conversion, X, for the copolymerization case:

$$X(mol\%) = \frac{n_1}{n_1 + n_2} x_1(mol\%) + \frac{n_2}{n_1 + n_2} x_2(mol\%) \tag{3.3}$$

where $\frac{n_i}{n_i + n_j}$ denotes the mole fraction of monomer i in the reaction mixture. This method has been previously reported by Chatzi et al.[15] For the post-process data analysis, ReactIR™ software was used.

Gravimetry. Gravimetry was used for the determination of conversion, X(mass %) and was based on total polymer. The following equation was used:

$$X = \frac{\text{wt. of dish with dry polymer} - \text{wt. of empty dish}}{\left[\begin{array}{c}(\text{wt. of ampoule and reaction mixture} - \text{wt. of empty ampoule})\times \\ (\text{wt. fraction of total monomer(s) in reaction mixture})\end{array}\right]} \tag{3.4}$$

For the copolymerization case, the mass % conversion was transformed into mole % conversion using the cumulative copolymer composition data in order to compare the gravimetric and ATR-FTIR data.

^{1}H-NMR spectroscopy. Cumulative copolymer compositions were determined using a Bruker AMX-500 Fourier transform ^{1}H-NMR spectrometer. The analyses were carried out in deuterated chloroform (chloroform-d, approx. 2% (w/v) solution) at room temperature. A standard one-pulse experiment was employed using 45 degree pulses. Sixteen transients, each 4.6 seconds in duration with no additional relaxation delay, were signal averaged and Fourier transformed. The relative amounts of monomer bound into the polymer were estimated using the areas under the appropriate absorption peaks. A good separation of the spectral peaks of the $-OCH_2$ group in BA ($\delta \approx$ 4.0 ppm) and the α-hydrogen in VAc ($\delta \approx$ 4.9 ppm) was achieved, thus allowing the unambiguous interpretation of the results. The following expressions:

$$\overline{F}_{BA} = \frac{\frac{A_{BA}}{2}}{A_{VAc} + \frac{A_{BA}}{2}} \tag{3.5}$$

$$\overline{F}_{VAc} = \frac{A_{VAc}}{A_{VAc} + \frac{A_{BA}}{2}} \tag{3.6}$$

were used to calculate the mol fractions ($\overline{F}_{BA}, \overline{F}_{VAc}$) of BA and VAc monomer, respectively, bound into polymer. A_{BA} and A_{VAc} represent the areas under the VAc and BA spectral peaks, respectively. The use of these spectral peaks for the determination of the cumulative copolymer composition has been reported previously.[27,28]

Gel Permeation Chromatography. The cumulative number- and weight-average molecular weights were determined using gel permeation chromatography. A Waters Associates gel permeation chromatograph equipped with a Waters Model 410 refractive index detector was employed. Three Waters Ultrastyragel packed columns (10^3, 10^4 and 10^6 Å) were installed in series. Tetrahydrofuran (THF, HPLC grade, EM Science) was filtered and used as the eluent at a flow rate of 0.3 mL/min at 38°C. Calibration of the instrument was performed with 10 standard samples of polystyrene (SHODEX) with peak molecular weights between $1.3x10^3$ to $3.15x10^6$ g mol^{-1}. Standards and samples were prepared in THF (0.2% (w/v) solutions) and filtered prior to injection through 0.45μm filters to remove high molecular weight gel, if present. Millennium 32™ software (Waters) was used for data acquisition and manipulation.

The absolute cumulative number- and weight average molecular weights were determined using a universal calibration curve. The Mark-Houwink, K and α, parameters determined in THF as a solvent are given in Table 3.2.

Table 3.2: Mark-Houwink parameters

Polymer	K (× 10^3) (mL/g)	α	Reference
Poly (butyl acrylate)	11	0.708	19
Poly (vinyl acetate)	15.6	0.708	29
Polystyrene	16	0.700	30

In the case of copolymers, weighted averages of K and α values were calculated using the cumulative copolymer composition data obtained earlier using ^{1}H-NMR spectrometry. The observed difference between the relative and absolute values of the number and weight average

molecular weights for most of the samples was minimal since the K and α values for the polymers and polystyrene standards were close.

RESULTS AND DISCUSSION

Butyl acrylate homopolymerizations

Two BA homopolymerizations in toluene were carried out with different monomer concentrations (see Table 3.1). In Figures 3.1 and 3.2, experimental data for BA/toluene ratios of 50/50 wt% and 20/80 wt% obtained using the ReactIR™ 1000 (open symbols) are compared to gravimetric data (solid symbols).

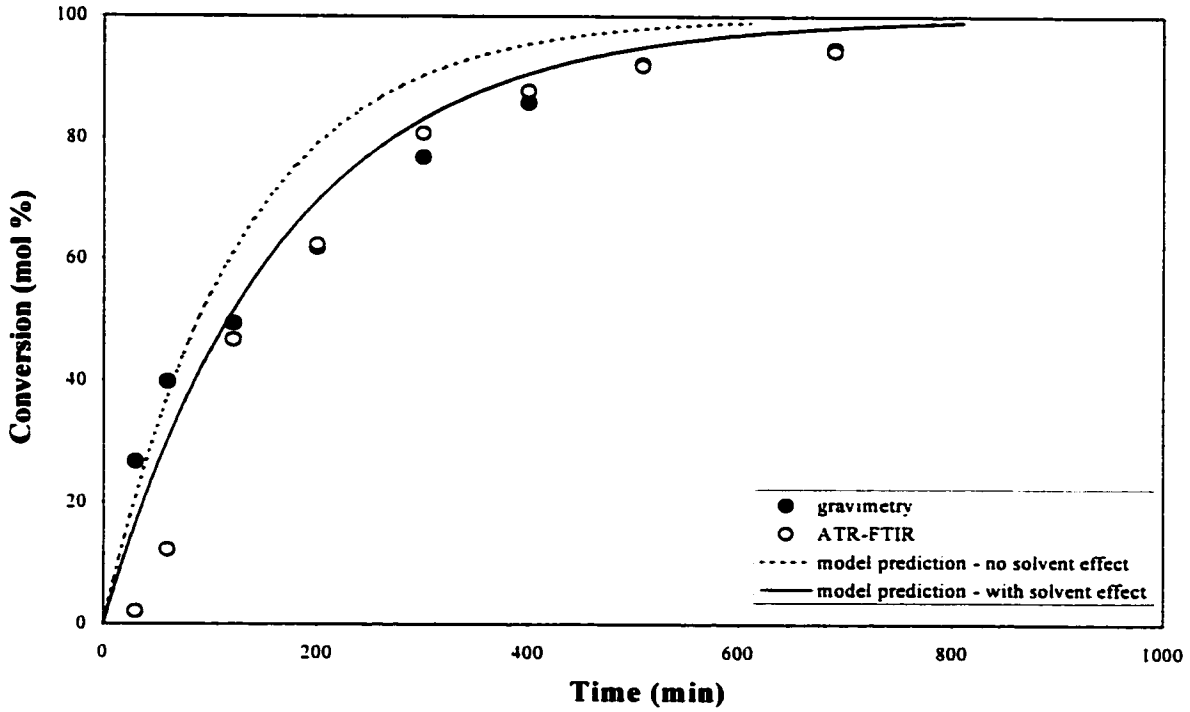

Figure 3.1 Conversion vs. time: BA/Toluene 50/50 wt%

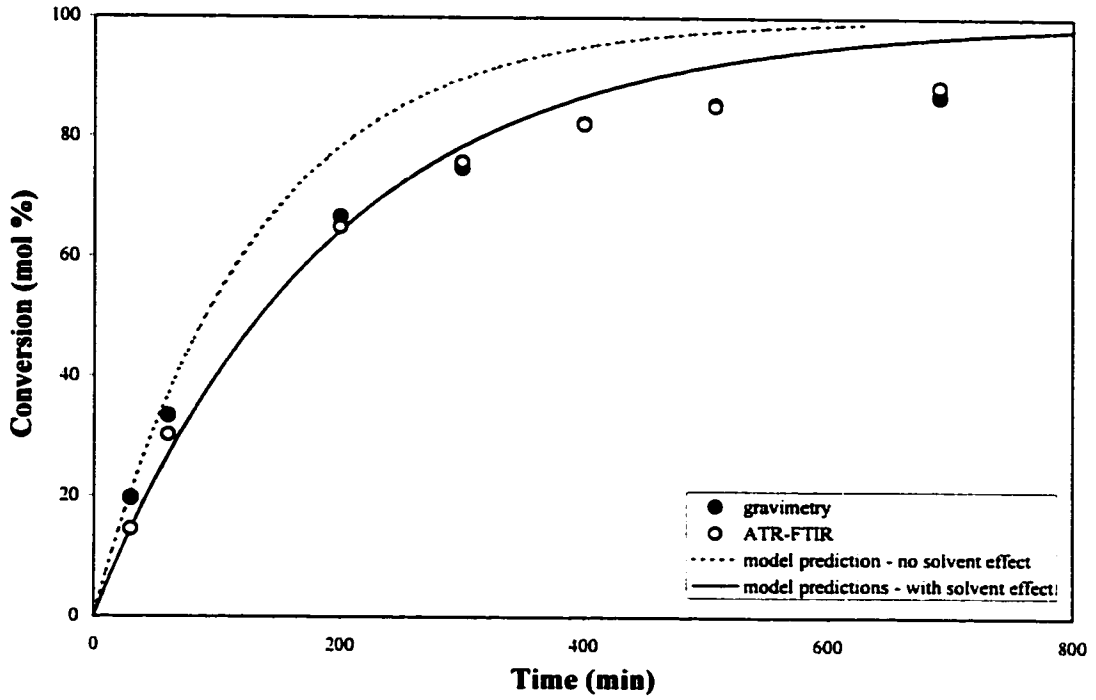

Figure 3.2 Conversion vs. time: BA/Toluene 20/80 wt%

The first step after the spectra were collected was to make peak assignments and determine which of the peaks could be used to calculate conversion. For the purposes of peak assignment, the spectra of BA monomer shown in Figure 3.3, was collected under similar conditions as the reaction spectra. The assignments for the major peaks are given in Table 3.3.[31,32]

Table 3.3: Vibrational assignments for butyl acrylate

Wavenumber cm^{-1}	Peak Assignment
1725	C=O str.
1640	C=C
1409	$=CH^2$ def.
1274	=CH rock
1189	C-O asym. str.
1065	$=CH_2$ rock
984.3	trans CH wag
968.9	$=CH_2$ wag
810.6	$=CH_2$ twist

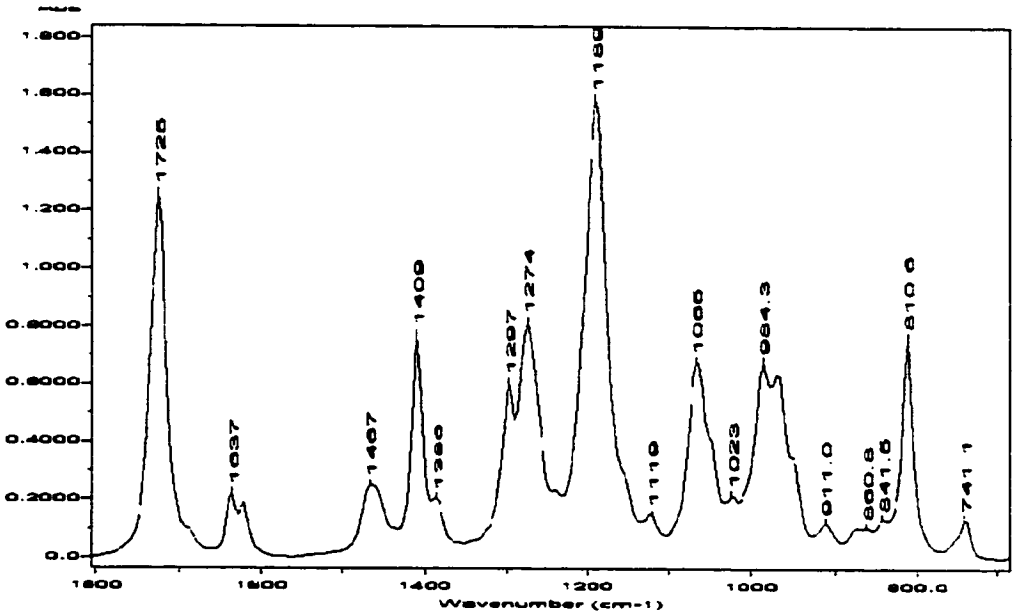

Figure 3.3 ATR-FTIR spectra of BA monomer

After careful examination of the spectra collected during the BA polymerization in toluene (see Figure 3.4), several peaks (1409 cm^{-1}, 1193cm^{-1}, 984.3 cm^{-1}, 968.9 cm^{-1}, and 810.6 cm^{-1}) were identified to be appropriate for use in the quantitative estimation of the conversion of BA monomer.

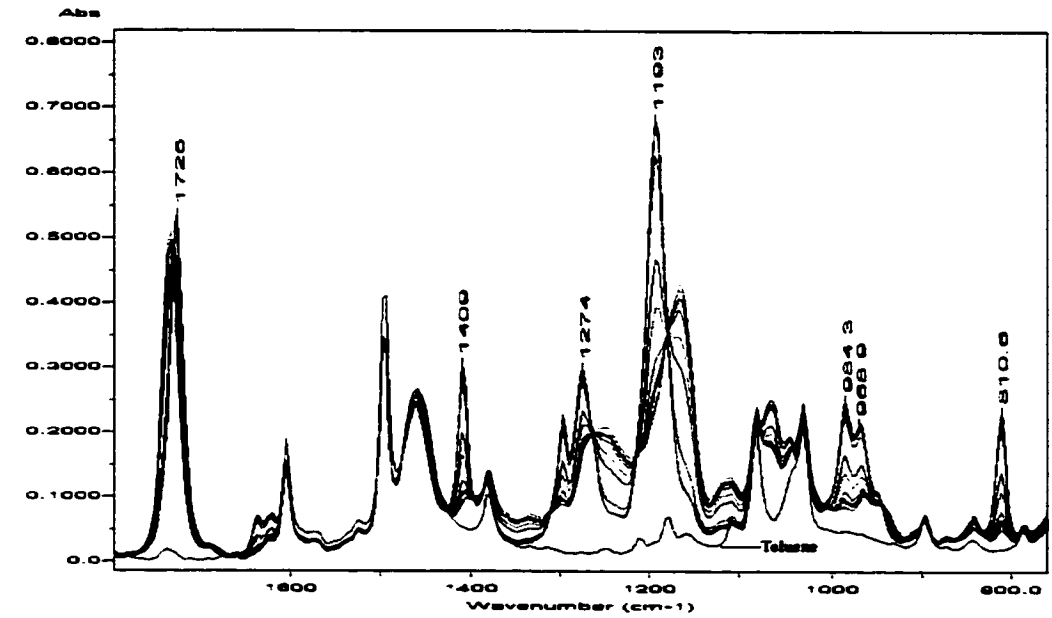

Figure 3.4 ATR-FTIR spectra of BA solution homopolymerization in toluene (50/50 wt%)

Because the subtraction of solvent was intentionally omitted, the number of peaks that could have possibly been used for monitoring monomer conversion was reduced. After baseline correction, the calculation using the peak height referenced to a two-point baseline for the absorbance band at 810.6 cm^{-1} (=CH_2 twist) was found to give the best predictions of monomer conversion compared to the gravimetric data. Conversion was calculated using equation 3.2. The absorbance (peak height) at time zero was the absorbance (peak height) of the reaction mixture collected prior to polymerization. The change of the absorbance (peak height) during the course of reaction is given in Figure 3.5.

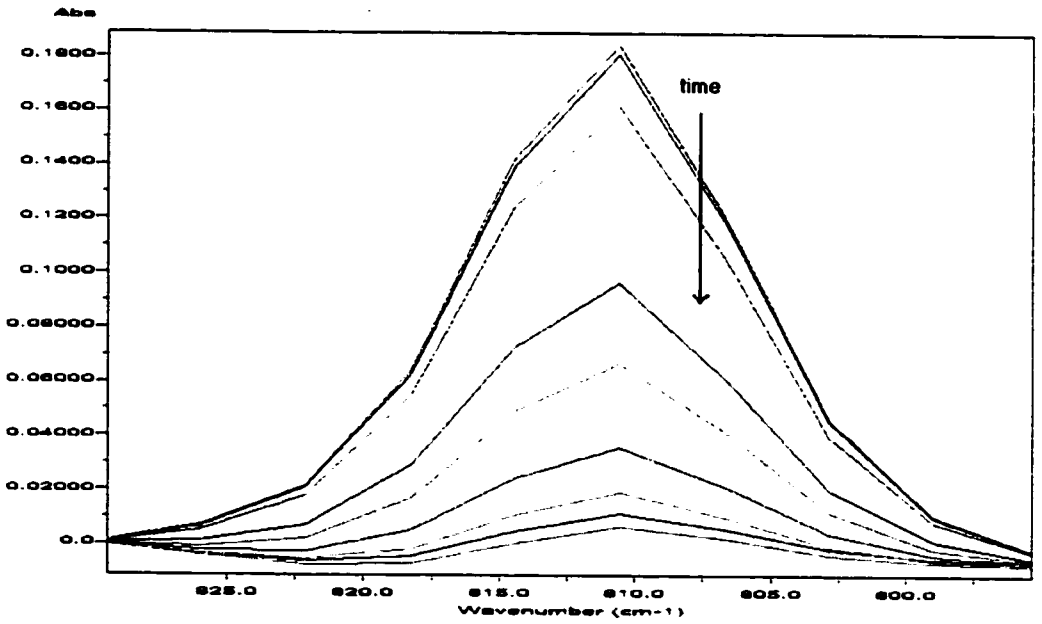

Figure 3.5 Changes in the absorbance of BA monomer during the course of reaction

The same peak (810.6 cm^{-1}) was used to obtain conversion vs. time data for both polymerization reactions (BA/toluene 50/50 wt% and 20/80 wt%). There was no need to subtract the solvent spectra from the overall spectra since toluene does not absorb in the range (i.e. 830-790 cm^{-1}) where the absorbance of BA has been observed. Good agreement between the data obtained by gravimetry and the ATR-FTIR probe was observed as shown in Figures 3.1 and 3.2. These

findings confirmed that the monitoring of BA homopolymerizations in solution using an ATR-FTIR probe in an off-line mode is not only possible but also sufficiently accurate. The observed disagreement between the two techniques at low conversions (Figure 3.1) could have been caused by an induction period in the ampoules used for the ATR-FTIR measurements. It is important to recall that each technique was used on separate ampoules.

In our attempt to model BA solution homopolymerizations, we were faced with the fact that BA rate constants are affected by the presence of solvent in the reaction mixture.[23] The value of the ratio of the propagation rate constant (k_p) and the square root of the termination rate constant (k_t), henceforth referred to as a lumped constant ($k_p/k_t^{0.5}$), depends on the concentration of BA in a reaction mixture. Its value increases with the concentration of BA. This effect was observed for the methyl methacrylate homopolymerization in benzene[33] as well as for BA and VAc homopolymerizations in toluene and benzene.[19,20] Both groups suggested that it was unlikely that k_p was significantly affected by the solvent concentration.[19,20,33] The variation of the lumped constant with solvent concentration might instead be explained by the chain-length dependence of k_t.[24] Thus, short chain radicals would have higher values of k_t compared to longer ones, and therefore have lower values of $k_p/k_t^{0.5}$. McKenna et al.[19] and Othman et al.[21] used this concept to explain variations in the value of the lumped constants for BA and VAc polymerizations in different solvents. The high number of chain transfer to solvent reactions that take place in these systems leads to the formation of a considerable fraction of short chain radicals. Since short radicals move and terminate more quickly, the value of the termination rate constant will increase and the value of the lumped constant decreases with an increase in solvent concentration. In light of the experimental difficulties involving the determination of the absolute

rate constants for these systems,[25] it is impossible to say with certainty that changes in k_t exclusively cause the variation of the lumped constant with solvent concentration. In Figures 3.1 and 3.2 two model predictions are shown for each run. Use of our JAVA™-based model[6] with bulk polymerization rate constants resulted in reasonable but not sufficiently accurate predictions (dashed lines in Figures 3.1 and 3.2). In light of the previous discussion, the value of the lumped constant was then changed with solvent (or monomer) concentration. Values for k_t at 60°C that showed the best fit to experimental data were 2.67×10^8 L·mol^{-1}·s^{-1} and 2.13×10^8 L·mol^{-1}·s^{-1} for 20 and 50 wt% of BA in the reaction mixture, respectively. The value of the lumped constant was increased from 4.89 to 5.47 as the concentration of BA increased. The chain transfer to monomer constant (the ratio of the propagation rate constant over the chain transfer to monomer rate constant), C_{fm} equaled 1.44×10^{-4}. McKenna et al.[19] reported $C_{fm} = 1 \times 10^{-4}$ while $C_{fm} = 6.6 \times 10^{-5}$ was obtained using Maeder and Gilbert's[34] parameters in an Arrhenius expression for C_{fm} at 60 °C. The value used for the chain transfer to solvent constant (the ratio of the propagation rate constant over the chain transfer to solvent rate constant) was $C_{fs} = 3.25 \times 10^{-4}$ which is close to $C_{fs} = 1.8 \times 10^{-4}$ reported by McKenna et al.[19] The chain transfer to CTA constant (the ratio of the propagation rate constant over the chain transfer to chain transfer agent rate constant) was $C_{fcta} = 1.9$. De la Fuente and Madruga[35] reported $C_{fcta} = 0.455$ to 1.056 for n-dodecyl mercaptan in the copolymerization of butyl acrylate with methyl methacrylate at 60°C depending on the feed composition and the method used for determination of the chain transfer constant. Use of the above parameters resulted in improved model predictions (see Figures 3.1 and 3.2).

Changes in the cumulative number- and weight-average molecular weights with conversion for BA/toluene 50/50 and 20/80 wt% respectively, are presented in Figures 3.6 and 3.7, respectively.

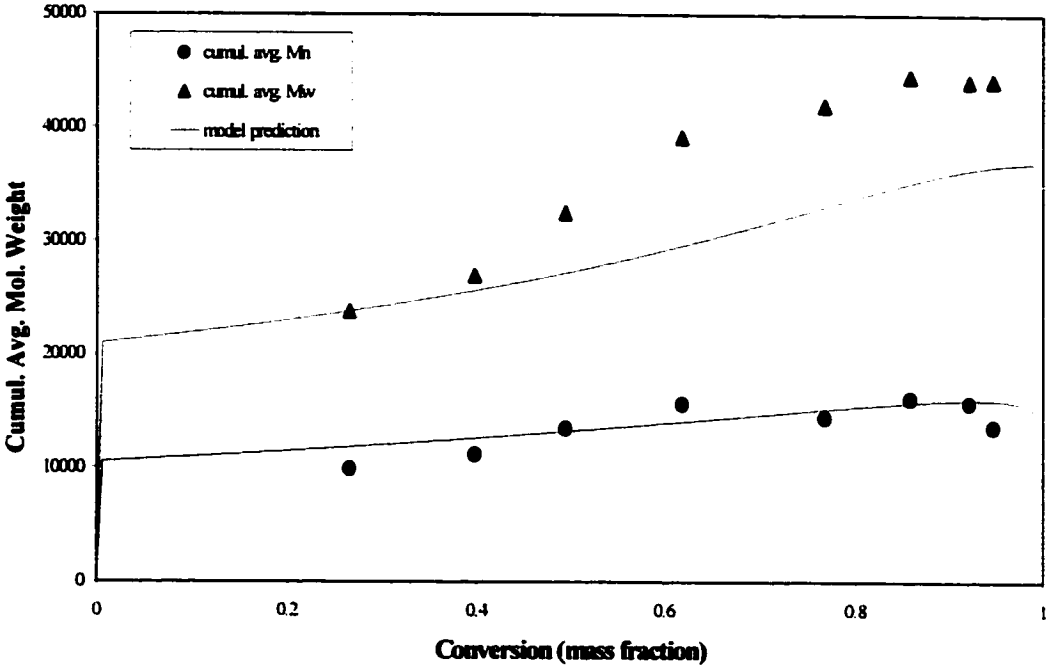

Figure 3.6 Cumulative average molecular weight vs. conversion: BA solution homopolymerization in toluene (50/50 wt%)

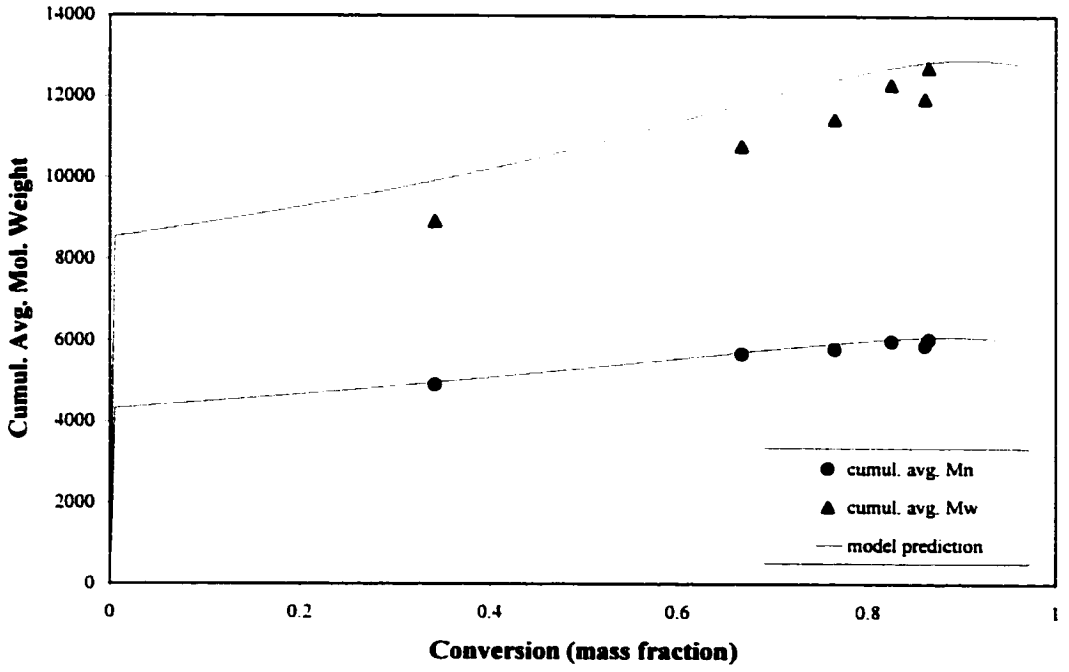

Figure 3.7 Cumulative average molecular weight vs. conversion: BA solution homopolymerization in toluene (20/80 wt%)

Comparing these two figures, it is evident that the cumulative number- and weight-average molecular weights increased with monomer concentration. The model predictions were obtained by accounting for the solvent effect. The molecular weight predictions were very sensitive to changes in the lumped rate constant: model predictions without the solvent effects were an order of magnitude higher than the experimentally observed values.

The individual influence of the chain transfer reactions on the molecular weight development was also investigated. Using the instantaneous molecular weight distribution method (for demonstration purposes only, since branching reactions are present for these polymerization systems), the instantaneous number- and weight-average molecular weights (M_n and M_w, respectively) can be expressed as:

$$M_n = \frac{(MW_m)}{\tau+\beta} \tag{3.7}$$

$$M_w = \frac{(MW_m)(2\tau+3\beta)}{(\tau+\beta)^2} \tag{3.8}$$

where MW_m represents the molecular weight of the repeat unit and τ, the molecular weight contribution due to termination by disproportionation and transfer to small molecules, and β, the molecular weight contribution due to termination by combination, are given as

$$\tau = \frac{k_{td}R_p}{(k_p[M])^2} + C_{fm} + C_{fs}\frac{[S]}{[M]} + C_{fcta}\frac{[CTA]}{[M]} \tag{3.9}$$

$$\beta = \frac{k_{tc}R_p}{(k_p[M])^2} \tag{3.10}$$

The individual terms in equation 3.9 were calculated in order to assess their change during the course of reaction. In both systems, $C_{fs}\frac{[S]}{[M]}$ was the dominant term throughout the course of the reaction and showed an increase of two orders of magnitude toward the reaction's end.

Vinyl acetate homopolymerizations

As for the case of BA, two homopolymerizations of VAc in toluene were carried out (see Table 3.1). The ATR-FTIR off-line monitoring of the VAc homopolymerizations was accomplished using the same method as in the BA homopolymerizations. The obtained results are shown in Figures 3.8 and 3.9 for VAc/toluene ratios of 50/50 and 20/80 wt%, respectively.

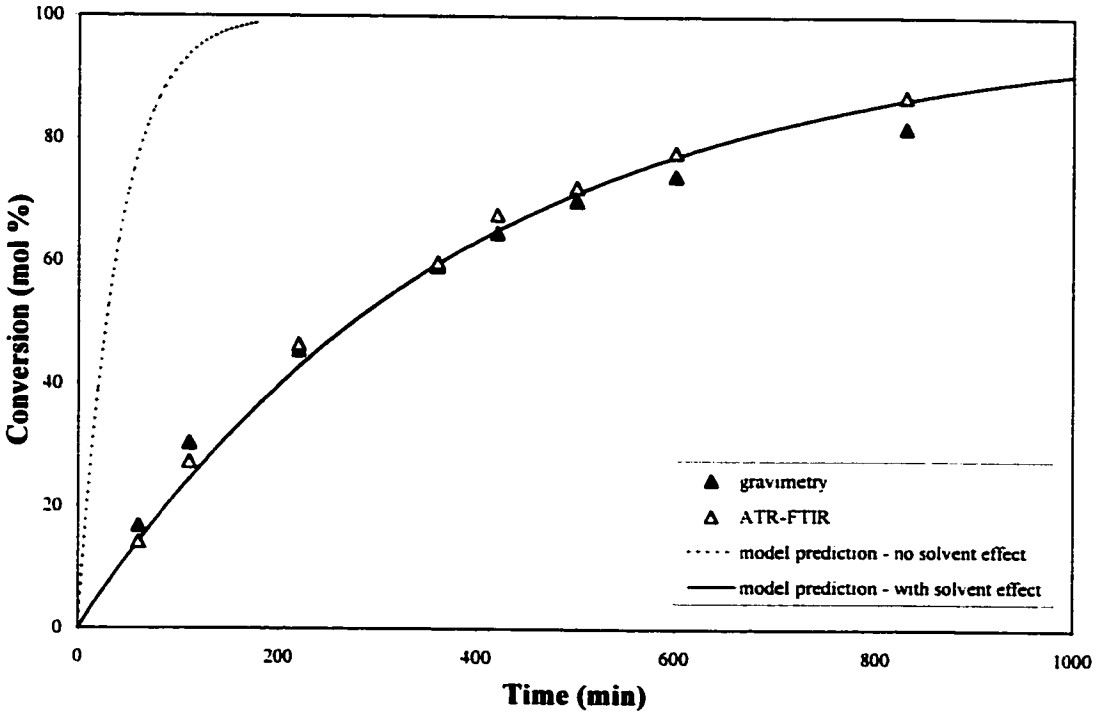

Figure 3.8 Conversion vs. time: VAc solution homopolymerization in toluene (50/50 wt%)

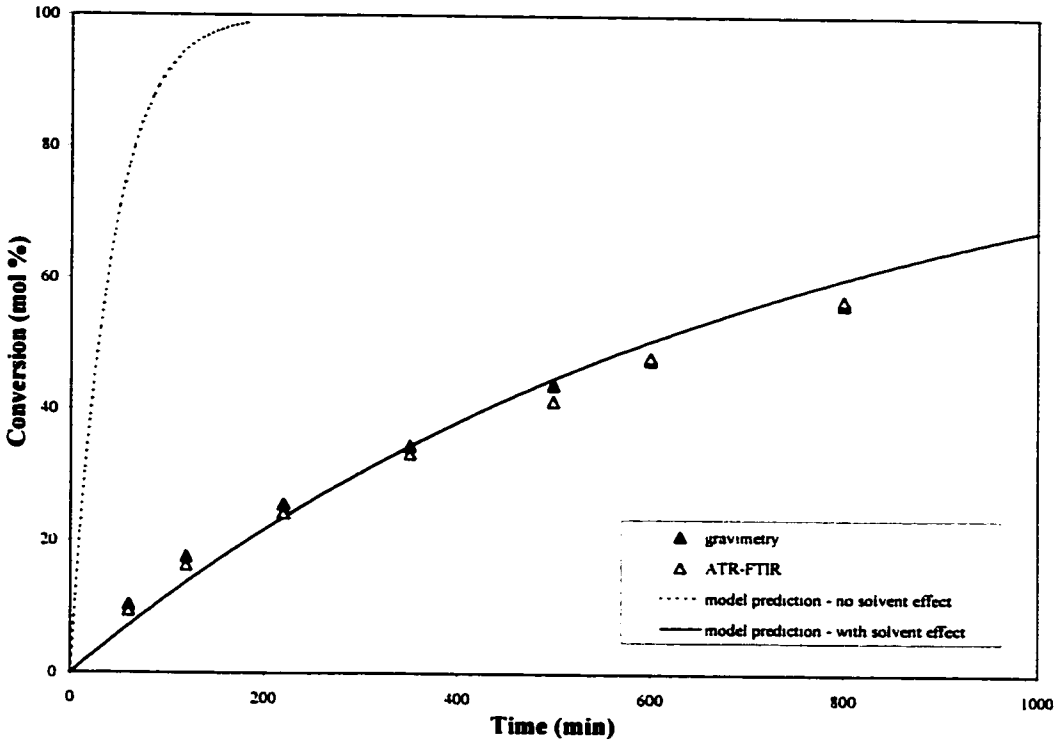

Figure 3.9 Conversion vs. time: VAc solution homopolymerization in toluene (20/80 wt%)

The ATR-FTIR spectra (range 1800-800 cm^{-1}) of VAc monomer shown in Figure 3.10 was used for the peak assignments. The assignments of the characteristic peaks are given in Table 3.4.[31,36]

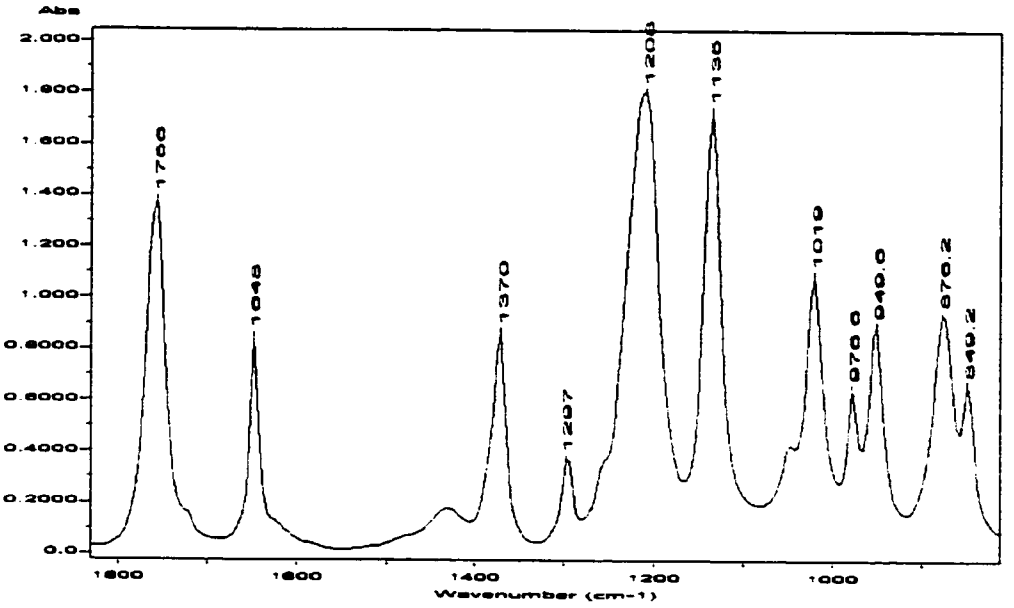

Figure 3.10 ATR-FTIR spectra of VAc monomer

Table 3.4 Vibrational assignments for vinyl acetate

Wavenumber cm^{-1}	Peak assignment
1725	C=O symmetric stretching
1648	C=C stretching
1370	CH_3 symmetric deformation
1290	C-O stretching
1208	C-C-O symmetric stretching
1135	C-O stretching
1019	C-O-C symmetric stretching
949.6	trans CH wag
876.2	$-CH^2$ wag

The characteristic change of the absorbances during the course of reaction that represented the changing concentration of monomer or polymer in the reaction mixture was observed with several peaks which are represented in Figure 3.11.

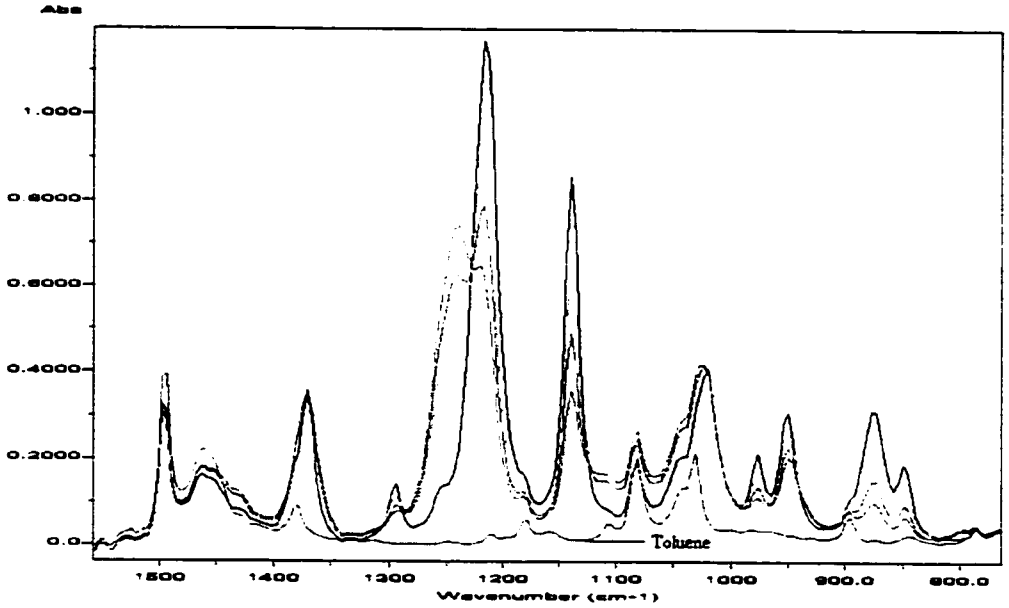

Figure 3.11 ATR-FTIR spectra of VAc solution homopolymerization in toluene (50/50 wt%)

For the sake of clarity, not all collected spectra are shown. After careful examination of the spectra, the absorbance bands for which there was no absorption of toluene were used for calculating conversion. Calculations performed using the peak height referenced to a two-point baseline for the absorbance band at 1293 cm^{-1} showed the highest degree of agreement between the gravimetric data and the ATR-FTIR data. Changes in the absorbance of VAc monomer at 1293 cm^{-1} during the course of the reaction are shown in Figure 3.12. Equation 3.2 was used to calculate monomer conversion. As in the case for BA, good agreement between gravimetry and ATR-FTIR was observed. Therefore, conversion of monomer in VAc solution homopolymerizations can be successfully monitored off-line using ATR-FTIR.

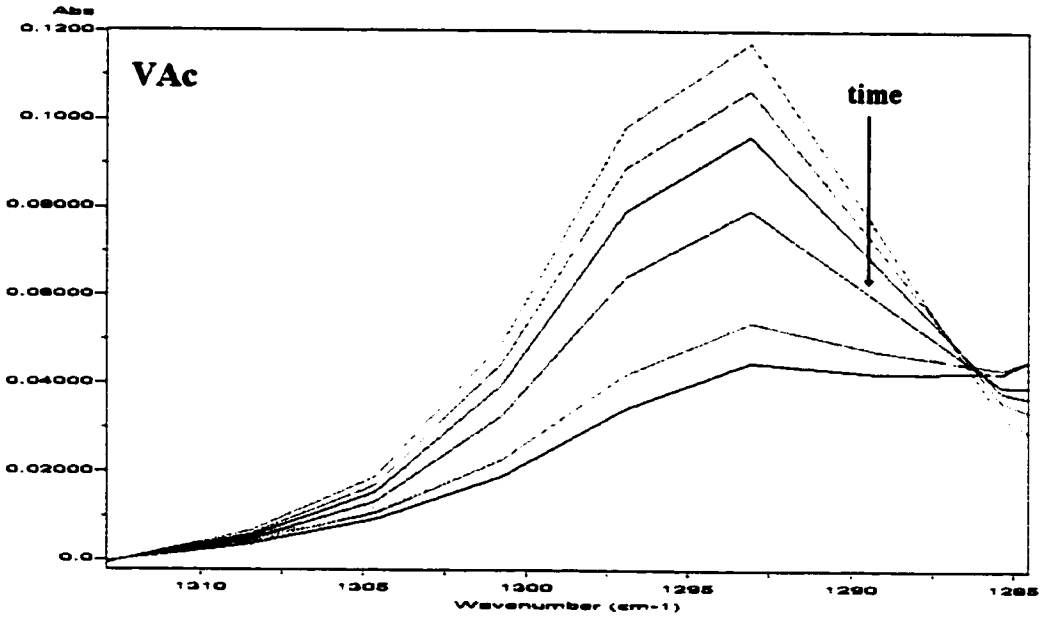

Figure 3.12 Changes in the absorbance of VAc monomer during the course of reaction

It is well known that toluene, like other aromatic solvents, acts as a strong retardant for VAc homopolymerization.[23] The solvent effect is more pronounced for VAc than for BA. Changes in the lumped rate constant ($k_p/k_t^{0.5}$) with solvent concentration were observed in toluene as well as in benzene.[20,21] As with BA, a chain length dependence for k_t is suspected.

In Figures 3.8 and 3.9, two models are presented: one that incorporates parameters for VAc bulk homopolymerization and another in which the solvent effect was taken into account. As previously mentioned, our approach was to adjust the termination rate constant to fit the model to the experimental data. For VAc/toluene 20/80 wt% the value of the termination rate constant was 2.17×10^{12} L·mol^{-1}·s^{-1} and that for the lumped rate constant was 0.1624; these gave the best fit to the experimental data. The value of the lumped rate constant depends on the ratio of monomer to solvent at constant initiator concentration. Therefore, when the concentration of monomer was increased to 50 wt% the value of the lumped rate constant was 0.3349 for the best estimate of k_t (5.1×10^{11} L·mol^{-1}·s^{-1}). The values of chain transfer constants used in the model for solution polymerizations were: $C_{fm} = 1.75 \times 10^{-4}$ which falls near the end of the range of values reported in the Polymer Handbook;[29] $C_{fs} = 20 \times 10^{-4}$, which is slightly lower than the range of values ($21\text{-}34 \times 10^{-4}$) reported by Ham,[37] and $C_{fcta} = 3.48 \times 10^{-4}$.

Changes in the cumulative number- and weight-average molecular weights with conversion are shown in Figures 3.13 and 3.14. The cumulative number- and weight-average molecular weights for the VAc/toluene 50/50 wt% run were much higher than for the VAc/toluene 20/80 wt% run because there was more solvent present in the former case.

In light of the changes introduced in the model used for the prediction of the bulk polymerization, the molecular weights were greatly affected by changes in k_t. As with the BA solution homopolymerizations, neglecting the solvent effect yielded model predictions for cumulative number- and weight-average molecular weights which were an order of magnitude higher than the experimental data.

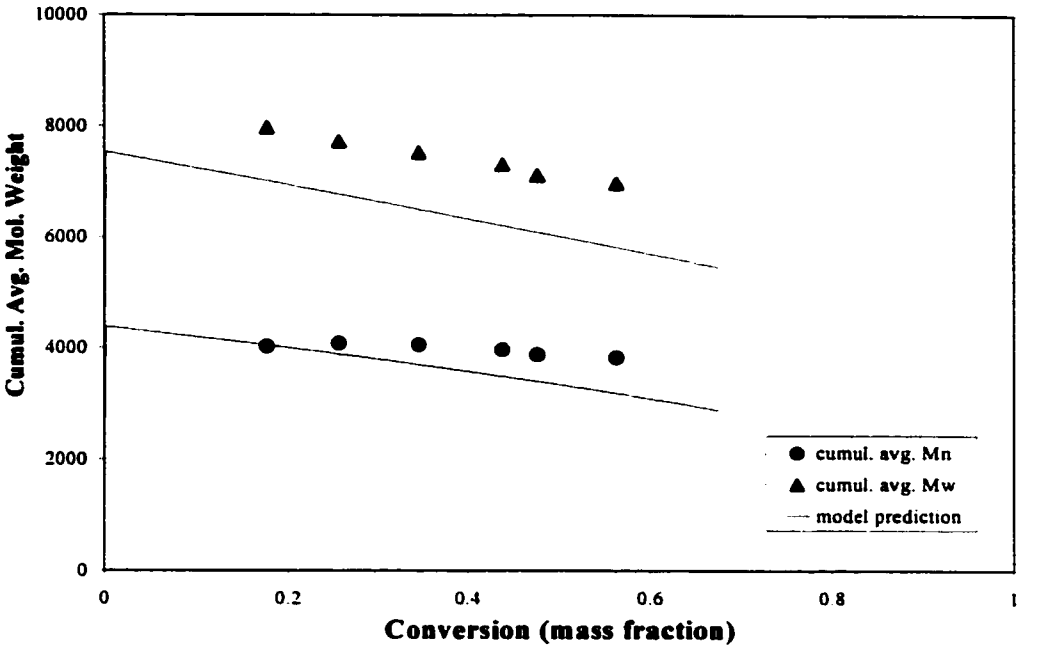

Figure 3.13 Cumulative average molecular weight vs. conversion: VAc solution homopolymerization in toluene (50/50 wt%)

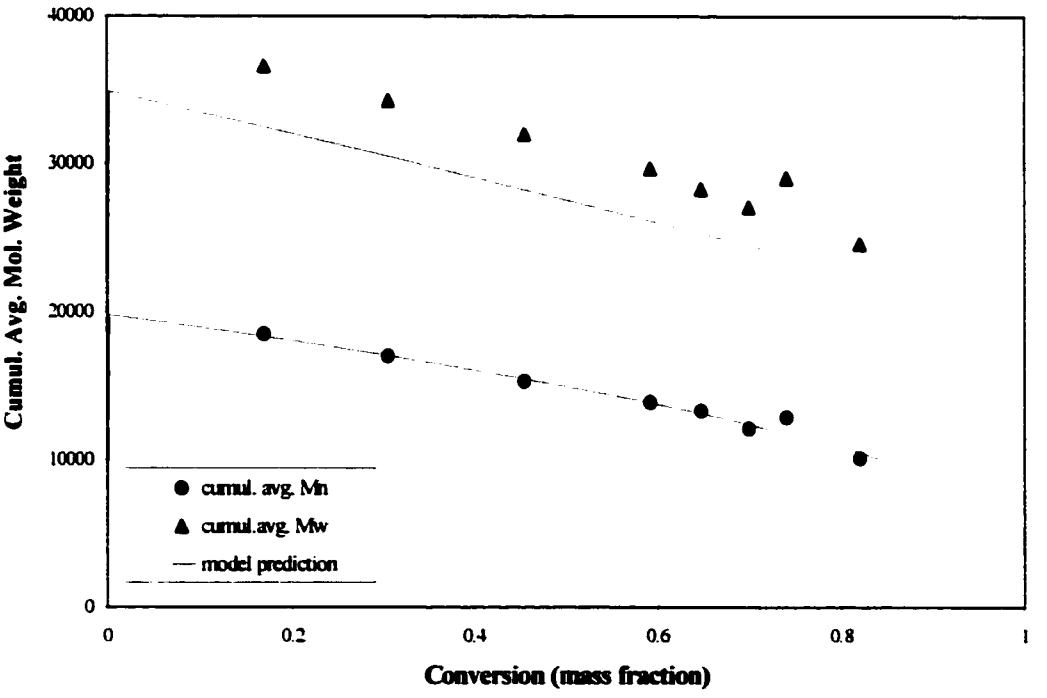

Figure 3.14 Cumulative average molecular weight vs. conversion: VAc solution homopolymerization in toluene (20/80 wt%)

The influence of the individual chain transfer reactions on the molecular weight development was also investigated. The individual terms in equations 3.9 and 3.10 were calculated in order to assess their change during the course of reaction. It was found that the term $k_{tc}*R_p/((k_p*[M])^2$ (eqn. 10) was dominant followed by C_{fs} during the course of the reaction. This is unlike the bulk polymerization case where the C_{fm} term dominates throughout the reaction.

BA/VAc copolymerizations

Two BA/VAc copolymerizations in toluene were carried out under the conditions described in Table 3.1. In Figures 3.15 and 3.16, experimental data obtained by traditional techniques (gravimetry and ^{1}H-NMR) and ATR-FTIR are presented along with model predictions.

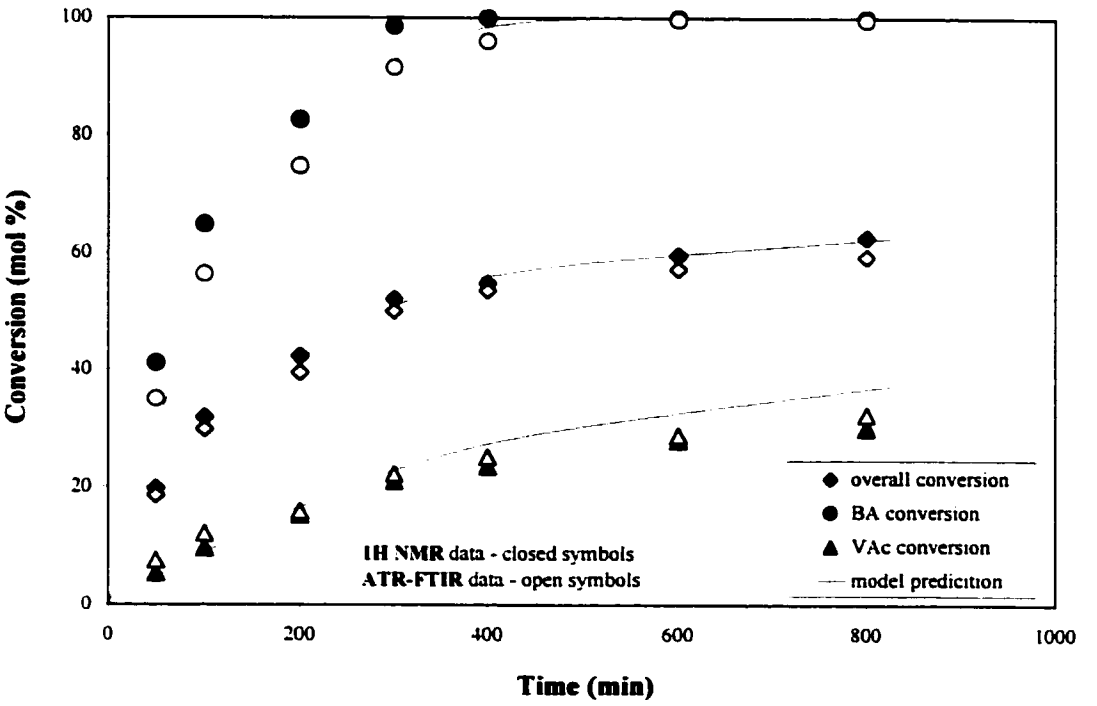

Figure 3.15 Conversion vs. time: BA/VAc (50/50 wt%) solution copolymerization in toluene (50 wt%)

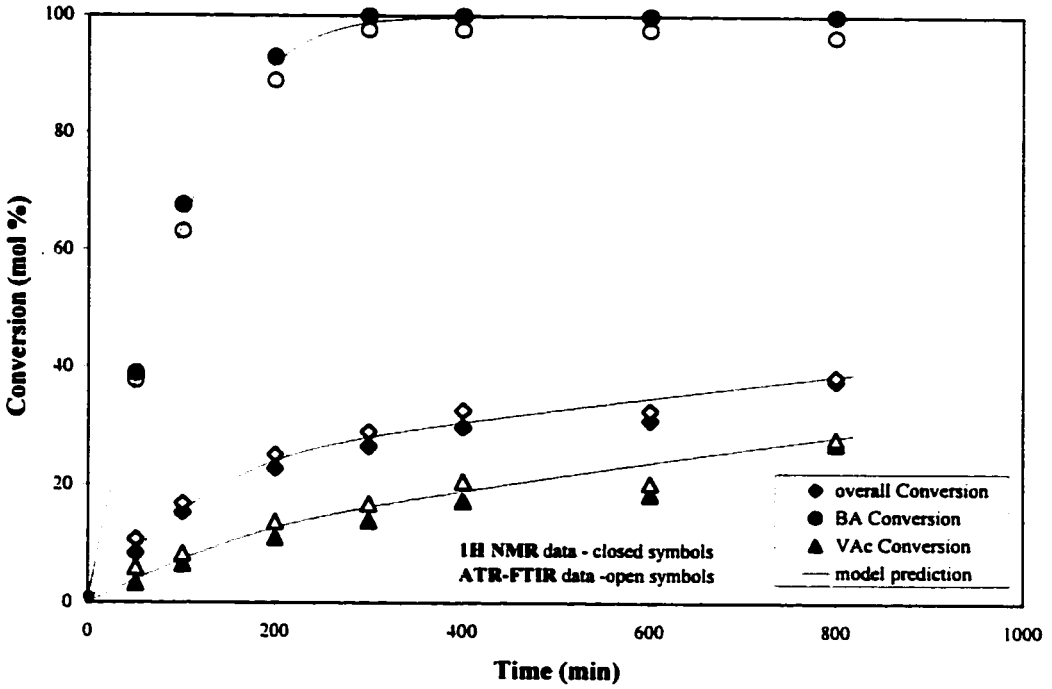

Figure 3.16 Conversion vs. time: BA/VAc (20/80 wt%) solution copolymerization in toluene (50 wt%)

For ATR-FTIR monitoring, the determination of characteristic peaks to represent the changing monomer concentrations was complicated by the presence of both monomers in addition to the solvent in the collected spectra. The same approach was used as in the case of the homopolymerizations. The spectra of pure monomers collected under the same conditions as the reaction spectra were compared to the spectra collected during the reaction. As a result, the peaks observed during the reactions could be easily assigned to each of the monomers. The absorbance peak previously used for the VAc homopolymerization to determine conversion overlapped with an absorbance peak for BA and it was necessary to use another absorbance peak. As described previously, there was no need to subtract solvent because toluene was not absorbing at the same wavelengths as the selected BA and VAc peaks. In Figure 3.17, characteristic spectra for a BA/VAc copolymerization are shown.

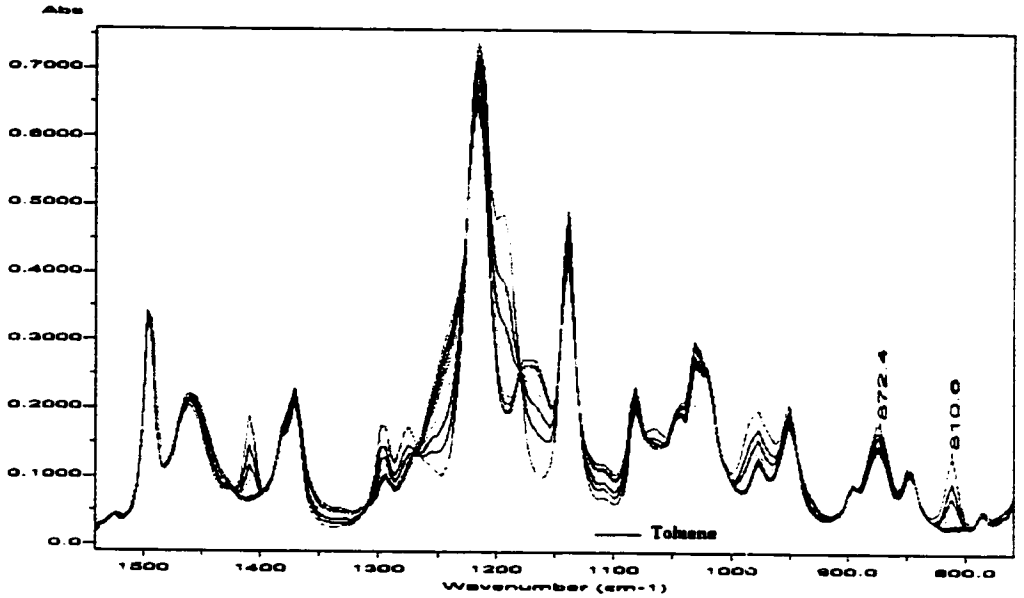

Figure 3.17 ATR-FTIR spectra of BA/VAc (50/50 wt%) solution copolymerization in toluene (50 wt%)

The absorbances of BA at 810.6 cm^{-1} and of VAc at 872.4 cm^{-1} were used to obtain the conversion vs. time data for both copolymerizations (BA/VAc/toluene 25/25/50 wt% and 10/40/50 wt%). Conversion of the individual monomers and the overall conversion were calculated using equations 3.2 and 3.3 after baseline correction. The peak height used in the calculation was referenced to a single point baseline and the peak height at time zero was the peak height determined for the reaction mixture prior to polymerization. Good agreement between the data obtained by the traditional approach using gravimetry and ^{1}H-NMR spectroscopy techniques and using ATR-FTIR spectroscopy was observed. As Chatzi et al.[15] suggested, ATR-FTIR can be a very powerful technique for the determination of not only overall conversion, but also of copolymer composition. Monitoring is not only possible but also sufficiently accurate.

As shown earlier, solution homopolymerizations of BA and VAc are affected by the type and concentration of the solvent. Therefore, it is expected that the solution copolymerization of these two monomers shows similar behavior. Recent work on BA/VAc copolymerization in

solution are scarce apart from that of McKenna and Heredia[38] where ethyl acetate was used as a solvent. They concluded that, similar to the homopolymerization reactions of VAc and BA, the lumped constant ($k_p/k_t^{0.5}$) was dependent on solvent concentration. Our approach in modeling the BA/VAc solution copolymerization in toluene was as follows: the previously determined rate constants for the solution homopolymerizations of BA and VAc in toluene were left unchanged for the particular toluene concentration (50 wt%) and as such, were used for the prediction of the BA/VAc solution copolymerizations. As seen in Figures 3.15 and 3.16, very good agreement between the experimental data and the model predictions was obtained for both BA/VAc ratios in the reaction mixture.

The cumulative number- and weight-average molecular weights for the obtained copolymers are shown in Figures 3.18 and 3.19.

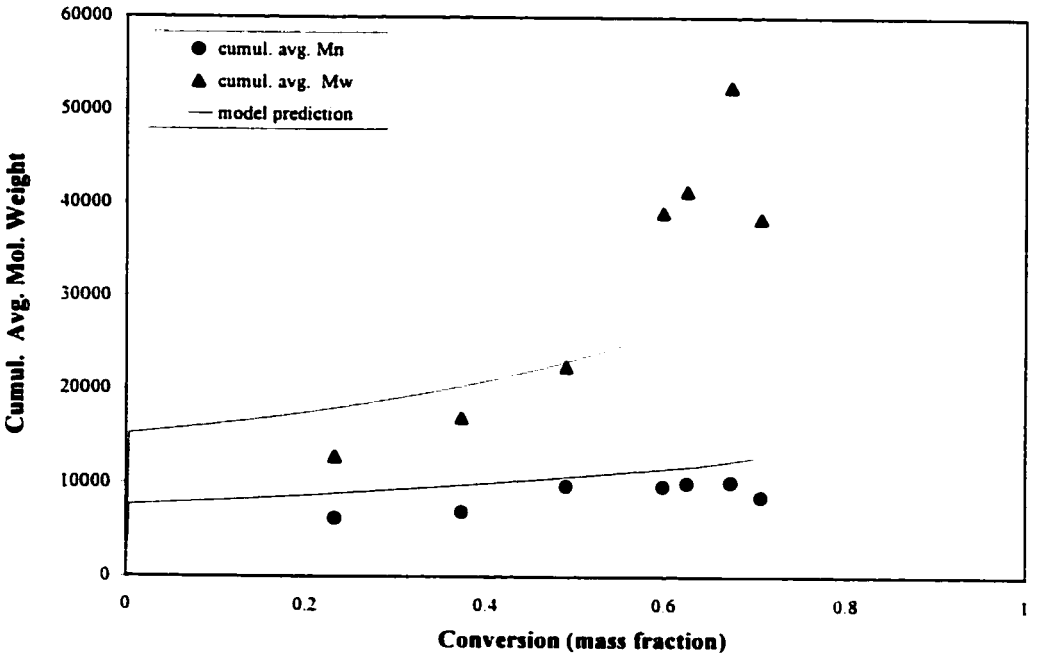

Figure 3.18 Cumulative average molecular weight vs. conversion: BA/VAc (50/50 wt%) solution copolymerization in toluene (50 wt%)

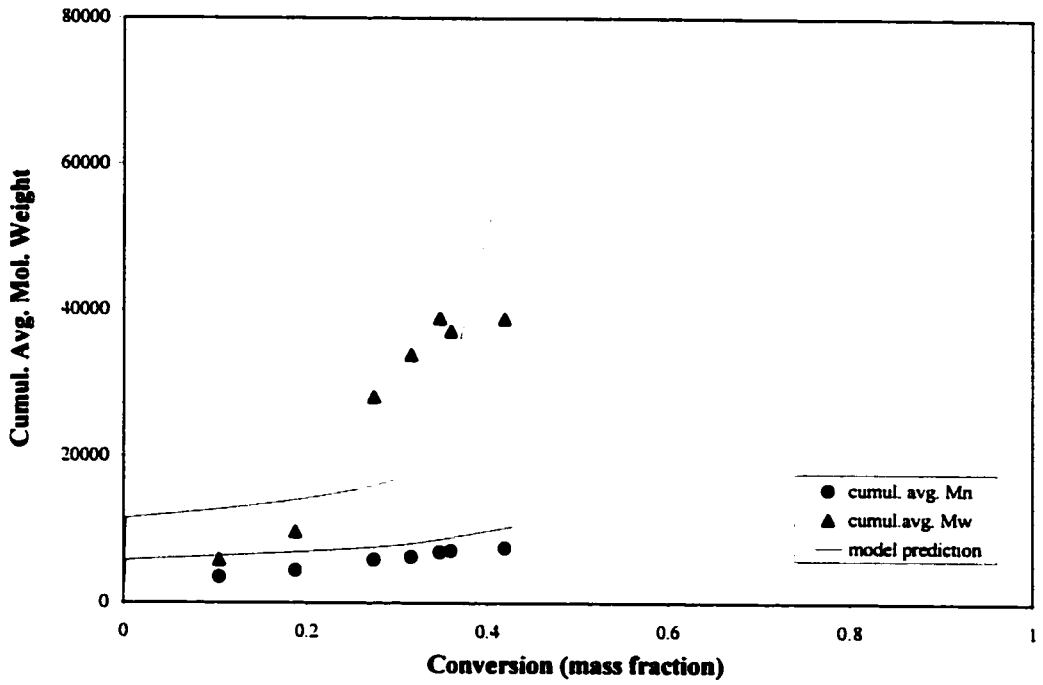

Figure 3.19 Cumulative average molecular weight vs. conversion: BA/VAc (20/80 wt%) solution copolymerization in toluene (50 wt%)

As for the homopolymerizations, a considerable improvement in molecular weight predictions was observed when the lumped constant was changed to incorporate the solvent effect.

CONCLUDING REMARKS

The results presented herein confirm that the monitoring of BA and VAc solution homo- and copolymerizations using an ATR-FTIR probe in an off-line mode is not only possible but also sufficiently accurate compared to traditional techniques (gravimetry and ^{1}H-NMR spectroscopy). These findings are especially important for systems such as BA/VAc copolymerization where there is a possibility of composition drift due to the differences in the reactivity ratios of the monomers. Even though measurements were made off-line, reliable

composition data were obtained without a significant time lag. Only a few minutes were enough to analyze a sample and obtain the results compared to gravimetry and ^{1}H-NMR where significant time lags (measured in days) were present. This advantage of ATR-FTIR measurements provides opportunities for appropriate steps to be taken, if necessary, when composition drift is observed. Our preliminary results for in-line monitoring of BA/VAc emulsion copolymerizations confirm that the approach developed for the off-line measurements is applicable to in-line measurements as well. These findings are useful for industrial scale polymerization monitoring and process control.

Previously reported solvent effects on BA and VAc homo- and copolymerizations in solution were observed in this study. Using previously reported knowledge on these and similar systems, we were able to improve the predictions of our model significantly. This was done by incorporating the change of the lumped constant with the solvent concentration through the change of the termination rate constant. Despite the fact that the change of lumped constant with solvent concentration is evident, there is no real physical evidence that only the termination rate constant changes with the concentration of solvent in these systems. This is especially true for VAc where suspected monomer-solvent interactions that influence k_p are quite likely.[23] Thus, until more accurate measurements of the individual rate constants for BA and VAc are obtained, this uncertainty will continue.

Acknowledgements

The authors wish to gratefully acknowledge financial support from the Natural Science and Engineering Research Council (NSERC) of Canada, the Canada Foundation for Innovation (CFI), and the Province of Ontario Research and Development Challenge Fund.

LITERATURE

1. M.A. Dubé and A. Penlidis, *Polymer*, **36** (3), 587 (1995)
2. A.E. Hamielec, J.F. MacGregor and A. Penlidis, *Makromol. Chem., Macromol. Symp.*, **10/11**, 521 (1987)
3. J. Gao and A. Penlidis, *J. Macromol. Sci. - Rev. Macromol. Chem. Phys.*, **C36**(2), 199 (1996)
4. J. Gao and A. Penlidis, *J. Macromol. Sci. - Rev. Macromol. Chem. Phys.*, **C38**(2), 651 (1998)
5. M.A. Dube, J.B.P. Soares, A. Penlidis, and A.E. Hamielec, *Ind. Eng. Chem. Res.*, **36**, 966 (1997)
6. C. Badeen, M.A.Sc. thesis, Department of Chemical Engineering, University of Ottawa, Ottawa, 2000
7. F.L. Marten and A.E. Hamielec, in *ACS Symposium Series*, H.N. Henderson and T.C. Bouton, Eds., American Chemical Society: Washington, DC, **104**, 43 (1979)
8. T.J. Crowley and K.Y. Choi, *J. Appl. Polym. Sci.*, **55**, 1361 (1995)
9. G. Storti, A.K. Hipp, and M. Morbidelli, *PolyM. Reac. Eng.*, **8** (1), 77 (2000)
10. O. Kammona, E.G. Chatzi, and C. Kiparissides, *J. Macromol. Sci. - Rev. Macromol. Chem. Phys.*, **C39**(1), 57 (1999)
11. G. Dotzlaw and M.D. Weiss, *Chem. Eng. Prog.*, **89**(9), 42 (1993)
12. C. Wu, J.D.S. Danielson, J.B. Callis, M. Eaton, and N.L. Ricker, *Process Control Qual.*, **8**(1), 1 (1996)
13. C. Wu, J.D.S. Danielson, J.B. Callis, M. Eaton, and N.L. Ricker, *Process Control Qual.*, **8**(1), 25 (1996)
14. J. Mijovic and S. Andjelic, *Polymer*, **38**(8), 1295 (1996)
15. E.G. Chatzi, O. Kammona, and C. Kiparissides, *J. Appl. Polym. Sci.*, 63 1997
16. R.F. Storey, T.L. Maggio, and L.B. Brister, *Polymer Preprints*, **40**(20), 964 (1999)
17. R.F. Storey and T.L. Maggio, *Macromolecules*, **33**, 681 (2000)
18. A. Pasquale and T.E. Long, *Macromolecules*, **32**, 7954 (1999)
19. T.F. McKenna, A. Villanueva, and A.M. Santos, *J. Polym. Sci.:Part A: Polym. Chem.*, **37**, 571 (1999)
20. T.F. McKenna and A. Villanueva, *J. Polym. Sci.:Part A: Polym. Chem.*, **37**, 589 (1999)
21. S. Othman, I. Barudio, G. Fevotte and T.F. McKenna, *Polym. Reac. Eng.*, 7(1), 1 (1999)
22. M. Kamachi, M. Fuji, S.-I. Ninomiya, S. Katsuki, and S.-I. Nozakura, *J. Polym. Sci.: Polym. Chem. Ed.*, **20**, 1489 (1982)
23. M.L. Coote, T.P. Davis, B. Klumperman and M.J. Monteiro, *J. Macromol. Sci. - Rev. Macromol. Chem. Phys.*, **C38**(4), 567 (1998)
24. G.T. Russell, R.G. Gilbert, and D.H. Napper, *Macromolecules*, **25**, 2459 (1992)
25. R.A. Hutchinson, J.R. Richards, and M.T. Aronson, *Macromolecules*, **27**, 4530 (1994)

26. B.C. Smith, Fundam*entals of Fourier Transform Infrared Spectroscopy*, CRC Press, Boca Raton (1996)
27. C. Pichot, M.-F. Llauro, and Q.-T. Pham, *J. Polym. Sci.: Polym. Chem. Ed.*, **19**, 2619 (1981)
28. M.A. Dubé and A. Penlidis, *Macromol. Chem. Phys.*, **196**, 1101 (1995)
29. *Polymer Handbook*, 4th ed., J. Brandrup, E.H. Immergut, and E.A. Grulke, Eds., Wiley, New York (1999)
30. American Polymer Standards Corp. a and K values. http://www.ampolymer.com/mark-%20houwink%20parameters.htm
31. N.B. Colthup, L.H. Daly, and S.E. Wiberley, *Introduction to Infrared and Raman Spectroscopy*, 3rd ed, Academic Press, Inc., Boston (1990)
32. D. Lin-Vien, N.B. Colthup, W.G. Fately, and J.G. Grasselli, Eds., In *Handbook of Infrared and Raman Characteristic Frequences of Organic Molecules*, Academic Press, Inc., Boston (1991)
33. M. Fernandez-Garcia, J.J. Martinez, and E.L. Madruga, *Polymer*, **39**(4), 991 (1998)
34. S. Maeder and R.G. Gilbert, *Macromolecules*, **31**, 4410 (1998)
35. J.L. de la Fuente and E.L. Madruga, *J. Polym. Sci.: Part A: Polym Chem.*, **36**, 2913 (1998)
36. Y. Terui and K. Hirokawa, *Vibrational Spectroscopy*, **6**, 309 (1994)
37. G.E. Ham, *Vinyl Polymerization*, Vol. 1, Marcel Dekker Inc., New York (1967)
38. T.F. McKenna and M.F. Heredia, *Polymer Journal*, **31**(1), 7 (1999)

Chapter 4

PAPER II

Butyl Acrylate/Vinyl Acetate Emulsion Polymerization:

In-line Monitoring Using ATR-FTIR Spectroscopy

Renata Jovanović and Marc A. Dubé*
Department of Chemical Engineering, University of Ottawa,
161 Louis Pasteur, P.O. Box 450 Stn. A, Ottawa, ON, K1N 6N5 Canada
* dube@genie.uottawa.ca

ABSTRACT:

A study of butyl acrylate/vinyl acetate (BA/VAc) batch emulsion copolymerization was carried out in a pilot-scale reactor. Conversion and copolymer composition were monitored off-line using standard techniques (gravimetry and ^{1}H-NMR spectroscopy) and in real time, *in situ* using ATR-FTIR spectroscopy. The real-time infrared peak profiles of monomers were used to calculate conversion and copolymer composition for in-line monitoring. The data obtained using the ReactIR™ 1000 reaction analysis system showed good agreement with data obtained using standard techniques. The limitations in real-time monitoring of BA/VAc emulsion polymerizations using ReactIR™ 1000 are also discussed.

Key words: butyl acrylate, vinyl acetate, polyvinyl alcohol, emulsion polymerization, ATR-FTIR, in-line monitoring, ReactIR™ 1000

INTRODUCTION

Better heat transfer due to lower viscosity and the absence of toxic solvents make emulsion polymerization an attractive choice in the production of architectural coatings, adhesives, caulks and sealants. Performed either in batch or semi-batch mode, emulsion polymerizations yield final products that can be used "as is", which makes this process even more interesting from an economic point of view.[1] Among the most common monomers employed in emulsion polymerization is vinyl acetate (VAc). Its emulsion homo- and copolymerizations with different monomers have been extensively studied over several decades.[2,3,4] One of the monomers that VAc can be copolymerized with is butyl acrylate. Due to differences in the glass transition temperatures of these two monomers (BA= -54 to -49 °C; VAc= 23-29 °C)[5] different copolymer compositions will lead to a range of mechanical properties in the final product. The final properties are also affected by the particle size and molecular weight distributions of the copolymer.

Obtaining desired copolymer properties is further complicated when the selected monomers have different reactivities. These are described by the reactivity ratios, parameters in the Mayo-Lewis equation.[6] Because the reactivity ratios of BA and VAc are quite different (r_{BA}=5.93, r_{VAc}=0.026),[7] composition drift during batch copolymerization is inevitable. Thus, monitoring or modeling of this and similar systems is of great importance. Furthermore, better product characterization and process control using in-line monitoring could lead to increased product quality and process safety in both batch and semi-batch emulsion polymerizations.

For emulsion polymerization processes, there is a considerable interest in continuously monitoring conversion, copolymer composition, molecular weight and particle size. The

objective in this study was to monitor conversion and copolymer composition. Continuous monitoring of conversion and copolymer composition has come a long way since the first reliable techniques were reported in the mid-eighties.[8] As those authors predicted, many of the techniques reported then as off-line techniques are now used on-line. Recent overviews on hardware sensors for conversion and copolymer composition monitoring are given by Hergeth[9] and Kammona et al..[10] On-line and in-line monitoring techniques have to be distinguished because the latter are performed *in situ* and thus, do not require sampling loops or by-passes.[11] When on-line techniques are used, the sensitivity of the reaction mixture to shear can present a serious obstacle because it can lead to demixing and/or flocculation inside the sampling loop or by-pass. Densitometry[12] and dilatometry[1] are currently used as on-line monitoring techniques while ultrasonic sensors[13] and gas chromatography are being used in both on-line[14] and in-line[15] modes. Calorimetry is employed as an on-line technique.[16] Considerable attention has been devoted to the utilization of spectroscopic techniques such as near infrared (NIR) [17-20] and mid infrared (MIR)[21-23] spectroscopy in conversion and copolymer composition monitoring because they can be employed *in situ* to give real-time structural and kinetic data.

A commercially available instrument, the ReactIR™ 1000 (ASI Applied Systems Inc.) based on ATR-FTIR (Attenuated Total Reflectance – Fourier Transform Infrared) spectroscopy has been used for in-line monitoring of polymerization reactions in some recent studies. It was used for monitoring the living carbocationic polymerization of isobutylene,[24-27] the free radical polymerization of styrene[28] and an ester-exchange polymerization mechanism.[29] Apart from the works of Full et al.[30] on the monitoring of tetrahydrofurfuryl methacrylate microemulsions, and Hua and Dubé[31] on the in-line monitoring of homo- and multicomponent polymerizations involving VAc, BA and methyl methacrylate monomers, there are no published studies on the

use of this reaction monitoring system for emulsion polymerization monitoring. An ability to monitor emulsion polymerizations of a commercially attractive system such as BA/VAc in-line would have a great impact on product quality as well as process control, safety, and economics.

In this study, high solids (50%) emulsion copolymerizations of BA and VAc were conducted in a pilot scale reactor. Partially hydrolysed poly(vinyl alcohol) was used as the emulsifier in order to enhance the rheological properties of the latexes as well as the properties of the final targeted products – adhesives. Polymerization processes were monitored in-line using ATR-FTIR spectroscopy. Our intention was to evaluate the results obtained using in-line ATR-FTIR spectrometry and compare them to results obtained by standard off-line techniques such as gravimetry and ^{1}H-NMR spectrometry.

EXPERIMENTAL PROCEDURES AND TECHNIQUES

Reagent purification

Butyl acrylate (BA) and vinyl acetate (VAc) (Sigma-Aldrich) were received inhibited by 0.05 ppm hydroquinone. To remove the inhibitor, VAc was distilled under vacuum while BA was washed three times with a 10% (vol/vol) sodium hydroxide solution, washed three times with distilled water, dried over calcium chloride and distilled. Distillations were done 24h prior to polymerization and the monomers were stored at –10°C. The emulsifiers, polyvinyl alcohol (PVOH) (Sigma-Aldrich) with a weight-average molecular weight of 9000-10000 g/mol and a degree of hydrolysis of 80% and sodium dodecyl sulfate (SDS) (BHD Inc) were used without further purification. The initiator, ammonium persulfate (APS) (J.T. Baker Chemicals), the sodium bicarbonate buffer, as well as the n-dodecyl mercaptan (Sigma-Aldrich) chain transfer

agent (CTA) were employed as packaged. All solvents (toluene, tetrahydrofuran (THF), chloroform-d, and others) used for sample characterization were not further purified.

Experimental procedure

All reactions were performed in a jacketed 5L pilot-scale stainless steel batch reactor. The reactor contents were stirred with a propeller turbine agitator at 200 rpm. The remote sensor for ATR-FTIR monitoring was inserted through an opening in the top head. The final position of the probe (approximately 2mm above the agitator blades) ensured monitoring of a well-mixed reactor content. At the top head were also located feeding, sampling and nitrogen ports, and a condenser. Three platinum resistance thermometers (PR-13) were used to detect the temperature of the process, and the heating and cooling liquids. The process temperature was controlled using a PID controller using LabVIEW™ (Graphical Programming for Instrumentation, National Instruments, 1998).

The emulsion polymerization experimental conditions are summarized in Table 4.1. In all runs, ammonium persulfate was used as initiator, $NaHCO_3$ as buffer and n-dodecyl mercaptan as chain transfer agent. Poly vinyl alcohol with a weight-average molecular weight of 9000-10000 g/mol and an 80% degree of hydrolysis was used as an emulsifier in all runs except in Run S where sodium dodecyl sulfate (SDS) was employed. Distilled de-ionized water was used in all runs. The total volume of the reaction mixture was approximately 2.5 L.

The following experimental procedure was employed in all runs. A day prior to the experiment, the monomers were purified according to standard techniques.[32] A PVOH solution was made using a magnetic stirrer and left covered overnight.

Table 4.1 Experimental conditions (all amounts in phm, parts per hundred parts monomer, unless otherwise indicated)

Run	Feed composition BA/VAc	Initiator	Surfactant	CTA	Buffer	Water	T (°C)
Run S	50/50	0.167	4.29*	0.861	0.167	245.73	60
Run 2	50/50	0.100	8.86	0.501	1.01	110.46	60
Run 3	20/80	0.159	8.86	0.502	1.00	110.52	60
Run 4	35/65	0.159	8.85	0.502	1.06	110.57	60
Run 5	50/50	0.039	8.86	0.499	1.01	110.40	80
Run 6	20/80	0.028	8.86	0.512	1.03	110.43	80
Run 7	35/65	0.013	8.86	0.502	0.442	110.43	80

*Sodium dodecyl sulfate was used as an emulsifier in this run.

When the set point temperatures were reached, the PVOH solution, most of the water, and the buffer were charged into the reactor and the reactor was closed. The ATR-FTIR probe was inserted, the agitation was started and the reactor contents were purged with nitrogen for about 15 min. When the process temperature set point was reached, a background spectrum was collected. Monomers and CTA were then charged to the reactor. The charging vessel and pipes were flushed with 100 mL of water. When the process temperature set point was again reached, the initiator solution was charged into the reactor and the ATR-FTIR reaction monitoring and process temperature monitoring were started simultaneously (reaction time, t=0). During the reaction, at suitable time intervals, samples were taken through a sampling port for gravimetric and ^{1}H-NMR spectroscopy measurements. Approximately 3g of sample was poured into a pre-weighed dish and allowed to dry.

Off-line product characterization

Gravimetry. Gravimetry was used for the determination of conversion, X (mass %), and was based on total polymer. The samples were placed in a pre-weighed dish and weighed. After evaporation of water at room temperature, the samples were dried in a vacuum oven (~30°C) until constant weight was reached. The following equation was used to calculate the % solids:

$$weight\ fraction\ solids = \frac{(wt.of\ dried\ sample\ and\ dish - wt.of\ empty\ dish)}{(wt.of\ dish\ and\ sample - wt.of\ empty\ dish)} \tag{4.1}$$

The conversion was calculated after correcting for the emulsifier, buffer, initiator and CTA present in the sample using the following expression:

$$X(wt.fraction) = \frac{[wt.fr.\ solids - (wt.fr.of\ PVOH + wt.fr.of\ APS + wt.fr.of\ buffer + wt.fr.of\ CTA)]}{(wt.fraction\ monomers\ initially)} \tag{4.2}$$

In order to compare the individual monomer conversions obtained by standard techniques to results obtained using the ATR-FTIR probe, the weight fraction conversion was transformed into mol fraction conversion for run S.

^{1}H-NMR spectroscopy. Cumulative copolymer compositions for run S (all other runs yielded insoluble polymers) were determined using a Bruker AMX-500 Fourier transform ^{1}H-NMR spectrometer. The analyses were carried out in deuterated chloroform (chloroform-d, approx. 2% (w/v) solution) at room temperature. The relative amounts of monomer bound into the polymer were estimated using the areas under the appropriate absorption peaks: BA ($\delta \approx 4.0$ ppm)

representing $-OCH_2$ group and VAc ($\delta \approx 4.9$ ppm) representing the α-hydrogen. Using areas under the peaks, the weight fractions of BA and VAc monomers bound into the polymer were calculated. The use of these spectral peaks for the determination of the cumulative copolymer composition has been reported previously.[33]

ATR-FTIR reaction monitoring system

Polymerization reactions were monitored in-line using an attenuated total reflectance (ATR) Fourier transform infrared (FTIR) spectrometer – ReactIR™ 1000 (ASI Applied Systems, Inc). This reaction monitoring system is designed for in-line monitoring of chemical reactions in the mid infrared spectral region (4000-650 cm^{-1}) using light conduit technology and a diamond composite (DiComp) remote sampling device. Light conduit technology consists of six mirrors and two tubes providing a purged path for the travel of the infrared beam from its source to the insertion probe and back to the detector. The DiComp insertion probe has a six-reflection bi-layer ATR element diamond surface (6mm diameter) at the top of a stainless steel body (length 7.25", diameter 0.625"). This reaction set up enables non-destructive in-line monitoring in hostile reaction environments without complicated changes in reactor design and sampling. Unlike the conventional transmission IR technique, in the ATR technique, the intensive absorbance of water in the MIR region (4000-600 cm^{-1}) presents no obstacle to obtain absorbance peaks of other latex components. This is due to the very short depth of penetration of the IR beam into the reaction medium (1-10 μm), which enables effective subtraction of the water contribution.[22] For the monitoring of BA/VAc emulsion polymerizations, the standard reaction acquisition mode was employed. Prior to the collection of background and reaction

spectra, the number of scans and resolution were selected to give the best signal to noise ratio. For the monitoring of BA/VAc emulsion polymerizations under the conditions used in Table 1, 256 scans and a resolution of 4 cm^{-1} were found to give a satisfactory signal to noise ratio. Under these conditions, the acquisition of spectra took 84.7s. To ensure continuous monitoring, the reaction spectra were acquired every 2 minutes.

The basis for monitoring polymerization reactions is the determination of the characteristic peaks that represent functional groups inside a monomer or polymer and monitoring their absorbance throughout the course of the reaction. The concentration of a component is proportional to the absorbance, which can be measured as peak height, peak height ratio, peak area or peak area ratio. Real-time peak profiles of monomers (changes in absorption during the course of reaction for a specific component) were used to calculate conversion and copolymer composition. The following expression was used to obtain the conversion of the individual monomers, x, in the reaction mixture:

$$x(mol\ fraction) = 1 - \frac{peak\ height\ at\ time\ t}{peak\ height\ at\ time\ t = 0} \tag{4.3}$$

where peak height at time t=0 represents the absorbance of the component in the reaction mixture prior to polymerization.

Overall conversion, X, can be expressed in mol or weight fraction using the following formulae:

$$X(mol\ fraction) = \frac{n_1}{n_1 + n_2} x_1(mol\ fraction) + \frac{n_2}{n_1 + n_2} x_2(mol\ fraction) \tag{4.4}$$

where $\frac{n_i}{n_i + n_j}$ denotes the mole fraction of monomer i in the reaction mixture or

$$X(weight\ fraction) = \frac{m_1}{m_1 + m_2} x_1(weight\ fraction) + \frac{m_2}{m_1 + m_2} x_2(weight\ fraction) \tag{4.5}$$

where $\frac{m_i}{m_i + m_j}$ denotes the mass fraction of monomer *i* in the reaction mixture. This method has been previously reported by Chatzi et al..[22]

RESULTS AND DISCUSSION

In order to follow a reaction using ATR-FTIR spectroscopy, a background spectrum of a mixture of water, surfactant, CTA and buffer was collected. The background spectrum (Figure 4.1) was automatically subtracted from the reaction spectra. Typical reaction spectra of a BA/VAc emulsion copolymerization are shown in Figure 4.2.

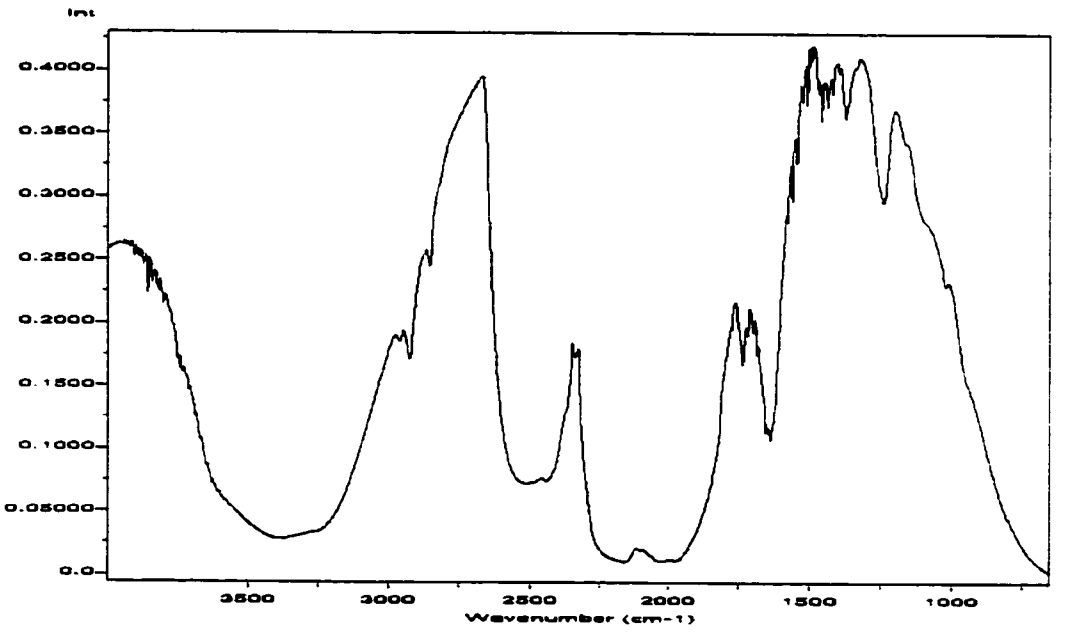

Figure 4.1 Typical background spectra for BA/VAc emulsion copolymerizations

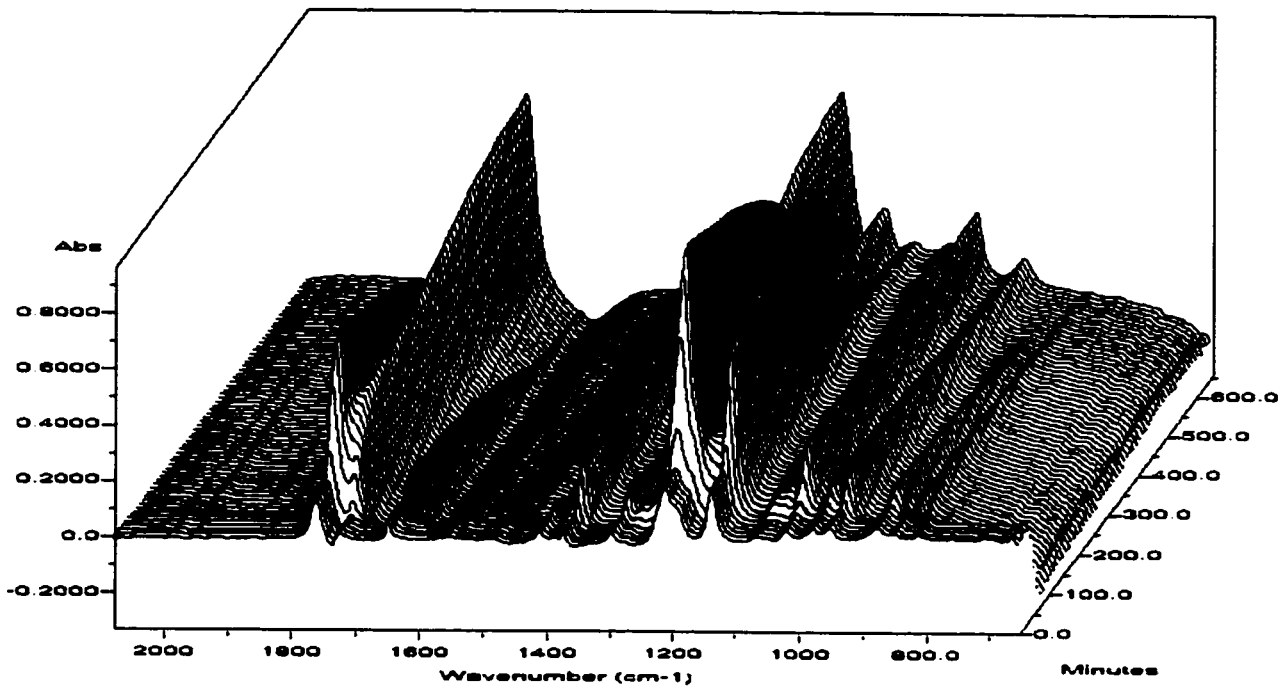

Figure 4.2. Typical reaction spectra for BA/VAc emulsion polymerization

There are several peaks that can be clearly assigned to monomer consumption or polymer build-up during the course of reaction. These characteristic peaks can be used for in-line monitoring of individual monomer conversion and overall conversion. In this work, the characteristic peaks of the monomers were used. The reaction spectra were compared to the spectra of the pure monomers in order to obtain the vibrational assignments for the peaks of interest. Details of this procedure and vibrational assignments for absorbances for BA and VAc monomers were previously described.[34] Among the several monomer absorbance bands that showed no interference with the absorbance bands of other components in the reaction mixture, the following were selected to follow the BA/VAc emulsion polymerization reaction: BA absorbance band at 810.4 cm^{-1} assigned to $=CH_2$ twist[35,36] and VAc absorbance at 1138 cm^{-1} assigned to C-O-C stretching.[35,37] Once identified, these absorbance bands were used for in-line

monitoring of BA/VAc emulsion copolymerizations. Real-time peak profiles (Figure 4.3) were used to obtain the individual monomer conversion based on equation 4.1 and the overall conversion was calculated based on equation 4.2.

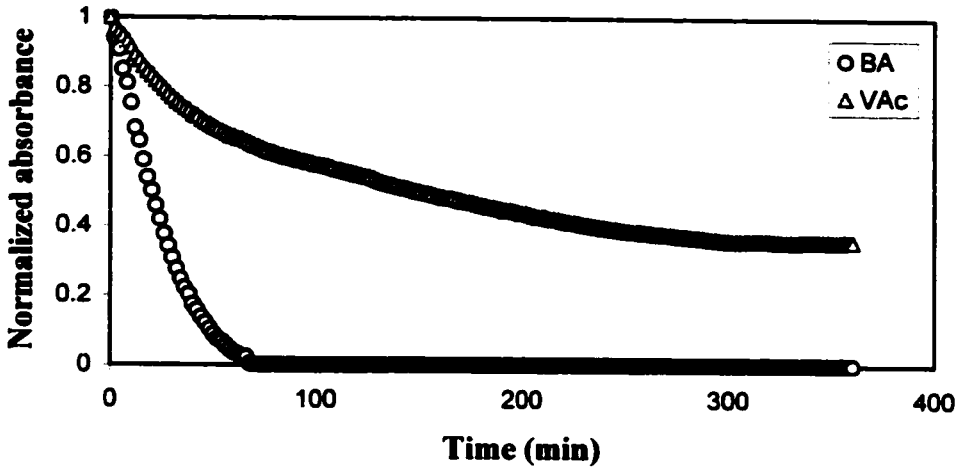

Figure 4.3 Normalized real-time peak profiles for BA and VAc monomers (Run 5)

In order to evaluate ATR-FTIR spectroscopy as an in-line monitoring technique, the results obtained with this technique should be compared to the results obtained using standard techniques: gravimetry for overall conversion and a combination of ^{1}H-NMR spectroscopy and gravimetry for conversion of individual monomers (copolymer composition). During this work a particular challenge arose due to the insolubility of the obtained polymers. The insolubility of the polymers was probably due to the combination of grafting of poly(vinyl alcohol) at the surface of particles and cross-linking due to the presence of OH groups from poly(vinyl alcohol).[4] It is well known that PVOH is not soluble in organic solvents and its solubility in water is strongly affected by its molecular weight and degree of hydrolysis.[38] Different combinations of solvents also resulted in poor solubility. This finding limited the use of standard techniques to gravimetry only. Therefore, it was not possible to obtain copolymer compositions using ^{1}H-NMR spectroscopy. Because of the great industrial interest in the use of PVOH as polymeric surfactant

and its positive effects on latex viscosity and final adhesive properties,[38] it was not replaced with an ionic surfactant in this project. Therefore, an alternative method was established to confirm the in-line monitoring data using ATR-FTIR spectroscopy. A BA/VAc emulsion polymerization was carried out under the same reaction conditions but with sodium dodecyl sulfate (SDS) as emulsifier. The use of this ionic emulsifier resulted in soluble polymers. Therefore, it was possible to employ standard off-line monitoring techniques. The results of this run and others that have been performed in our lab[31] were used to confirm the close agreement between the in-line monitoring ATR-FTIR data and off-line gravimetric and ^{1}H-NMR spectroscopy data.

In Figure 4.4, the results obtained using SDS as a surfactant are shown. The overall conversion monitored in-line using ATR-FTIR spectroscopy (open symbols) and off-line using gravimetry (closed symbols) showed good agreement. Individual monomer conversion data obtained using in-line and off-line techniques also showed satisfactory agreement.

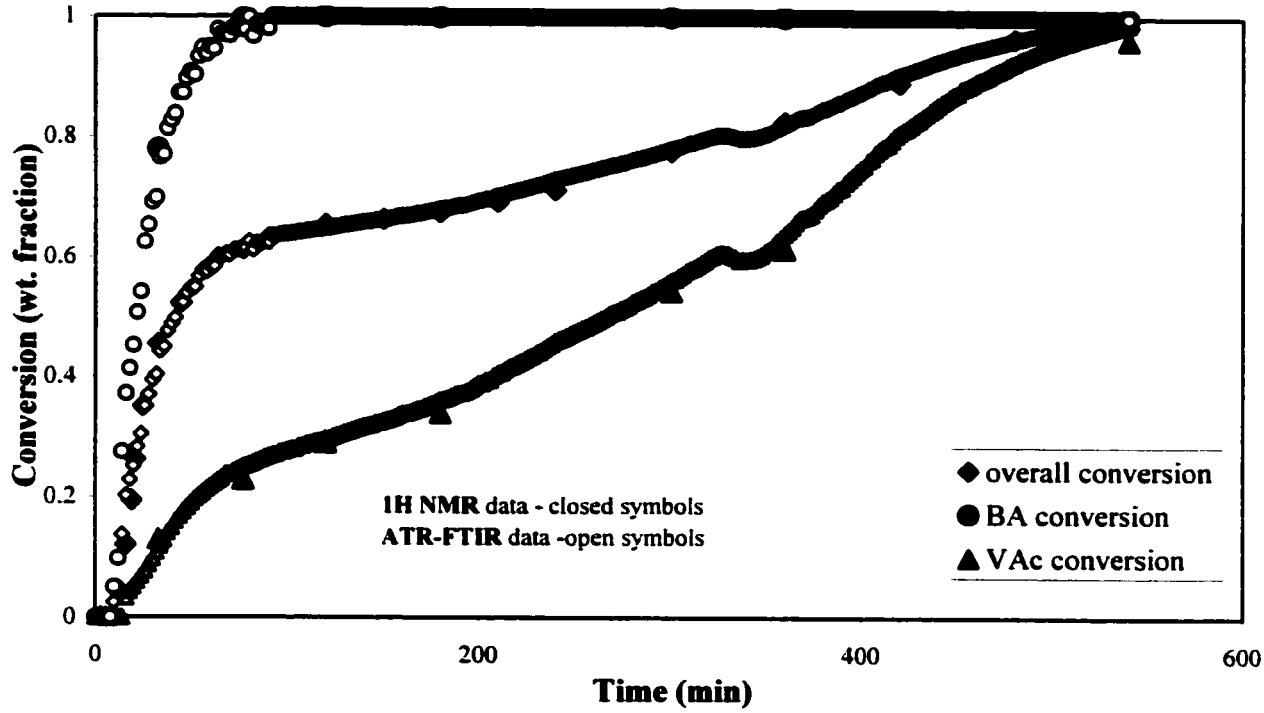

Figure 4.4 Conversion vs. time: BA/VAc (50/50 wt%) with SDS as emulsifier

Based on these and the results obtained for emulsion co- and terpolymerizations of other monomers[31] we concluded that if the overall conversion data obtained in-line and off-line showed close agreement, there is no evidence that individual monomer conversion data are not followed in-line sufficiently accurately. This is also due to the fact that the overall conversion data obtained using gravimetry are combined with ^{1}H-NMR spectrometry data in order to obtain individual monomer conversions. The error analysis on ATR-FTIR data obtained in an off-line mode showed that the associated error in the data is approximately ±2.5%.[31] A similar error analysis performed on BA and VAc emulsion polymerizations for gravimetric data showed an error of ±0.77% and ^{1}H-NMR data for BA ±0.0114% and VAc ±0.0338%.[39]

In Figures 4.5 through 4.8, the results of runs 2, 5, 4 and 7, respectively are shown. In all figures, open symbols represent in-line monitoring data obtained using ATR-FTIR spectroscopy and closed symbols represent off-line gravimetric data. Clearly, the ATR-FTIR data compared well to the gravimetric data for overall conversion. As mentioned earlier, it was not possible to compare the *individual* monomer conversion data obtained using ATR-FTIR spectroscopy to standard techniques due to the insolubility of polymers. As discussed earlier, these are monitored with sufficient accuracy when ATR-FTIR and gravimetric data show good agreement for overall conversion.

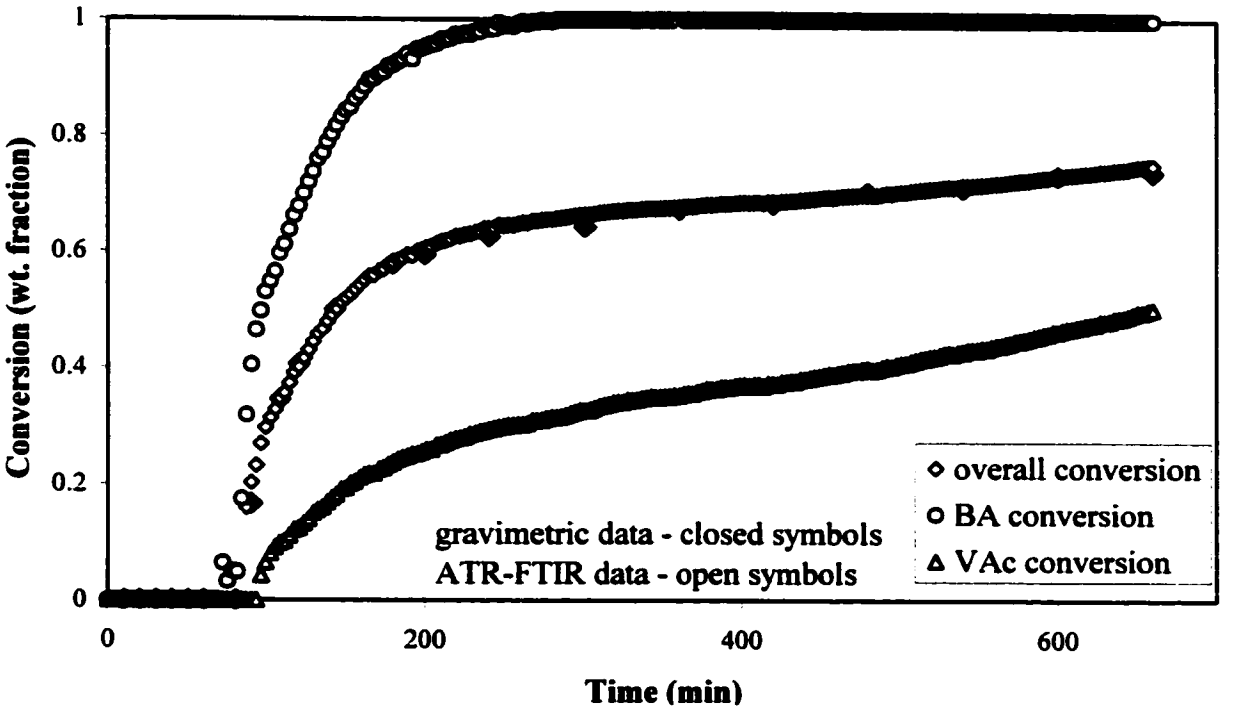

Figure 4.5 Conversion vs. time: BA/VAc 50/50 wt% at 60°C (Run 2)

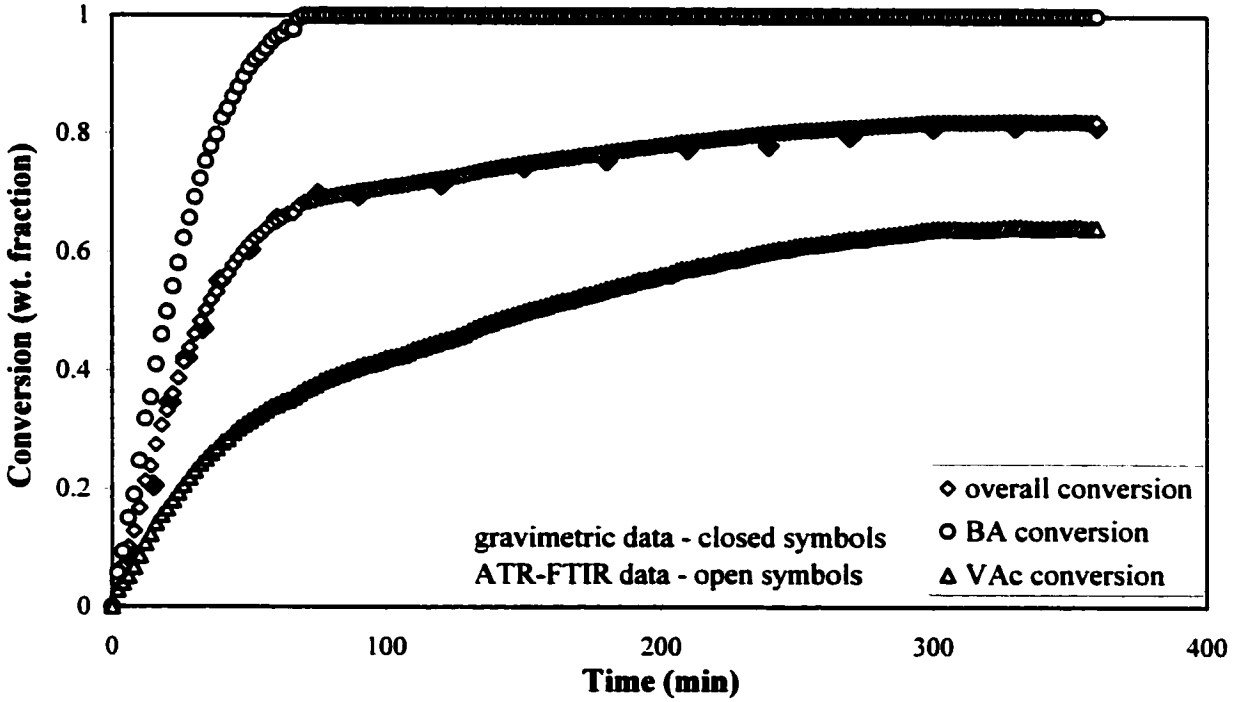

Figure 4.6 Conversion vs. time: BA/VAc 50/50 wt% at 80°C (Run 5)

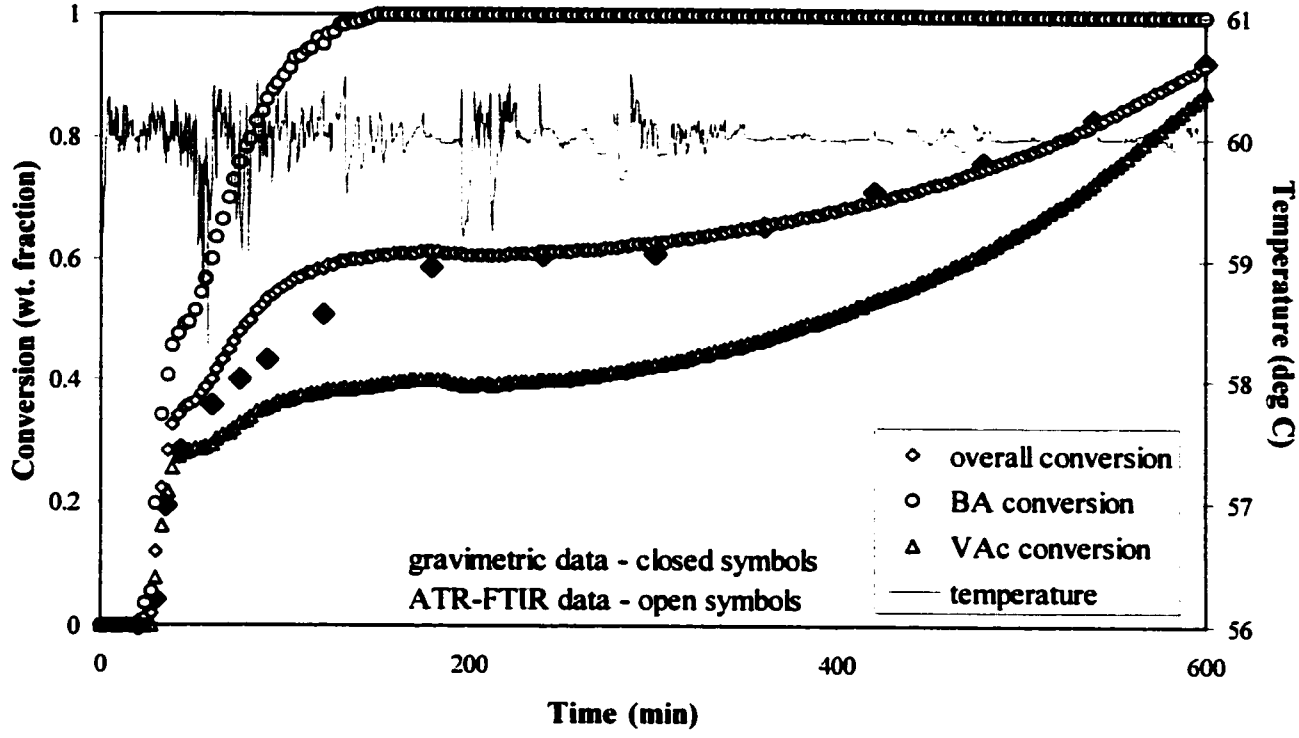

Figure 4.7 Conversion vs. time: BA/VAc 35/65 wt% at 60°C (Run 4)

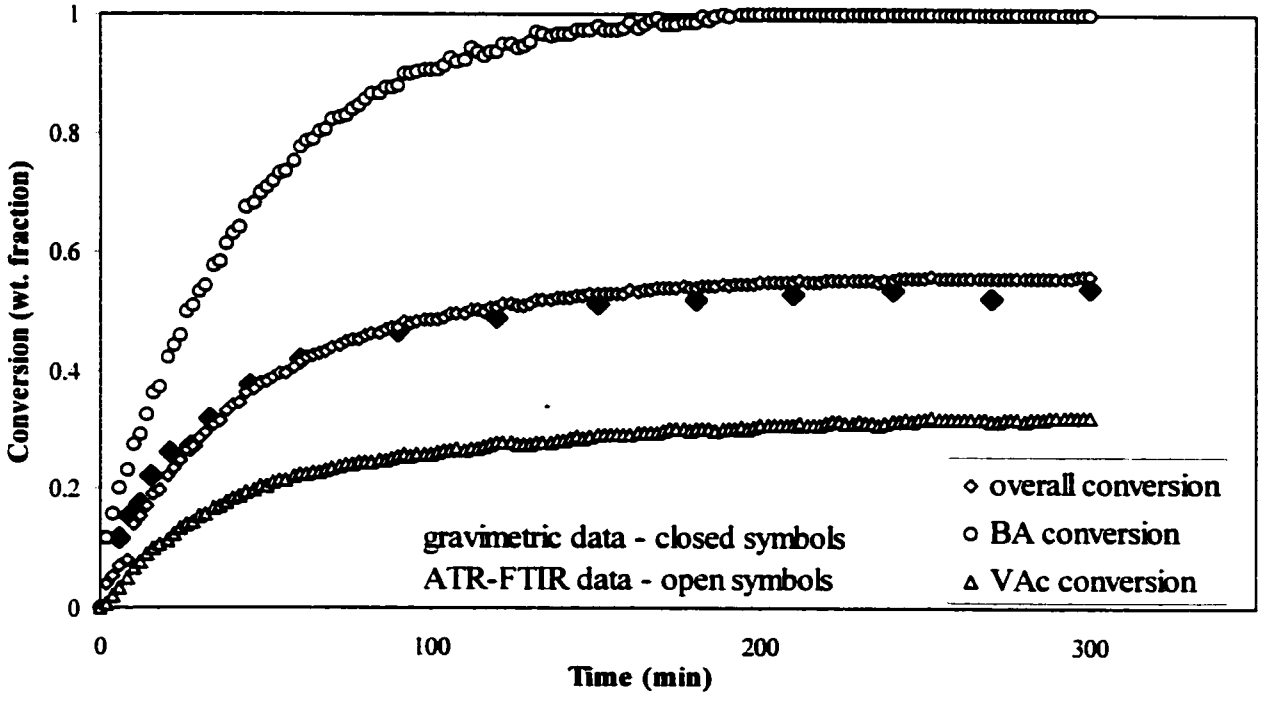

Figure 4.8 Conversion vs. time: BA/VAc 35/65 wt% at 80°C (Run 7)

Increases in polymerization temperature placed a greater challenge to in-line monitoring due to the much higher rate of reaction. The acquisition of reaction spectra performed every two minutes (256 scans, resolution $4cm^{-1}$) ensured continuous monitoring. As can be seen in Figures 4.6 and 4.8, the in-line and off-line monitoring data for overall conversion are in close agreement under these conditions as well. The discrepancy between the gravimetric and ATR-FTIR spectrometry data observed for run 4 between approximately 40 to 60% conversion is explained later.

Limiting conversions observed in all cases (e.g. Figure 4.6 shows a limiting conversion of 80%) are consistent with previous experimental observations.[39] Some of the experiments were repeated and showed similar limiting conversions. In addition, a characteristic two-stage rate effect was observed. This effect has been observed in other BA/VAc emulsion polymerizations.[39] During the first period of the reaction (up to ~40%), the copolymerization proceeds almost entirely as a BA homopolymerization. When BA is almost completely consumed, VAc monomer starts to react to a greater extent. This was also confirmed by ATR-FTIR spectroscopy. The normalized real-time peak profiles (see Figure 4.3) showed that the BA curve is initially much steeper than that for VAc, indicating that BA monomer is consumed at a much faster rate than VAc monomer. At about 70 minutes after the beginning of the reaction, the BA absorbance reached zero (i.e. BA monomer was completely consumed) while approximately 70% of the VAc monomer was unreacted. This is consistent with literature findings, indicating that the initial copolymer formed is richer in PBA while in the latter stages, it is richer in PVAc.

Apart from the capability of using ATR-FTIR spectroscopy to successfully monitor chemically heterogeneous reactions such as emulsion polymerizations, there are other advantages to this instrument. ATR-FTIR is able to follow induction periods successfully (e.g.

see Figure 4.7). Knowing that induction is present, allows one to take proper corrective action, such as the addition of extra initiator, early in the reaction. While searching for a stable recipe for the BA/VAc copolymerization, there were several occasions where catastrophic coagulation occurred. ATR-FTIR spectroscopy indicated the occurrence of catastrophic coagulation inside the reactor (e.g. see Figure 4.9). The catastrophic coagulation in BA/VAc emulsion polymerization can be recognized by the broadening of absorbance peak at (1138 cm^{-1}) as well as the disturbed pattern along the time axes as indicated in Figure 4.9. Even though there were no quantitative measurements of coagulum taken, the importance of these characteristic signs in the reaction spectra lays in the fact that, in each case, they were observed before the separation of phases was observed in the samples taken from the reactor. An early detection of catastrophic coagulation in the reactor can save time and energy that would be otherwise spent on the removal of coagulum from the reactor.

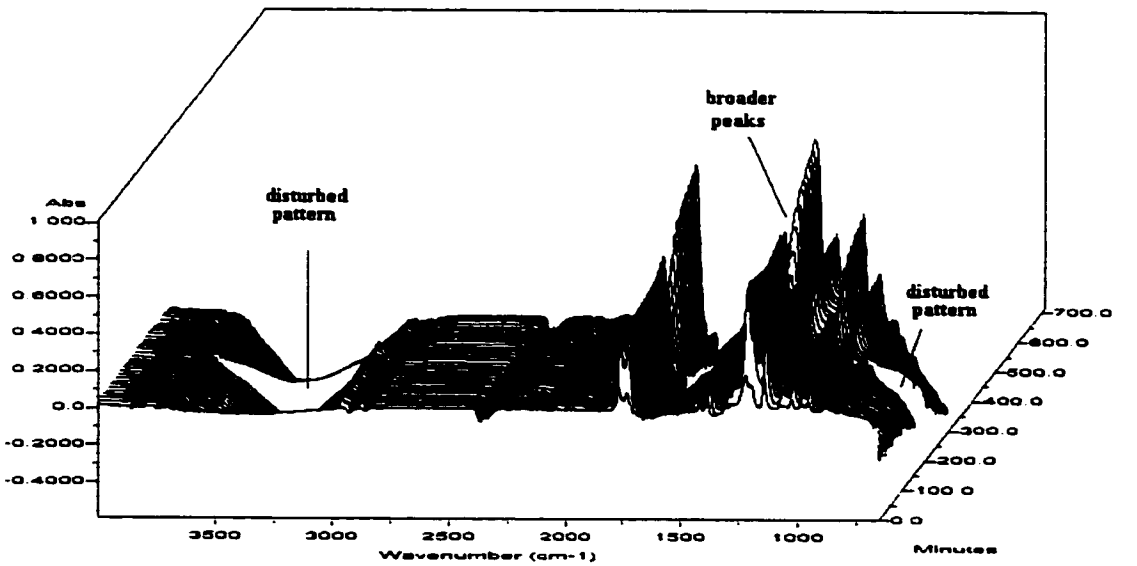

Figure 4.9 Characteristic reaction spectra when catastrophic coagulation occurs

Despite the encouraging results of our work, some limitations in the use of the instrument were encountered. The most important limitation would be the need for very strict temperature control. Polymerization reactions in our lab are usually performed under isothermal conditions but there are two particular cases where temperature drift can considerably contribute to the discrepancy between the data obtained using ATR-FTIR spectroscopy and gravimetric data. Under conditions where a temperature off-set is approximately 2-3°C and subsequent stabilization period is longer than 20 minutes, the probe readings showed disagreement with the gravimetric data even after the set point was re-established. Another case was the sharp decrease or increase in temperature (approximately 2°C) followed by the shorter stabilization period (less than ~20 minutes) compared to reaction time (4-5 hours) as in BA/VAc 35/65 wt% at 60°C. During that period, disagreement (between 5-10 wt%) in the data obtained by gravimetry and ATR-FTIR spectroscopy was observed. After the set point was established, the difference between the gravimetric and ATR-FTIR data diminished. In both cases, the trend observed in the process temperature was followed by the ATR-FTIR probe readings but in an inverted way. The overestimation of the probe readings was observed in cases where the temperature was lower than the set point and the underestimation in cases where the temperature was higher than the set point.

A number of homo- and multicomponent polymerizations of different monomers (BA, VAc, MMA) in solution and emulsion were successfully monitored using the ATR-FTIR probe in an off-line or in-line mode.[31,34] Despite this, the results obtained in-line for emulsion polymerization BA/VAc (20/80 wt%) showed a greater discrepancy than expected (see Figures 4.10 and 4.11). The experiments were repeated several times and yielded the same outcome: the

ATR-FTIR and gravimetric data displayed a disagreement near the middle of the reaction. However, near the end of the reaction, improved agreement was observed.

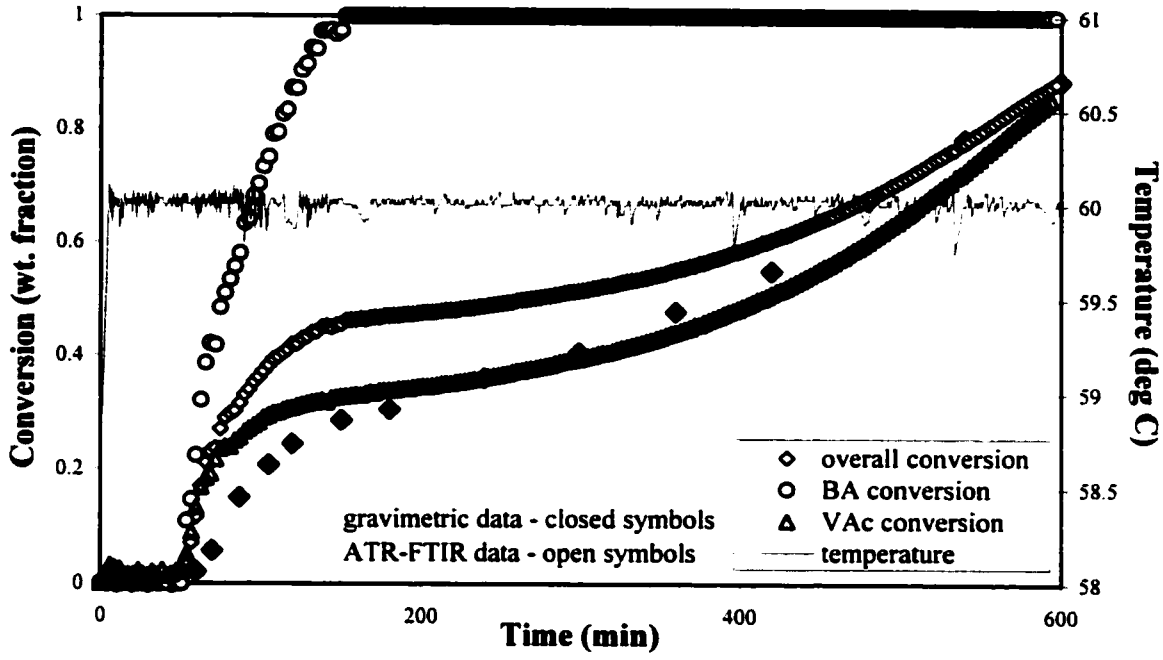

Figure 4.10 Conversion vs. time: 20/80 wt% at 60°C

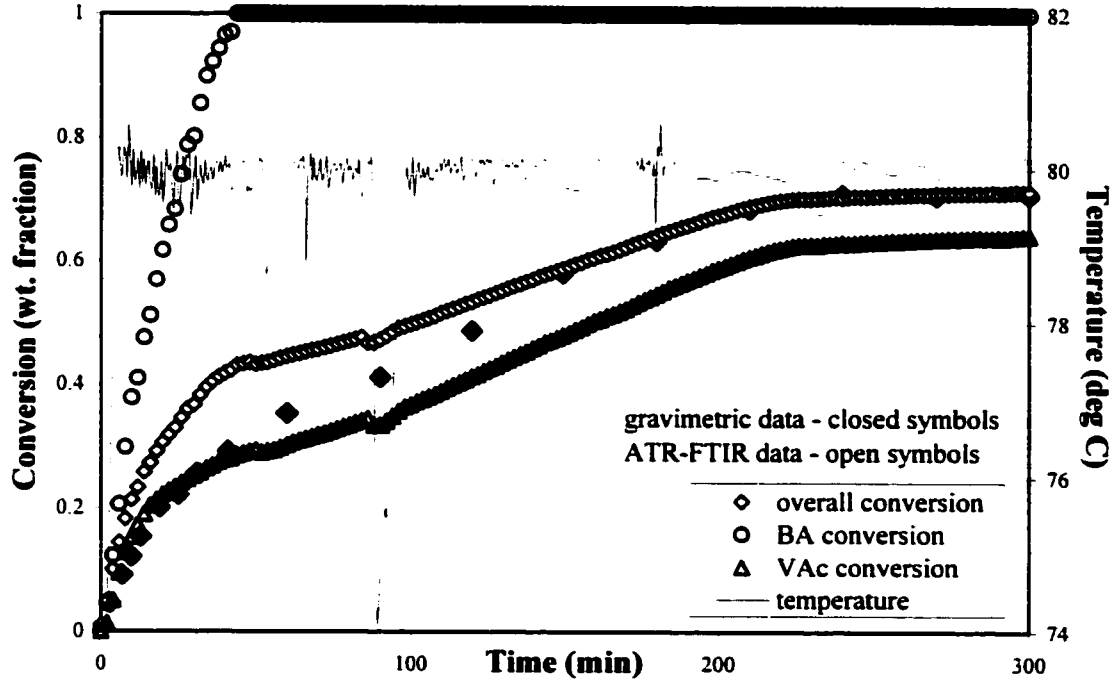

Figure 4.11 Conversion vs. time: 20/80 wt% at 80°C

These errant reaction profiles were similar to those observed under poor temperature control. However, in this case, temperature control was satisfactory as can be seen in Figure 4.10. Temperature control was less favorable in run 6 (see Figure 4.11) but the discrepancy between the ATR-FTIR and gravimetric data started before any temperature excursions. Good agreement between the two techniques was established at about 60% conversion. These two runs were repeated twice with the same outcome. These results led us to question the role of the solubility of the monomers and the phase changes during the course of the reaction for this particular feed composition, where the weight fraction of more water soluble and less reactive monomer is high. Thus, a question that still remains to be answered is "*what does the ATR-FTIR probe really "see"?*". Is there a possibility that the partitioning of monomer(s) in different phases and phase changes during the polymerization can trigger these unexpected results? Are there other systems or feed compositions that are not possible to track with ATR-FTIR spectroscopy? If these are issues for batch polymerizations, what can be expected in a semi-batch experiment where there is an additional issue: concentration change? Evidently, more experimental work has to be done in order to answer some of these questions.

CONCLUSIONS AND RECOMMENDATIONS

The presence of several components in the reaction mixture for BA/VAc emulsion polymerizations resulted in complex ATR-FTIR spectra. Nonetheless, it was possible to isolate and assign the limited number of absorbances for each monomer. Real time peak profiles for these characteristic monomer peaks were used to calculate individual monomer conversions and

the overall conversion. Our results showed that in-line monitoring of BA/VAc emulsion polymerizations using ATR-FTIR spectroscopy is possible and sufficiently accurate when compared to traditional off-line techniques. The insolubility of the polymers limited the direct comparison to overall conversion only, but the alternative method led to indirect favorable conclusions about the individual monomer conversions.

When used in an in-line mode, the ATR-FTIR probe can trace the length of an induction period correctly, and more importantly, can lead to early observation of catastrophic coagulation in the reactor. This work also showed that ATR-FTIR in-line monitoring can be a valuable tool in cases where standard techniques cannot be employed (e.g. due to limitations in polymer solubility in organic solvents).

There are limitations to the application of ATR-FTIR spectroscopy. This study has shown that temperature control is one of the key parameters for the successful application of ATR-FTIR spectroscopy in an in-line mode. Very strict temperature control is necessary for accurate in-line monitoring. Our assumptions on the influence of the solubilities and the phase changes in the copolymerization systems where one of the monomers is more water soluble and less reactive, require more investigation before being unquestionably stated as one of the limitations of the ATR-FTIR spectroscopy.

The results shown here are of considerable interest for the future development of ATR-FTIR spectroscopy as a tool in emulsion polymerization in-line monitoring. Despite the need for additional experimental work on in-line monitoring of these and other systems, these results are an important first step toward ATR-FTIR-based process optimization and control of emulsion polymerizations.

Acknowledgements

The authors wish to gratefully acknowledge financial support from the Natural Science and Engineering Research Council (NSERC) of Canada, the Canada Foundation for Innovation (CFI), and the Province of Ontario Research and Development Challenge Fund.

LITERATURE

1. R. Gilbert, *Emulsion Polymerizations: a mechanistic approach*, Academic Press, London, 1995
2. G.E. Ham, *Vinyl Polymerization*, Vol. 1, Marcel Dekker Inc., New York (1967)
3. M.S. El-Aasser and J.W. Vanderhoff, *Emulsion Polymerizatoin of Vinyl Acetate*, Applied Science Publishers, London, (1980)
4. D.C. Blackley, *Polymer Latices*, ed.2, vol 2, Chapman & Hall, London, (1997)
5. R.J.Andrews and E.A. Grulke,in *Polymer Handbook*, 4th ed., ed. J. Brandrup, E.H. Immergut, and E.A. Grulke, John Wiley and Sons, Inc., New York, 1999
6. F.R. Mayo and F.M Lewis, *J. Am. Chem. Soc.*, **66**, 1594 (1944)
7. M.A. Dubé and A. Penlidis, *Polymer*, **36** (3), 587 (1995)
8. D.C.H. Chien and A. Penlidis, *J. Macromol. Sci. – Rev. Macromol. Chem. Phys*,**1**, 1 (1990)
9. W.D. Hergeth, in *Polymeric Dispersions: Priciples and Applications*, ed. J.M. Asua, Kluwer Academic Publishers, Dordrecht, 1997
10. O. Kammona, E.G. Chatzi, and C. Kiparissides, *J. Macromol. Sci. – Rev. Macromol. Chem. Phys.*, **C39**(1), 57 (1999)
11. P. Dallin, *Process Control Qual.*, **9**(4), 167 (1997)
12. F.J. Schork and W.H. Ray, *J. Appl. Polym. Sci.*, **34**, 1259 (1987)
13. G. Storti, A.K. Hipp, and M. Morbidelli, *Polym. Reac. Eng.*, **8**(1) 2000
14. A. Urretabizkaia, J.R. Leiza, and J.M. Asua, *AIChE J.*, **40**, 1850 (1994)
15. M. Alonso, M. Alivers, L. Puigjaner, and M. Recasens, *Ind. Eng. Chem. Res.*, **26**, 65 (1987)
16. T.F. McKenna, S. Othman G. Fevotte, A.M. Santos, and H. Hammouri, *Polym. Reac Eng.*, **8**(1), 1 (2000)
17. G. Dotzlaw and M.D. Weiss, *Chem. Eng. Prog.*, **89**(9), 42 (1993)
18. P.D. Gossen, J.F. MacGregor, and R.H. Pelton, *Appl. Sprctros.*, **47**,1852 (1993)
19. C. Wu, J.D.S. Danielson, J.B. Callis, M. Eaton, and N.L. Ricker, *Process Control Qual.*, **8**(1), 1 (1996)
20. C. Wu, J.D.S. Danielson, J.B. Callis, M. Eaton, and N.L. Ricker, *Process Control Qual.*, **8**(1), 25 (1996)
21. . J. Mijovic and S. Andjelic, *Polymer*, **38**(8), 1295 (1996)
22. E.G. Chatzi, O. Kammona, and C. Kiparissides, *J. Appl. Polym. Sci.*, **63**, 799,1997
23. E.G. Chatzi, O. Kammona, A. Kentepozidou, and C. Kiparissides, *Macromol. Chem Phys.*, **198**, 2409 (1997)
24. R.F. Storey, A.B. Donnalley, and T.L. Maggio, Macromolecules, **31**, 1523 (1998)
25. T.L. Maggio and R.F. Storey, *Polymer Prep.*, **40**(2), 958, (1999)
26. R.F. Storey and A.B. Donnalley, *Macromolecules*, **32**, 7003 (1999)

27. R.F. Storey and T.L. Maggio, *Macromolecules*, **33**, 681 (2000)
28. A.J. Pasquale and T.E. Long, *Macromolecules*, **32**, 7954 (1999)
29. J.R. Bradley and T.E. Long, *Polymer Prep.*, **40**(1), 546 (1999)
30. A.P. Full, J. Puig, L. Gron, and E. Kaler, *Macromolecules*, **25**(20), 5157 (1995)
31. H. Hua and M.A. Dubé, In-Line monitoring of Emulsion Homo- and Copolymerizations Using ATR-FTIR Spectroscopy, *Macromolecules* (2001) (to be submitted)
32. M. Stickler, *Makromol. Chem., Macrmol. Symp.*,**10/11**, 17 (1987)
33. M.A. Dubé and A. Penlidis, *Macromol. Chem. Phys.*, **196**, 1101 (1995)
34. R. Jovanovic and M.A. Dubé, Off-line monitoring of butyl acrylate and vinyl acetate homo- and copolymerizations in toluene, submitted to *J. Appl. Polym. Sci.*, (2000), (submitted)
35. N.B. Colthup, L.H. Daly, and S.E. Wiberley, *Introduction to Infrared and Raman Spectroscopy*, 3rd ed, Academic Press, Inc., Boston (1990)
36. D. Lin-Vien, N.B. Colthup, W.G. Fately, and J.G. Grasselli, *Handbook of Infrared and Raman Characteristic Frequences of Organic Molecules*, Academic Press, Inc., Boston (1991)
37. Y. Terui and K. Hirokawa, *Vibrational Spectroscopy*, **6**, 309 (1994)
38. H.J. Jaffe and F.M. Rosenblum, in *Handbook of Adhesives*, 3rd ed., I. Skeist, Van Nostrand Reinhold, New York, 1990
39. M.A. Dubé and A. Penlidis, *Polymer International*, **37**, 23 (1995)

Chapter 5

PAPER III

Butyl Acrylate /Vinyl Acetate Latexes and Latex-Based Adhesive Properties

Renata Jovanović and Marc A. Dubé*
Department of Chemical Engineering, University of Ottawa,
161 Louis Pasteur, P.O. Box 450 Stn. A, Ottawa, ON, K1N 6N5 Canada
* dube@genie.uottawa.ca

ABSTRACT:

Butyl acrylate/vinyl acetate (BA/VAc) emulsion copolymerizations in the presence of poly(vinyl alcohol) emulsifier (PVOH, MW = 9000-10000 g/mol, DH = 80%) were carried out in a pilot scale reactor in batch mode. Relationships between the inherent properties of BA/VAc copolymers (e.g. copolymer composition, particle size and distribution), latex properties (rheology, solids content) and adhesive performance (tensile and shear strength of adhesive bond) were investigated. The use of PVOH resulted in insoluble BA/VAc copolymers possibly due to the grafting of PVOH onto the polymer particle surfaces. Therefore, the influence of molecular weight and distribution on adhesive performances was not determined. The copolymers formed showed increased heterogeneity with increased BA content. An indicator of the heterogeneity was the existence of the glass transition temperatures (T_g) determined using dynamic mechanical analysis. The average tensile strength of the adhesive bond of the copolymers with a wood substrate increased with increases in BA content while the average shear strength was decreased. No trends were observed when particle size and degree of polydispersity were considered.

Key words: butyl acrylate, vinyl acetate, polyvinyl alcohol, emulsion polymerization, DMA, rheology, wood adhesives, tensile strength of adhesive bond, shear strength of adhesive bond, structure-property relationship

INTRODUCTION

Poly(vinyl acetate)-based adhesives are among the most common adhesives used for bonding of different surface[1] especially porous ones.[2] The final properties of adhesives based on vinyl acetate homopolymers[3] or copolymers with ethylene[4,5] are primarily reported in the open literature. Even though emulsion-based copolymers such as butyl acrylate/vinyl acetate (BA/VAc) can also be employed as adhesives, the investigation of BA/VAc emulsion-based copolymers has been largely concentrated on the polymerization kinetics and/or inherent copolymer properties (e.g. copolymer composition, molecular weight, particle size and distribution)[6,7] and rarely on the final product properties.[8] Some of the relationships between polymerization reaction conditions and inherent properties BA/VAc copolymers are emphasized below.

Different polymerization modes lead to different extents of heterogeneity BA/VAc copolymers. Performed in a batch mode, BA/VAc emulsion polymerizations result in heterogeneous copolymers, while in a semi-batch mode, more homogeneous copolymers are possible.[9] In batch mode, the produced polymer particles, formed primarily during the early part of the reactions, have a core-shell structure. The core is BA-rich while shell tends to be PVAc-rich. In semi-batch mode, particles are formed over the course of reaction and possess a more homogenous structure.[9] Mirsa et al.[10] have found that the size of the particles is affected by copolymer composition when the BA/VAc polymerization is performed in the semi-batch mode, which is not the case in the batch mode.

The properties of BA/VAc dry latex films have also received considerable attention.[9,10,11] Mechanical properties of these films depend on the chemical structure of the polymer, particle

size and morphology, and drying conditions. Taking all of these into consideration, the increasing interest in the dynamic mechanical analysis (DMA) of polymer films obtained from latexes is not surprising. The confirmation of the core-shell structure of BA/VAc copolymers obtained in emulsion in the batch mode can be obtained using DMA. Two distinctive glass temperature transition peaks observed for the loss modulus are the confirmation of the heterogeneity of the particle structure.[9,12] These authors also concluded that the heterogeneity increases with the increase in BA content. When the same copolymer was obtained in the semi-batch mode, only one peak was observed indicating the homogeneity of the obtained copolymer.[9]

In addition to BA/VAc adhesive performance, there is a considerable lack of information on the use of polymeric surfactants (i.e. poly(vinyl alcohol), PVOH) and BA/VAc latex rheology. The closest system investigated is PVAc homopolymerizations. As a polymeric surfactant PVOH can be used alone (4-5 wt %) or in combination with small amounts of anionic emulsifier.[13] The association between the vinyl acetate units of PVOH and those of the formed polymer provides a means whereby PVOH molecules can be firmly fixed to the particle surface and thus stabilize the particles.[14] Dunn et al.[13] demonstrated that it is difficult to correlate the effect of PVOH on the rate of polymerization with its molecular weight, degree of hydrolysis and adsorption on poly(vinyl acetate) particles. On the other hand, Nakamae et al.[15] showed that particle size and rheological properties of the latex depend on the degree of hydrolysis of PVOH. Partially hydrolysed PVOH enhances the properties of the adhesive such as solvent, oil and heat resistance, machinability, setting time and wet tack.[16] Disadvantages of PVOH as emulsifier include: grafting reactions between propagating vinyl acetate chains and PVOH and promotion of the agglomeration of small particles.[14]

In this work, BA/VAc emulsion copolymers obtained in the presence of PVOH emulsifier were investigated. Inherent BA/VAc copolymer properties such as copolymer composition, particle size, and degree of polydispersity were related to the dynamic mechanical behavior of the dry polymer films and properties of the final product such as latex rheology and adhesive performance.

EXPERIMENTAL PROCEDURES AND TECHNIQUES

Materials. Six BA/VAc emulsion copolymerizations were carried out in a pilot scale reactor in batch mode. The experimental design included three different feed compositions (50/50, 35/65 and 20/80 wt%) at two different polymerization temperatures (60 and 80°C). A detailed description of the synthesis was given previously.[17] All latexes were prepared using ammonium persulphate as initiator and PVOH as polymeric surfactant. The targeted solids content was 50 wt%. In all cases, limiting conversion was observed. Reaction conditions, final conversions and copolymer compositions for all runs are summarized in Table 5.1. After polymerization, the latexes were filtered through an 80 mesh screen to remove the low amount of grit formed during the reaction.

Copolymer composition. Because of the insolubility of the copolymers obtained, the determination of copolymer composition using the standard method that combines ^{1}H-NMR spectroscopy and gravimetry was not possible. Therefore, Attenuated Total Reflectance Fourier Transform Infrared Spectroscopy was used. A detail description of the use of this technique for the determination of copolymer composition was given elsewhere.[17,18] The results are presented in Table 5.1.

Table 5.1 Reaction Conditions, Conversion, Solids Content and Polymer Composition

Name	Feed composition wt. Fraction BA (mole fraction BA)	Polymerization temperature (°C)	Overall Conversion (wt. fraction)	Solids content (wt. fraction)	Cumulative polymer composition	
					$\bar{F}_{BA}$	$\bar{F}_{VAc}$
Run 2	0.50 (0.40)	60	0.74	0.381	0.57	0.43
Run 3	0.20 (0.14)	60	0.88	0.448	0.16	0.84
Run 4	0.35 (0.24)	60	0.93	0.460	0.29	0.71
Run 5	0.50 (0.40)	80	0.76	0.415	0.51	0.49
Run 6	0.20 (0.14)	80	0.71	0.386	0.21	0.79
Run 7	0.35 (0.24)	80	0.54	0.287	0.53	0.47

$\bar{F}_i$ denotes the cumulative fraction of monomer *i* bound as copolymer

Molecular weights and molecular weight distribution (MW and MWD). The determination of MW and MWD was not possible due to the insolubility of the BA/VAc copolymers.

Particle size analysis. All final latexes were analyzed for particle size using a Brookhaven BI-200SM light scattering goniometer equipped with a Lexel 2-W argon ion laser operating at 514.5 nm and a Brookhaven BI-2030AT 201-channel correlator. The measurements were carried out at 90°, and the correlator was operated in the exponential sampling mode, the last four channels being used for baseline measurements. As a dispersion medium, a solution of sodium dodecyl sulfate (1g/L) was used.

Viscosity. Viscosity measurements were performed using an RS 5000 rheometer (Rheometric Scientific, Inc.). A Couette geometry with a fixed cup (32 mm) and mobile bob (29.5 mm) was used. Approximately 16 mL of sample was placed between the cup and bob and

covered with a thin silicone oil layer to prevent possible evaporation. Measurements were performed in a controlled strain rate mode. All measurements were performed at 23°C.

Dynamic Mechanical Analysis (DMA). DMA was performed on a Rheometrics Solids Analyser RSA II (Rheometrics, Inc.). A film fixture was used. Latex samples were cast at room temperature and allowed to dry over a two-week period. Specimens for analysis (23 mm × 2.2 mm × 0.3 mm) were cut from the samples. The exception was the dry film obtained from run 5, where due to the nature of the dry polymer film, the tests were done in a compression mode using a parallel plates fixture. The specimens were 5 mm in diameter and 0.3 mm thick. In case of run 7, several attempts to obtain a consistent film failed, possibly due to the high water content (low conversion). The evaporation of water left voids and bubbles inside the film making it unsuitable for dynamic mechanical measurement. Temperature sweeps were conducted between –70 to 50 °C (depending on the behaviour of the film) at a frequency of 1Hz. Prior to each temperature sweep, a strain sweep was performed at the lowest temperature and 23°C in order to determine the linear viscoleastic region and to select an initial strain for the temperature sweep. The initial strain ranged from 0.02-0.06%. The soak time was 30s.

Adhesive testing. Two tests were performed: a standard test method for tensile properties of adhesive bonds (D 879-95) and a modified standard test (D 905-94) for strength properties of adhesive bonds in shear by compression loading. Hard maple wood with specified properties (no defects or unusual discoloration) was used as a substrate for both tests. The wood blocks were conditioned at 24°C for seven days prior to assembly. The tests were performed on the copolymers obtained at the lower polymerization temperature (60°C). For both tests, the open assembly time was 15 min and the samples were clamped and allowed to dry for fifteen days prior to testing. The clamps were removed after 7 days. The specimens (Figure 5.1) were cut

from the blocks and tested. An Instron universal testing machine was used to perform both tests and the employed speed in both tests was 0.221 mm/min. The testing apparatus required by the standard shear test (ASTM D 905) was not available and therefore, the modified shear test was performed using a custom built jig for the Instron testing machine. The form and dimensions of the test specimens of the standard test method were altered to ensure that the pure shear was acting on the bonding surfaces under the test conditions employed.

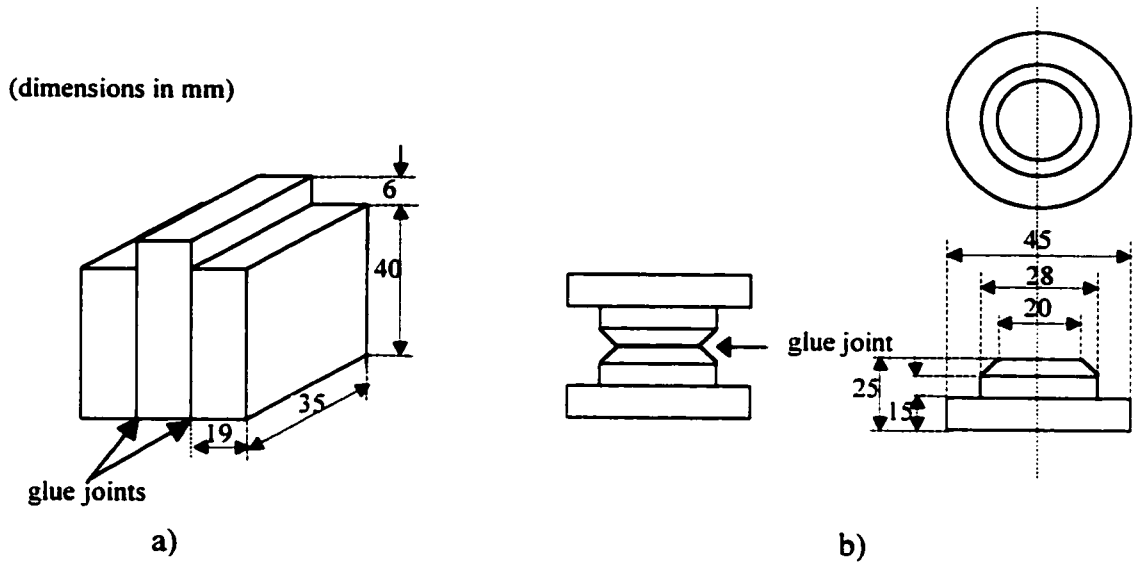

Figure 5.1 Specimens for adhesive testing a) shear strength, b) tensile strength

RESULTS AND DISCUSSION

The objective of this study was to investigate the relationships between the performance properties of BA/VAc emulsion-based adhesive, polymerization conditions, inherent polymer properties as well as latex properties. The determination of some of the most important properties such as molecular weight and molecular weight distribution was not possible due to the insolubility of the dry copolymers. The insolubility was the result of the use of a polymeric surfactant PVOH. When the selected recipe (run 2) was performed using sodium dodecyl

sulphate, an ionic surfactant, the obtained copolymers were soluble in organic solvents. A possible explanation lies in the morphology of the latex particles when PVOH is used as a surfactant. The particle is of a core-shell structure, where the core is PBA-rich and the shell is PVAc-rich due to the use of a batch polymerization mode.[8] Because the particle is surrounded with a PVOH layer, there is a possibility of grafting of PVOH onto the particle surface. In addition, there is a possibility of cross-linking due to the presence of hydroxyl groups. Knowing that the only solvent for PVOH is water (depending on its molecular weight and degree of hydrolysis), water and/or organic solvents (e.g. THF, toluene, hexane, dichloro benzene and others) were used to dissolve the copolymers. A limited degree of swelling was reached in all cases. The degree of swelling was not further experimentally investigated.

Rheology and particle size of latexes

In Figure 5.2, the viscosity profiles of final the latexes are shown. The latexes are denoted by the runs in which they were obtained (e.g. the latex obtained in run 2 is denoted as L2). All the latexes displayed the typical flow behaviour found in concentrated colloidal dispersions: the existence of a Newtonian plateau at low shear rates followed by shear thinning at intermediate rates. The existence of a high-shear Newtonian plateau was not confirmed due to the limitations of the rheometer. The sensitivity of the instrument was the reason for the higher dissipation of the results at lower shear rates. The high solids content in these cases is believed to have been achieved due to the use of polymeric surfactant. When the same solids content was attempted for the same emulsion polymerization system (run 2) with a polar surfactant, the catastrophic coagulation occurred.

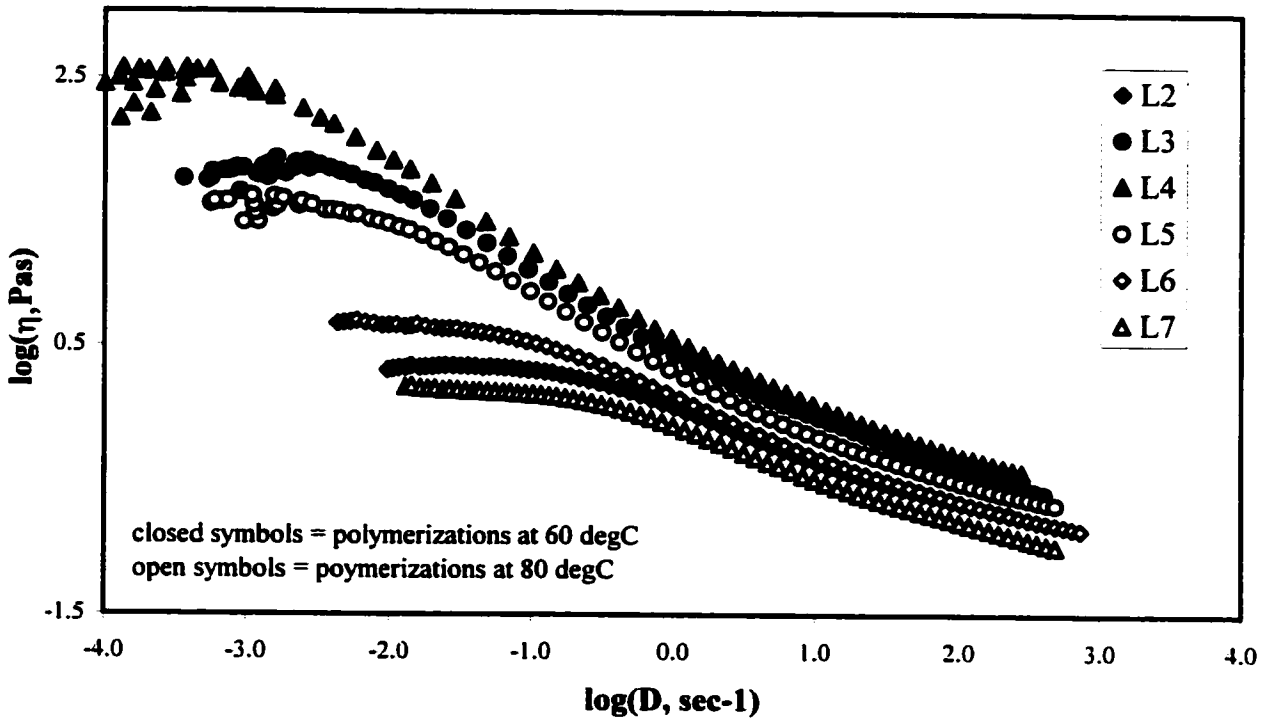

Figure 5.2 Viscosity of Latexes as a Function of Shear Rate

Even though the differences among the latexes are small especially in the region of intermediate shear rates, the existence of two distinctive behaviors is noticeable. The characteristics of latexes are summarized according these two behaviors in Table 5.2.

The first group of latexes (L4, L3, L5) has larger viscosities over the range of shear rates especially in the lower shear rate region than the second group (L2, L6, L7). This is not unexpected considering that the solids content is the most important factor influencing latex rheology. In the first group, latexes have a solids content ranging from 42-46 % while the second group's ranges from 29-38%. The first group also has slightly larger particle diameters compared to the second one. Polydispersity is the second most important factor influencing the rheological behavior of latexes. At high solids contents the more polydisperse latex might show an equivalent viscosity to less a polydisperse one.

Table 5.2 Latex Characteristics

Group	Latex	Solids content (%)	Particle diameter (nm)	Polydispersity
1	L4	46.0	236	0.215
1	L3	44.8	224	0.150
1	L5	41.5	214	0.174
2	L6	36.8	205	0.181
2	L2	38.1	209	0.146
2	L7	28.7	210	0.181

The viscosity of latexes L4 and L3 confirm this. At a similar high solids content and almost twice the high polydispersity, the viscosity of latex L4 is close to that exhibited by latex L3 especially at intermediate shear rates.

With the exception of latex L2, the particle diameters are slightly greater at a lower polymerization temperature (60°C). There is no trend in particle size observed when the copolymer composition is considered. This has been previously reported for the case when the latexes are obtained in a batch mode.[8] On the other hand, there is a trend observed at the higher polymerization temperature (80°C) where the particle size decreased with the decrease in BA content.

Dynamic mechanical properties of dry BA/VAc copolymers

The heterogeneity of the copolymer structure was confirmed by the results of dynamic mechanical analysis. The loss modulus spectra (Figures 5.3 and 5.4) showed two distinctive peaks corresponding to the glass transition temperatures (T_g) of the PBA-rich and PVAc-rich domains in the copolymers. In Table 5.3, the results of the dynamic mechanical analysis are summarized.

Table 5.3 Glass Transition Temperatures of BA/VAc Dry Copolymers

Run	Copolymer composition (BA/VAc)	Tg (°C)	ΔTg
Run 2	57/43	-33/38	71
Run 3	16/84	-29/24	53
Run 4	29/71	-31/28	59
Run 5	51/49	-28/43	71
Run 6	21/79	-31/18	49

It can be seen that the copolymers formed in the polymerization reactions at 60°C showed a decrease in the PBA glass transition temperature with the increase of BA content in the copolymer. Simultaneously, the second glass transition temperature corresponding to the PVAc domain increased. Similarly, for the copolymers obtained at 80°C, the increase in the BA content in the copolymer led to an increase in the second T_g corresponding to PVAc.

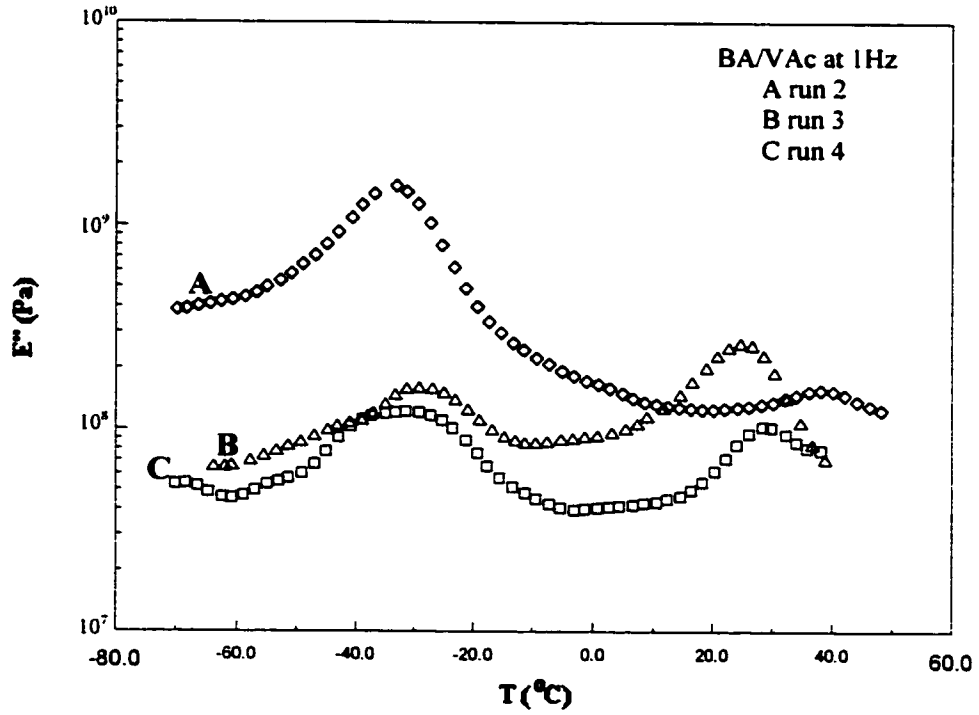

Figure 5.3 Isohronal (f = 1 Hz) Temperature Dependence of Loss Modulus for BA/VAc Copolymer Films (Polymerization Temperature 60°C)

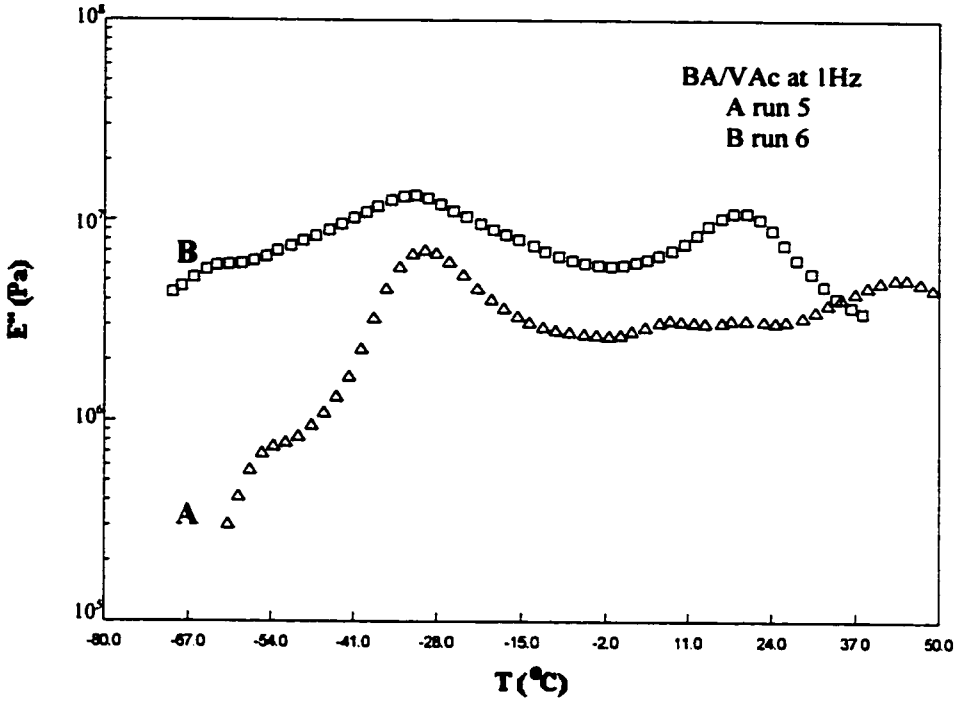

Figure 5.4 Isohronal (f = 1 Hz) Temperature Dependence of Loss Modulus for BA/VAc Copolymer Films (Polymerization Temperature 80°C)

However, the trend observed for the first T_g corresponding to the PBA glass transition was opposite to that observed for copolymers formed at 60°C: the increase in BA content in the copolymer led to an increase in the glass transition temperature. Copolymers formed at both polymerization temperatures showed increases in the distance between the two transition peaks of loss modulus curve when the BA content was increased. This indicates the increasing degree of the heterogeneity within the particles and the increasing size of the homopolymer domains within the copolymer films with increasing of BA content.

Adhesive performance

The strength of the adhesive bonds under tensile and shear stresses was determined as an indicator of the performance of BA/VAc emulsion based adhesives. The tests were undertaken for the BA/VAc latexes obtained at 60°C. The results of these tests are summarized in Table 5.4. The bond strength was calculated as the maximum force necessary to break the bond over the adhesive bond area.

Table 5.4 Strength of BA/VAc Adhesive Bond under Shear and Tensile Stress

Run	Total number of specimens	Average shear strength (kPa)	Total number of specimens	Average tensile strength (kPa)
Run 2	5	1152.28	2	8630.4
Run 3	5	11372.96	2	6164.57
Run 4	5	8065.93	2	6575.54
A commercial adhesive*	2	11977.9	2	4109.71

*Commercial PVA-based carpenter glue (a.k.a. "white glue")

Only slight increases in the average tensile strength were observed with the increased BA content in the copolymer. In contrast, the same adhesives under shear stress exhibited a decrease in shear strength with an increase in BA content. While all BA/VAc adhesives showed greater average tensile strengths compared to a commercial PVAc-based adhesive in the case of shear strength, the commercial glue was superior in all cases with exception of the run 3 (lowest BA content). Even though the number of specimens tested was small, the obtained results indicated an improved performance of BA/VAc wood adhesives under tensile stress when the BA content was increased.

Not only does the copolymer composition but also the heterogeneity of the polymer particles and film structure have an effect on the adhesive strength. The heterogeneity measured

as the difference in T_g values obtained using dynamic mechanical analysis increased with increasing BA content. Thus, all conclusions related to the BA content conform to that related to the heterogeneous adhesive film morphology. As opposed to particle structure, a trend between the particle size of different latexes and adhesive performance was not observed.

CONCLUSIONS

The investigation of different properties and their relationships for BA/VAc emulsion based adhesives led to the following conclusions. Performed in batch mode, BA/VAc emulsion polymerizations resulted in heterogeneous core-shell particle structures, where the core was PBA-rich while the shell was PVAc-rich. In addition, the use of the PVOH as emulsifier in this case led to insoluble polymers possibly due to the grafting of the PVOH onto the particle surface and cross-linking as the result of the presence of OH groups. When considering the obtained results, the molecular weight and degree of hydrolysis of the PVOH used in this study should be taken into account. Therefore, future studies should focus on the effect of molecular weight and degree of hydrolysis of the PVOH used as emulsifier on BA/VAc emulsion based copolymers.

On the other hand, the use of PVOH enabled us to obtain the latexes with a higher solids content compared to those using ionic surfactants. Rheological measurements confirmed that the solids content was the most important factor affecting the flow properties of BA/VAc latexes. In addition, all latexes with slightly higher viscosity had larger particle sizes. The particle size appeared to be affected by polymerization temperature, where a lower polymerization temperature resulted in slightly larger particle diameters. The exception was the latex with 53

mol% BA in the copolymer. However, a trend connecting particle sizes and copolymer compositions was not observed.

The dynamic mechanical analysis of dry polymers confirmed the heterogeneity of the BA/VAc particle structure. The existence of two glass transitions determined as the maximums at the loss modulus curves clearly indicated the heterogeneous nature of the copolymers obtained in batch mode. The heterogeneity in the particle structure measured as the difference between two glass transition temperatures showed an increase with the increase in BA content in the case of copolymers obtained at 60°C.

Increased BA content in BA/VAc copolymers showed the opposite effect on BA/VAc adhesive performance. This was measured as the adhesive bond strength under the shear and tensile stresses. The average tensile strength of the BA/VAc bond showed a slight increase while the shear strength showed a decrease with the increased BA content in the copolymer. This was also combined with the increase of heterogeneity of copolymers obtained with the increase of BA content.

In order to eliminate the heterogeneity and investigate only copolymer composition as factors affecting adhesive performance, a study where the adhesives are obtained in semi-batch mode would be suitable. The variability observed among the samples having the same feed composition, indicates that the adhesive application method should be improved. In addition, a larger number of samples should be included in future studies.

Acknowledgements

The authors wish to gratefully acknowledge financial support from the Natural Science and Engineering Research Council (NSERC) of Canada, the Canada Foundation for Innovation (CFI), and the Province of Ontario Research and Development Challenge Fund.

Assistance by Ms. A. Delgado of the National research Council for the DMA measurements, by Dr. M. Munro (Department of Mechanical Engineering, University of Ottawa) for the adhesive strength tests, and by Mr. F. Cotton (École Polytechnique – Montreal) for the viscosity measurements is also gratefully acknowledged.

LITERATURE

1. E.M. Petrie, *Handbook of Adhesives and Sealants*, McGraw-Hill, New York, 2000
2. A. Pizzi, *Advanced Wood Adhesives Technology*, Marcel Dekker, Inc., New York, 1994
3. H.J. Jaffe, F.M. Rosenblum, and W. Daniels, in *Handbook of Adhesives*, 3rd ed., I. Skeist, Van Nostrand Reinhold, New York, 1990
4. R.J.Lorenz, *Adhesives Age*, **40**(11), 42 (1997)
5. P.J. Scott, A. Penlidis, and G L Rempel, *J. Polym. Sci. Part A-Polym. Chem.*, **31**(2), 403 (1993)
6. M.A. Dubé and A. Penlidis, *Polymer International*, **37**, 23 (1995)
7. G.A. Vandezande and A. Rudin, in "Polymer Latexes. Preparation, Characterization, and Applications, ed. E.S. Daniels, E.D. Sudol, and M.A. El-Aasser, ACS Symp. Ser., **492**,134 (1992)
8. J L. Down, MA. Macdonald, J. Tetreault, and R.S. Williams, *Studies in Conservation*, 41(1), **19** (1996)
9. M.S. El-Aasser, T. Makgawinata, J.W. Vanderhoff, and C. Pichot, *J Polymer Sci.:Poymer Chem. Ed.*, **21**, 2363 (1983)
10. S.C. Mirsa, C. Pichot, M.S. El-Aasser, and J.W. Vanderhoff, *J. Polym. Sci.: Polym. Letters Ed.*, **17**, 567 (1979)
11. H.Y. Erbil, *Polymer*, **37**(24), 5483 (1996)
12. . C. Jourdan, J.Y. Cavaille, and J. Perez, *J. Polym. Eng. Sci.*, **28**(20), 1318,
13. A.S. Dunn, in *Emulsion Polymerization of Vinyl Acetate*, ed. M.S. El-Aasser, and J.W. Vanderhoff, Applied Science Publishers, London, 1980
14. D.C. Blackley, *Polymer Latices: Science and Technology*, Vol.2, Chapman & Hall, London, 1997
15. M. Nakamae, K. Yuki, T. Sato, and H. Maruyama, *Colloids and Surfaces A: Phusiochemical and Engineering Aspects*, **153**, 367 (1999)
16. H.J. Jaffe and F.M. Rosenblum, in *Handbook of Adhesives*, 3rd ed., I. Skeist, Van Nostrand Reinhold, New York, 1990
17. R. Jovanovic and M.A. Dubé, Butyl Acrylate/Vinyl Acetate Emulsion Polymerization: In-line Monitoring Using ATR-FTIR Spectroscopy, *Macromolecules*, 2001 (to be submitted)
18. E.G. Chatzi, O. Kammona, and C. Kiparissides, *J. Appl. Polym. Sci.*, **63**, 799 (1997)

Chapter 6

CONCLUSIONS AND RECOMMENDATIONS

In adhesive production, as in the production of any other polymer, the ultimate goal is to achieve a desired set of properties of the final product. This thesis is a contribution toward this objective. Within the scope of this thesis, the following conclusions and recommendations for future work, have been reached.

BA and VAc solution homo- and copolymerizations. This work was performed as a preliminary study on the use of ATR-FTIR spectroscopy for monitoring BA and VAc polymerizations. The major objective of determining BA and VAc characteristic absorbances and using them for ATR-FTIR off-line monitoring was successfully completed. The absorbances of BA at 810 cm^{-1} and VAc at 1293 cm^{-1} were employed for off-line monitoring of BA and VAc homopolymerizations in toluene. The obtained results were favourably compared to those obtained by standard off-line monitoring techniques (i.e. gravimetry and ^{1}H-NMR spectroscopy). BA/VAc copolymerizations in toluene were also successfully monitored using ATR-FTIR spectroscopy. These findings were the basis for the next part of the project: in-line monitoring of BA/VAc emulsion polymerizations. In future work, it is recommended to employ in-line ATR-FTIR monitoring for BA/VAc solution copolymerizations performed at the pilot-scale in the semi-batch mode. These experiments would approximate actual production conditions more closely than bench-scale polymerizations in the batch mode and disclose possible limitations for continuous monitoring using ATR-FTIR spectroscopy. Some pilot-scale batch experimentation may be necessary prior to the performance of the semi-batch experiments due to the former's more straightforward nature in terms of ATR-FTIR monitoring.

The solution polymerization experiments were also used to gain more knowledge about the solvent effect in BA and VAc solution polymerizations. The experiments confirmed the

existence of solvent effects on BA and VAc homo- and copolymerizations in toluene. The lumped rate constant $k_p/(k_t)^{0.5}$ was found to be dependent on solvent concentration. It is often assumed that this dependence is due to solvent effects on the termination rate constant. On the other hand, there is no physical evidence that the propagation rate constant is not affected. This uncertainty is due to limitations of the existing experimental techniques to obtain absolute values of the rate constants for systems with a combination of high propagation and termination rate constants such as BA and VAc. In this project, the dependence of the lumped constant was incorporated into a free radical polymerization model developed by Badeen and Dubé (2000). In the model, the lumped constant was changed with solvent concentration. This considerably improved the model predictions, especially for the case of VAc polymerizations. Improvements to molecular weight predictions for both BA and VAc polymerizations were also obtained. Future investigations of solvent effects on BA and VAc homo- and copolymerization in toluene should include experiments covering a wider range of solvent concentrations. This could probably contribute to more accurate model predictions, especially at higher conversion levels. In addition, an investigation of the influence of chain transfer reactions, especially those involving the effects of chain transfer agent (e.g. n-dodecyl mercaptan) on molecular weight development in the presence of solvent is needed.

BA/VAc emulsion copolymerizations. The objective of this part of the thesis was to use the knowledge gained during the ATR-FTIR off-line monitoring of BA and VAc solution homo- and copolymerizations to establish the use of ATR-FTIR in an in-line mode for monitoring BA/VAc emulsion copolymerizations. Again, the characteristic monomer peaks were used and conversion and copolymer composition results obtained in-line using ATR-FTIR spectroscopy

were compared to off-line results using gravimetry and ^{1}H-NMR spectroscopy. The experiments included three different compositions and two polymerization temperatures.

The unexpected insolubility of the obtained polymers and the intention to use poly (vinyl alcohol) as the emulsifier despite this, placed an additional challenge on the verification of results obtained using ATR-FTIR spectroscopy. Under these conditions, only gravimetry as a standard technique for off-line monitoring of overall conversion was possible to verify the data obtained using ATR-FTIR spectroscopy. This left the confirmation of the individual monomer conversions monitored by ATR-FTIR spectroscopy to be performed indirectly. This confirmation was obtained using BA/VAc emulsion polymerizations with sodium dodecyl sulfate emulsifier as well as emulsion polymerizations of other monomers performed in our laboratory that yielded soluble polymers. In these cases, when overall conversion data obtained using the ATR-FTIR spectroscopy and gravimetry were in close agreement, the individual monomer conversion data obtained by ATR-FTIR spectroscopy and the combination of gravimetry and ^{1}H-NMR spectroscopy showed good agreement as well. This analogy was used to confirm the accuracy of in-line monitoring of individual monomer conversions using ATR-FTIR spectroscopy in this project.

The findings confirmed the close agreement between conversion data obtained using ATR-FTIR spectroscopy for BA/VAc for two BA/VAc feed compositions, 50/50 and 35/65 wt% at two polymerization temperatures. In these cases, monomer compositions were also monitored with sufficient accuracy using ATR-FTIR spectroscopy. According to the previous discussion, this led to the conclusion that in-line monitoring of BA/VAc emulsion polymerizations using ATR-FTIR spectroscopy is possible and accurate. A recommendation for future work is to perform these same experiments in the semi-batch mode to more closely mimic industrial

conditions. BA/VAc emulsion polymerizations are typically performed in the semi-batch mode because they lead to more homogeneous products.

During the project, two limitations were discovered when using this technique. Firstly, the BA/VAc 20/80 wt% feed composition showed disagreement between data obtained using gravimetry and ATR-FTIR at low and medium conversions, whereas at high conversions, agreement was established. Even though the experiments were replicated at both polymerization temperatures, the outcomes were the same. More experimental evidence is needed at this particular feed composition before any solid conclusions can be reached. One recommendation for future work is to conduct experiments with different emulsifiers to establish whether the use of PVOH is a factor. In addition, experiments at different BA/VAc feed compositions between 35/65 and 20/80 wt% should be conducted to determine at what feed composition this effect begins. This could lead to a possible explanation involving phase changes during the polymerization which may also be the culprit.

The second observed limitation was that the accuracy of ATR-FTIR in-line monitoring depends strongly on temperature control. Two particular cases were discovered. One, where a small (up to 2°C) temperature off-set, followed by a stabilization period (up to 20 min), resulted in disagreement between the various monitoring techniques during this period. When the temperature returned to set point, the agreement between the data was re-established. The other case occurred when the temperature instability lasted much longer than approximately 20 min or the offset was much higher than 2°C. In this case, the disagreement between the monitoring techniques continued beyond the re-establishment of the set point. It is recommended to improve the temperature control of the reactor, on the one hand, and to pursue an investigation of a means to compensate for any temperature effects, on the other.

With the respect to the production of insoluble copolymers, it is recommended that other off-line techniques for determining individual monomer conversion, such as gas chromatography, be used.

BA/VAc emulsion-based adhesives. The investigation of structure-property relationships for BA/VAc emulsion-based adhesives confirmed the influence of the batch polymerization mode on the particle structure. Obtained particles had a heterogeneous structure, which was confirmed using dynamic mechanical analysis. The structure probably was a core-shell with a PBA-rich core and a PVAc-rich shell. Possibly, the PVOH emulsifier may have formed grafts on the particle surfaces. The grafting, combined with possible cross-linking through OH groups, was likely responsible for the insolubility of the BA/VAc copolymers obtained. As a recommendation, the use of electron microscopy for further confirmation of the particle morphology would be appropriate. In addition, knowing that the molecular weight and degree of hydrolysis of PVOH affects its properties, a study to investigate the effects of these two factors on the solubility of BA/VAc emulsion copolymers is also recommended. Furthermore, their influence on the latex rheology could also be investigated.

The adhesive performance measured as the strength of the adhesive bond under shear and tension stresses revealed the effects of the BA/VAc copolymer composition and heterogeneity on the BA/VAc adhesive bond strength. The increase in BA content in BA/VAc copolymers decreased the average shear strength of the adhesive bond while the average tensile strength slightly increased. The comparison with the commercial glue reviled the slightly higher average tensile strength of the BA/VAc copolymers while in the average shear strength only the copolymer with the lowest BA content showed equivalent average shear strength as a commercial glue.

Dynamic mechanical analysis of the dry BA/VAc latex films reviled an increase in heterogeneity of the particle morphology with the increase in BA content. As a measure of the heterogeneity, the difference between two glass transition temperatures, determined as peaks on the loss modulus curve, was used. Because of the relationships between the copolymer composition and heterogeneity, the observed adhesive performances might have been affected by both factors. Thus, to eliminate heterogeneity as a factor and consider only BA/VAc copolymer composition, BA/VAc emulsion polymerizations should be performed in semi-batch mode. The use of a common semi-batch control policy to compensate for the difference in the reactivity ratios of monomers would ensure the production of homogenous copolymers.

The observed variation in the results obtained at each composition indicates that further investigations should involve a much larger number of samples. In addition, the method of adhesive application should be improved in order to reduce sample to sample variability. Furthermore, the influence of the amount of the BA/VAc adhesive applied to a substrate, the use of different substrates (other wood types or veneer) as well as the duration of the bond open time and drying conditions on BA/VAc adhesive performance should be investigated. Finally, the performance of BA/VAc emulsion-based adhesives as pressure sensitive adhesives should be investigated.

Appendix A

SAMPLE CALCULATIONS

BA/VAc (50/50 wt%) emulsion polymerization at 80°C (**Run 5**) is selected to illustrate the calculation procedure. A sample calculation is given for the first row in the appropriate table if not otherwise indicated.

a) Polymerization recipe

Table A.1 Polymerization recipe

Ingredient	Weight (g)	Wt. fraction	phm
BA	566.1000	0.2264	0.5000
VAc	566.1000	0.2264	0.5000
APS	0.4498	0.0002	0.0004
PVOH	100.3248	0.0401	0.0886
CTA	5.6269	0.0023	0.0049
BUFF	11.4551	0.0046	0.0101
DDW	1249.9215	0.5000	1.1040
Sum	2499.9781	1.0000	

*phm = parts per hundreds monomers
**DDW = distilled deionized water

Weight fraction of an ingredient

$$w(i) = \frac{weight\ of\ ingredient}{total\ weight} \qquad w(BA) = \frac{566.1000}{2499.9781} = 0.2264$$

Parts per hundred parts monomer of an ingredient

$$phm(i) = \frac{weight\ of\ ingredient}{total\ weight\ of\ monomers} \qquad phm(BA) = \frac{566.1}{566.1000 + 566.1000} = 0.5000$$

b) Experimental log sheet and calculations based on gravimetric data

Table A.2 Experimental log sheet and calculations based on gravimetric data

#	Time (min)	Empty dish (g)	Sample + dish (g)	Dry sample + dish (g)	Solids	Conversion
1	3	1.270	2.238	1.342	0.074	0.059
2	6	1.268	2.266	1.356	0.088	0.091
3	15	1.258	1.794	1.333	0.140	0.205
4	21	1.268	1.523	1.320	0.204	0.346
5	27	1.266	1.672	1.363	0.238	0.421
6	33	1.270	3.651	1.890	0.260	0.471
7	39	1.278	1.781	1.427	0.297	0.551
8	50	1.261	1.949	1.482	0.321	0.604
9	60	1.265	2.469	1.679	0.344	0.656
10	75	1.264	1.770	1.448	0.363	0.698
11	90	1.269	1.930	1.508	0.362	0.696
12	120	1.263	2.207	1.613	0.371	0.715
13	150	1.267	2.229	1.637	0.384	0.744
14	180	1.272	1.585	1.394	0.390	0.757
15	210	1.272	2.133	1.615	0.398	0.776
16	240	1.267	2.126	1.611	0.401	0.781
17	270	1.281	2.739	1.876	0.408	0.797
18	300	1.271	1.718	1.456	0.415	0.811
19	330	1.266	2.800	1.903	0.415	0.813
20	360	1.275	1.624	1.420	0.415	0.813

Solids

$$Solids = \frac{(wt.of\ dried\ sample\ and\ dish - wt.of\ empty\ dish)}{(wt.of\ dish\ and\ sample - wt.of\ empty\ dish)}$$

$$Solids = \frac{(1.342 - 1.270)}{(2.238 - 1.270)} = 0.074$$

Conversion (wt. fraction)

$$Conversion(wt.fraction) = \frac{[\%\ solids - (wt.fr.\ of\ PVOH + wt.fr.of\ APS + wt.fr.of\ buffer + wt.fr.of\ CTA)]}{(wt.\ fraction\ monomers\ initially)}$$

$$Conversion(wt.fraction) = \frac{(0.074 - (0.0401 + 0.0002 + 0.0046 + 0.0023))}{(0.2246 + 0.2246)} = 0.059$$

c) Calculations based on ATR-FTIR data

First 60 min of the real time peak profiles for both monomers obtained using ATR-FTIR probe are shown in order to illustrate the calculations. Calculations are shown for the second row in Table A.3.

Table A.3 ATR-FTIR probe readings and calculations

Spectra #	Time (h)	Time (min)	A (810)	x(BA)	A (1138)	x(VAc)	X (wt.fr.)
1	0.000556	0.033333	0.011927	0	0.081274	0	0
2	0.033611	2.016667	0.011245	0.057206	0.078931	0.028827	0.043017
3	0.066944	4.016667	0.010825	0.092432	0.077968	0.040677	0.066555
4	0.100278	6.016667	0.010144	0.149525	0.07707	0.051729	0.100627
5	0.133611	8.016666	0.009676	0.188692	0.075804	0.067306	0.127999
6	0.166944	10.01667	0.008983	0.246829	0.07426	0.086299	0.166564
7	0.200278	12.01667	0.008131	0.318306	0.072579	0.106978	0.212642
8	0.233611	14.01667	0.007702	0.354218	0.071308	0.122619	0.238419
9	0.266944	16.01667	0.00704	0.409771	0.069827	0.140846	0.275309
10	0.300278	18.01667	0.006435	0.460441	0.06867	0.155075	0.307758
11	0.333611	20.01667	0.005979	0.498711	0.067789	0.165918	0.332315
12	0.366944	22.01667	0.005466	0.541681	0.066653	0.179899	0.36079
13	0.400278	24.01667	0.004999	0.580897	0.065589	0.192984	0.386941
14	0.433611	26.01667	0.004498	0.622903	0.064554	0.205723	0.414313
15	0.466944	28.01667	0.004085	0.65751	0.063543	0.218158	0.437834
16	0.500278	30.01667	0.00367	0.692317	0.062556	0.230304	0.46131
17	0.533611	32.01667	0.003295	0.723757	0.061604	0.242016	0.482886
18	0.566944	34.01667	0.002947	0.752943	0.060879	0.250939	0.501941
19	0.600278	36.01667	0.002648	0.777979	0.060148	0.259941	0.51896
20	0.633611	38.01667	0.002417	0.797345	0.059491	0.268018	0.532681
21	0.666944	40.01667	0.002075	0.826006	0.058613	0.278824	0.552415
22	0.700278	42.01667	0.001883	0.842099	0.058187	0.28407	0.563085
23	0.733611	44.01667	0.001648	0.861787	0.057357	0.294275	0.578031
24	0.766944	46.01667	0.00145	0.878421	0.056672	0.302703	0.590562
25	0.800278	48.01667	0.001243	0.895822	0.056165	0.308948	0.602385
26	0.833611	50.01667	0.001053	0.911727	0.055647	0.315321	0.613524
27	0.866944	52.01667	0.000897	0.924824	0.05512	0.321795	0.62331
28	0.900278	54.01667	0.000802	0.932775	0.054679	0.327232	0.630004
29	0.933611	56.01667	0.000668	0.943958	0.054168	0.333517	0.638737
30	0.966944	58.01667	0.00053	0.955566	0.053656	0.339811	0.647689
31	1.000278	60.01667	0.000427	0.964177	0.053419	0.342731	0.653454

A(810) = absorbance measured as the peak height for BA at 810 cm^{-1}

A(1138) = absorbance measured as the peak height of VAc at 1138 cm^{-1}

Individual monomer conversion $x(i)$

$$x(i)(mol\ fraction^{*}) = 1 - \frac{peak\ height\ at\ time\ t}{peak\ height\ at\ time\ t = 0}$$

$$x(BA) = 1 - \frac{0.011245}{0.011927} = 0.057181^{**}$$

$$x(VAc) = 1 - \frac{0.078931}{0.081274} = 0.028828^{**}$$

Overall conversion $X(wt.\ fraction)$

$$X(wt.fraction) = \frac{m_{BA}}{m_{BA} + m_{VAc}} x_{BA}(wt.fraction) + \frac{m_{VAc}}{m_{BA} + m_{VAc}} x_{VAc}(wt.fraction)$$

$$X(wt.fraction) = \frac{566.1000}{566.1000 + 566.1000} 0.057206 + \frac{566.1000}{566.1000 + 566.1000} 0.028827 = 0.043003^{**}$$

* For the individual monomer conversions mol and mass fractions have the same values.

** The difference from the sample calculations and the calculations reported in Table A.3 is due to the number of significant digits included in the calculations. The probe readings and calculations reported in Table A.3. were performed with 15 significant digits in the ATR-FTIR software.